Pumping coral-spawn slicks for large scale reef rehabilitation

F.J. Vons

TU**Delft**

Van Oord
Marine ingenuity

Challenge the future

Pumping coral-spawn slicks for large scale reef rehabilitation

by

F.J. Vons

June 19, 2019

Master of Science
in Hydraulic Engineering

at the Delft University of Technology,

People involved

Supervisor:	Prof. dr. ir. Mark van Koningsveld	TU Delft & Van Oord
Thesis committee:	Dr. ir. Myron van Damme	TU Delft
	Dr. ir. Matthieu de Schipper	TU Delft
	Dr. Christopher Doropoulos	CSIRO
	Remment ter Hofstede	Van Oord

TUDelft Delft University of Technology

Preface

This report is written with the objective to describe knowledge development on harvesting coral embryos from the ocean surface which can be used for large scale reef rehabilitation. This research contains information for biologist, ecologists or engineers who want to contribute to this goal. For people without an engineering background, it should be possible to develop a coral harvest pump when consulting this thesis.

The research has been performed in collaboration with Van Oord, a Dutch marine contractor based in Rotterdam, that has provided me with an excellent environment to conduct my work. Being able to ask questions to environmental- and pumping experts, helped me through my research. Furthermore, Van Oord gave me the exceptional possibility to execute field tests at the Great Barrier Reef in Australia for which I am very grateful.

Because both ecology and engineering play a big role in this research, assistance of many people was required. First I want to thank Mark van Koningsveld, for finding time within his busy schedule to help me shaping my research and teach me how this can be conducted on a scientific level. Next, Myron van Damme earns a special word of thanks. Due to his far-reaching dredging and pumping knowledge, he helped me building a mathematical model that calculates the stressors in a pumping system. Thirdly, I want to thank Remment ter Hofstede and Christopher Doropoulos for their biological knowledge and helped me write the coral sections. As final member of my committee, I want to thank Matthieu de Schipper for his advice during my research.

Furthermore, the project team in Australia, containing researchers from CSIRO and Van Oord earn a special word of thanks. Christopher Doropoulos and Russ Babcock, thanks for the inspiring coral knowledge and introducing the wonderful world of Australia to me. My passion for coral has grown enormously and will hopefully develop even more over the coming years. Furthermore, I want to thank Mark van Koningsveld, Jesper Elzinga and Remment ter Hofstede for all their help. It was very inspiring to work together with three specialist that gained a lot of knowledge through the awesome environmental and coral engineering projects which you were involved in. Finally, I want to thank Keri Constanti-Carey and Andrew Chryss who helped me enormously during the coral strength tests in Australia, without their experience it wouldn't have been possible to execute the tests.

Next to the team in Australia, also AquaUnique earns a word of thanks. They helped me execute the laboratory tests in Steenbergen and facilitated a perfect work environment to execute the tests.

F.J. Vons
Delft, June 19, 2019

Abstract

Coral reefs are degrading across the entire Great Barrier Reef. Rehabilitation of the Great Barrier Reef is crucial for Australia, both socially and economically because it provides $6 billion in revenue and 63,000 jobs. The Queensland state government issued a challenge within the "Small Business Innovation Research" program to quickly restore ecological functions provided by the reef. Van Oord and CSIRO participated in this challenge by testing a concept designed to scale-up rehabilitation efforts. This concept involves rehabilitation of the reef by increasing the number of larvae deployed onto the reef. To achieve this, coral-spawn slicks should be collected from areas with healthy coral populations that show a redundancy of embryos. During transport, these slicks should then be stimulated to grow into settlement competent larvae. Subsequently, they can be deployed at a degraded coral reef. The collection phase should be executed with pumps to reach considerable volumes of coral embryos for significant ecological scale. Unfortunately, the mortality rate of coral embryos due to pumping is so far unknown, yet crucial to determine. Therefore, the objective of this research is to develop a method for designing a pumping system that can pump coral embryos and larvae into a vessel-based container or hopper with maximal survival rates.

To achieve this objective, the strength of coral embryos and larvae as well as the stressors in a pumping system are investigated. In order to design and optimise the pumping process for survival, it is useful to have a framework that estimates the balance between strength of coral embryos and larvae and stressors. In literature, comparable strength and stress balances are known in, for example, thermal stress onto corals. The cause of failure (or mortality) is a combination between the strength, the exposed stress (or load) for a certain period of time and the capability to regain strength. Failure happens when the strength cannot withstand the stress (or load). These failure effects are also described through threshold limit values (TLV) which indicate a limit that the stresses may not exceed. Examples of such limits are time weighted average, short-term exposure limit and ceiling limit. Within the design of a pumping system, these values are expected to be acute (e.g. in the pump) and chronic stress (e.g. in the pipeline). In order to distinguish between pumping systems, the stressors in the system can be calculated by using tools such as a mathematical model.

The coral life cycle commences with gametes that contain eggs which are fertilised in the slick at the ocean surface, before developing into embryos. Because the buoyancy of coral embryos is positive until 36h following spawning, dispersion is limited. Hence, they are easiest collected within this period of time. The pumping related strength of coral embryos and larvae is therefore investigated in this research. The assumption is made that the strength of the embryos and larvae differ in the first period following spawning. In order to gain insight in the strength limits of coral embryos and larvae within this period, strength tests are executed. During the mass-spawning event in November 2018, fertilised eggs were collected and used in a Couette-rheometer test at the Heron Island Research Station. These tests consist of a cylinder rotating at different speeds in a container filled with water and embryos. Due to the rotation of the cylinder, the coral embryos and larvae experience stress. The living coral embryos are counted before and after each experiment by use of a microscope experiment in order to define the survival rate. After 5-7 hours the embryos have developed a considerable strength (larger than can be applied by the Couette-Rheometer). Therefore, it is recommended to start the collection process after 5-7 hours following spawning. Nevertheless, the tests do not define the exact strength of the embryos. Hence, it is advisable to investigate the exact strength in further research.

To design a pumping system that can pump coral embryos and larvae with low mortality, the stressors in the system should be minimal. The main technical criteria of the pumping system include low shear stresses, low-pressure fluctuations and low flow accelerations. Practical criteria such as availability, scalability and handling should also be considered in the design. A mathematical model was designed to calculate the previously described factors by calculating the magnitude of the stressors in a pumping system. Based on the model, it can be concluded that the pipeline configuration of a coral slick collection

system should contain minimum pipe length, maximum diameter, minimal surface to encounter (e.g. bends and connections), low rpm and flow velocities and submerged in- and outflows openings.

Laboratory tests in the Netherlands and field tests in Australia have been executed in order to validate the relation between the strength of coral embryos and larvae and stressors in a pumping system. During laboratory tests, pumping system aspects that contribute most to damage have been investigated, and potential practical issues have been identified. Damage rates were estimated for different pumps and pipeline configurations using different proxies such as, hydrogell balls, peas, berries and fish eggs. From these tests, the Hidrostal and Diaphragm pump resulted in low damage rates and were selected to be applied during the field tests. Additionally, a skimmer (intake) to collect the floating particles was designed and tested, both in the laboratory as well as the field.

The field test has been executed in the Southern Great Barrier Reef around the Heron and Wistari reef. Currently, this part of the reef boasts the highest level of coral cover throughout the entire reef, and is almost at its historical maximum. Therefore, it was chosen as research location because of its expected large supply of coral spawn. The main goal of the field study was to investigate the possibility to pump coral embryos following the mass spawning in November 2018. The experimental setup consisted of a tug vessel with two pumping systems, each with a different pump (i.e. the Hidrostal and Diaphragm pump) and the same configuration. A total of total twelve tanks was used for cultivation of which six plastic and six steel. The total number of living coral embryos that have been pumped was approximately 29 million from which 19% developed into competent larvae within five days. The competent larvae were pumped through the same system to investigate their survival rate, which was around 88%. This indicates that deployment of larvae onto degraded reefs should be possible by pumping without much loss and that coral larvae are less fragile compared to coral embryos.

The objective of this research was to develop a method for designing a pumping system that can pump coral eggs, embryos or larvae, from the sea surface onto a vessel housing an aquaculture facility. By using the previously described criteria, it is concluded that coral embryos and larvae are able to survive pumping related stressors. Further research should aim to find the exact strength of coral embryos after which a more precise model can be created to estimate mortality. Furthermore, limitations for pressure differences should be determined. For now, the assumption is made that for designing a pumping system, atmospheric pressure should be the minimum local pressure which is conservative. Additionally, the controlled deployment of the competent larvae onto degraded reefs should be further investigated because this project was not focused on that phase. To conclude, the project needs up-scaling towards hopper sizes, with a broader range of coral species and various weather conditions.

Given the previous described challenge, this research proofs that it is possible to pump coral embryos, after which they can grow into competent larvae and be deployed onto degraded reefs. Significant quantities of new recruits can be collected at healthy reefs and by using hopper size vessels, the collection of coral embryos from slicks become promising.

Contents

1

Introduction

Wide-spread disturbance events have resulted in significant declines in coral across the entire Great Barrier Reef (De'ath et al., 2012; Mellin et al., 2019). About one-third of the coral died in 2016 and 2017 because of extreme heat (Hughes et al., 2018). As a result, the production of new coral larvae has decreased. Reduced supply of larvae is a key factor inhibiting the rehabilitation of degraded reefs, as are a limited settlement of larvae onto the reef and high post-settlement mortality rates (Gilmour et al., 2013; Hughes et al., 2018). The growth of new coral is dependent on the combination of larvae supply, successful recruitment of those larvae, and post-settlement survival and growth (Connell et al., 2010; Doropoulos et al., 2015). Healthy reefs, in contrast to degraded reefs, produce more larvae than is needed for persistence of the coral reefs (Babcock et al., 1986; Harrison et al., 1983).

The Great Barrier Reef is crucial for Australia both socially and economically, providing over $6 billion in revenue and 63,000 jobs (Garrett, 2018). The Queensland state government issued a challenge within the "Small Business Innovation Research (SBIR)" program, to quickly restore ecological functions provided by the Great Barrier Reef (Martyn, 2018). The goal of this program is to support innovators to develop and test new, commercially viable solutions to complex challenges for restoration of the Great Barrier Reef. Van Oord DMC collaborates with the Commonwealth Scientific and Industrial Research Organisation (CSIRO, Australia) in this challenge to scale-up rehabilitation efforts. The idea is to rehabilitate the reef by harvesting coral-spawn slicks from areas with healthy coral reefs where there is a redundancy of embryos. Subsequently these slicks should be stimulated to grow, during transport, into competent larvae, and be deployed at a degraded coral reef (Doropoulos et al., 2019).

Over the last years several new technologies have been introduced for reef rehabilitation. One of them is the Reef-Guard which is an innovative mobile laboratory designed by marine contractor Van Oord, for reef rehabilitation. It has been developed in close collaboration with coral experts from all over the world. The ReefGuard employs the concept of nurturing coral larvae and young coral recruits under controlled conditions, to enhance their survival rates after re-introduction in nature (Van Koningsveld et al., 2017). For the rehabilitation challenge within the SBIR project, this current state of the art technique still requires an upscaling with two to three orders of magnitude to achieve rehabilitation of the Great Barrier Reef at an ecologically relevant scale (Doropoulos et al., 2019).

One approach to increase the magnitude is to upscale the coral spawn collection process by making use of vessels which contain hopper capacity. These vessels could be used to gather vast quantities of coral spawn using pumps and store the collected coral spawn in the hopper. Van Oord and CSIRO estimated that 2 - 2.5 billion live larvae inside a hopper are needed to reach ecologically significant rates (Doropoulos et al., 2019). To achieve this, around 3 billion live embryos should be pumped from the sea surface when a mortality rate of 25% due to pumping is considered. However, that rate is only estimated and therefore crucial to further investigate. At 230 embryos L^{-1}, a TSHD with 14,000 m^3 capacity would contain 2.4 billion live embryos following the anticipated pumping mortality rate. The collected embryos will be allowed to further develop within the hopper into competent larvae until being deployed at a degraded reef. After pumping, transportation, releasing and settling of the fragile

organisms, it is expected that these will develop into approximately 140.000 mature colonies that will contribute further to the reef rehabilitation process through natural spawning (Doropoulos et al., 2019).

Coral embryos are fragile, and therefore, minimal stresses should be present in the pumping and releasing system. Important aspects when optimising a pumping system to reduce stress on embryos are: pressure fluctuations, shear stresses and flow accelerations (Ulanowicz, 1976). A study that pumped fish eggs from *Coregonus artedi* using a diaphragm pump to minimise damage showed that mortality rates were approximately 30% (George et al., 2017). Coral embryos are not protected by a shell (Heyward and Negri, 2012). Hence, mortality rates are expected to be higher.

1.1. Scope

In light of the above-described innovation, the research presented in this report focuses on pumping coral-spawn slicks from the sea surface towards a storage facility (60 m^3) on board a vessel while achieving low pumping system related mortality. As stated in the before, the collection phase should be executed with pumps to reach considerable volumes (30 m^{3}h^{-1}) of coral embryos for significant ecological scale. The cultivation of the coral embryos and larvae is not part of the scope of this research nor is the investigation whether the competent larvae settle on a target reef and grow into mature colonies.

1.2. Research objective and research questions

Following the above context, it is clear that a crucial step in this proposed approach to reef rehabilitation is the pumping of coral embryos and larvae and the associated mortality rate. To contribute to this effort, the following research objective is defined:
The collection phase should be executed with pumps to reach considerable volumes of coral embryos for significant ecological scale.

To develop a method for designing a pumping system that can pump coral eggs, embryos or larvae (number of survivors > 0), from the sea surface onto a vessel housing an aquaculture facility.

To be able to achieve this objective a main research question and four sub-questions are posed below.

Main question
How can a pumping system (discharge > 30 m^{3}h^{-1}) be designed to maximise the amount of embryos and larvae pumped from coral-spawn slicks, into a vessel based container or hopper with maximal survival rates (number of survivors > 0)?

Sub-questions
To answer the main research question, it has been broken down into several sub questions (SQs). These SQs contribute to the main research question and divide the research into two main parts that focus on the strength of the coral embryos and larvae on the one hand and the stresses in the pumping system on the other. Therefore, laboratory tests and a prototype field test are executed.

Theoretical framework
SQ1: What are the basic elements of a theoretical framework, that can act as a design tool, where the survivability of coral embryos and larvae is related to the strength of the particles and stresses occurring in the pumping system?

This theoretical framework is based on existing literature. The relation between the strength and the exceeded stresses is first evaluated theoretically and subsequently validated with experiments.

Strength of coral embryos and larvae

SQ2: What is the strength of live coral embryos and larvae in the 48 hours following spawning in relation to shear stress?

Underlaying questions are:

- What aspects of pressure in the pumping system are relevant for coral embryo and larvae survival?
- What is the maximum stress coral embryos and larvae can handle?
- How can we test the strength of coral embryos and larvae?
- Is there an ideal time frame to pump the coral embryos and larvae after spawning?

Before a pumping system can be designed, certain thresholds of the coral embryos and larvae should be known. The minimum pressure limit is focusing on the "expansion" of the organisms and the maximum stress test will address which stress levels cause mortality. These values are the thresholds values in the model that estimates the stresses present in the pumping system.

Stresses in the pumping system
SQ3: Which pumping systems are able to pump coral embryos and larvae with maximal survival rates?

Underlying questions are:

- What are the selection criteria for a pumping system related to embryos and larvae survival?
- Can the theoretical selection criteria be confirmed in a laboratory test setup?
- Which parts of a pumping system reduce coral embryos and larvae survival?
- How can the stressors in a pumping system be approximated by a practice based mathematical model?
- How do pumps, available on the market, score on certain given critical selection criteria?
- What are the two best scoring pumping systems regarding high survival?

It is unknown whether pumping systems can pump coral slicks with high survival rates. When designing such a pumping system, criteria like stress levels, pressure differences, accelerations and handling should be considered.

Testing pumping systems in the field
SQ4: Is it possible to pump coral embryos and larvae during a prototype scale test and how can the pumping system be optimised?

Underlying questions are:

- How do selected pumping systems score and behave in a prototype scale test? (c.f. SQ3)
- Can the found strengths of coral embryos and larvae within field tests experiments be confirmed? (c.f. SQ2)
- What optimisations in the tested pumping system are required to maximise quantities of pumped coral embryos and larvae with minimal mortality?

The predicted performance of pumping systems is validated during a prototype scale test at the Great Barrier Reef in Australia (field test). Two different setups are used: from the ocean surface onto the deck of the tug vessel and deck to deck pumping (as contingency).

1.3. Methodology
A strength-stress framework is developed to relate applied stress and coral mortality. It can be used to indicate if the pumping system exerts critical stress that exceed the strength threshold values of coral embryos and larvae. The values of strength and stresses are required to design and engineer a

pumping system that operates with preferred discharge volumes while maintaining low mortality rates.

Because exact coral strength is so far not described in literature, experiments are executed to determine this threshold at Heron Island Research Station, Australia. By collecting live coral embryos and exerting stress onto the particles, the strength and mortality rates are determined.

To approximate the stressors in the pumping system, a model is built that calculates the specific values for pressure and shear stress in various sections of the pumping system.

Because many aspects of the interaction between coral embryos or larvae and the pumping system related stresses are unknown, different pumps and pipeline configurations are tested under laboratory conditions using surrogates for coral embryos and larvae. By investigating the failure rates of the surrogates when changing the configuration, optimisations are found and used in the final design to build a system with expected maximum survival rates. The laboratory tests have been executed in Steenbergen in cooperation with Aqua Unique (specialists in building swimming pools and ponds). The two best pumping systems are used in a prototype scale test on the Southern Great Barrier Reef in Australia during the mass coral spawning event in November 2018.

The results found during the experiments and the field research are used to validate the model, which can act as a tool to assess the effect of different pumping systems beforehand in future applications and configurations.

1.4. Field test, Australia

During the mass spawning event in November 2018, field tests were executed to investigate the potential of using coral slick collection for large scale reef rehabilitation. The aim was to harvest coral slicks from the ocean's surface and allow the organisms to develop until they were competent larvae (approx. 5 days), after which it is possible to deploy them onto a degraded coral reef. On the degraded reef, they have the opportunity to settle and to outgrow into full-fledged coral colonies.

The field test is executed in the Southern Great Barrier Reef around the Heron and Wistari reef part of the Capricorn-Bunker group and adjacent inshore reefs. This area currently has the highest level of coral cover throughout the entire reef, almost at its historical maximum (AIMS, 2018). Therefore, there is good potential to find high volumes of high density healthy coral-spawn slicks for large scale collection (Doropoulos et al., 2019). Multiple colonies of *Acropora spathulata* were collected from the reef and stored on the vessel after which their spawn was collected following the spawning event. Furthermore, the wild coral-spawn slicks that were collected from the ocean surface contained an entire community of corals representative of what is found on the reef.

The experimental setup on board of a tug vessel (Figure 1.1) contained two pumping systems (Figure 1.2), each with a different pump, and twelve tanks for cultivation (Figure 1.3).

Figure 1.1: Tug vessel; PT Fortitude

Figure 1.2: Hidrostal(blue) and Diaphragm pump(red)

Figure 1.3: Cultivation tanks on deck of the vessel

The main goal of the field study was to investigate the possibility to pump coral embryos that were formed during the mass spawning in November after which they could grow into competent larvae on board. Furthermore, it is investigated if coral embryos better survive in a steel tank or in a plastic one

until larval competency. No further investigations took place to check if the larvae could settle on a reef (this will be tested in a follow up phase). The five main goals of the field test were described as follows:

1. Ability to locate and concentrate coral slicks for collection (Figure 1.4 and Figure 1.5);
2. Ability to collect coral slick at high densities (Figure 1.6)
3. To measure survival of pumped embryos and larvae for both 1) deck to deck and 2) surface to deck pumping and comparing pump types used;
4. Test survivorship of embryos and larvae in untreated steel storage tanks relative to plastic tanks' (Figure 1.3);
5. Confirm ability of harvested ship-reared larvae to settle and metamorphose on reef substrata on-board.

Within this thesis the second and third key processes are investigated and described.

Figure 1.4: Locating slicks

Figure 1.5: Concentrating slicks

Figure 1.6: Collection device

The team executing field test of the feasibility study can be found in Figure 1.7 and consists of researchers from CSIRO, Van Oord (VO) and the TU Delft (TUD). The time table presented in Figure A.1 indicates the development of the project from January 2018 until March 2019.

Figure 1.7: Project team during field test in Australia from left to right: M. van Koningsveld (VO & TUD), F. Vons (VO & TUD), R. Babcock (CSIRO), R. ter Hofstede (VO), C. Doropoulos (CSIRO), J. Elzinga (VO) K. Salee (CSIRO)

1.5. Research impact and outcome

The collection of coral slicks by pumping large amounts has never been executed. The strength of coral embryos in the current literature is unknown and this knowledge is needed to design pumping

systems with low mortality rates. When demonstrated that large quantities of coral embryos and larvae can be pumped and stored alive on a vessel, this provides a large potential for large scale coral reef restoration, as coral slick can be collected at healthy reefs, and transported to degraded reefs as a huge supply of coral recruits.

1.6. Outline of the report

This report is divided into two main parts, namely, defining the strength of coral embryos and larvae and calculating stressors in the pumping system. Both are required to estimate the survival of coral embryos and larvae after pumping and are introduced in Chapter 2. The more in-depth research regarding the strength of coral is discussed in Chapter 3 in which relevant literature is reviewed and the results of laboratory tests are presented. Calculation of the stressors in a pumping system is described in Chapter 4. A mathematical model is built from which the most critical features and results are given. To validate the model, laboratory tests and field tests are executed and presented in Chapter 5. A discussion of the research is given per subject in the corresponding chapters and a final discussion, conclusions and recommendations of the project in Chapter 6.

2

Strength and Stresses

It is necessary to define the strength of coral embryos and the stressors in a pumping system to estimate the pumping related mortality. In this chapter, current knowledge is described, and the relation between coral strength and pumping stresses is considered.

The strength of coral embryos and larvae should be known to estimate the pumping related mortality. So far, these values are not described in literature. Resilience is described as a dynamic developmental process where adaptation is still reversible (Cicchetti, 2010). There are two critical conditions appointed: a) exposure to significant stress and b) the achievement of positive adaptation despite the stresses. A study dealing with strength/stress relations is, for example, investigating the effect of thermal stress on coral reefs (Gilmour et al., 2013). Stress receivers have different critical threshold values for the level of maximum acceptable stress this is elaborated upon in Section 2.1. The response to stresses is different for each type of receiver and depends on multiple parameters such as exposure duration, and exposure intensity Gough et al,. (2011) and these are further explained in Section 2.2. A simplification of species response to stresses is provided in Section 2.3. Finally, an introduction to the stressors in a pumping system is presented in Section 2.4.

2.1. Threshold limit values

The threshold limit value (TLV) is the level to which the receiver can be exposed without adverse effects (Paull, 1984). Threshold values are present in different industries and, for example, Galante et al., (2014) defined three types of threshold limits within the chemical industry:

1. Time weighted average: stress is experienced over a longer period (hours) and the integrated stress becomes fatal.
2. Short-term exposure limit: constant stress is experienced for a short period (minutes) and the integrated stress becomes fatal.
3. Ceiling limit: absolute exposure limit that should not be exceeded at any time.

When pumping coral embryos from the ocean's surface onto a vessel, the pumping period is in the order of minutes. Therefore, the most applicable TLV for this process are likely the short-term limit and ceiling limit. The short-term exposure limit is explained as chronic stress, which is relatively constant. An example of chronic stress is a particle that flows through a pipeline and experiences shear stress along the pipe wall until the outflow. Ceiling limits are explained as acute stress experienced by the particle in, for example, the pump. Figure 2.1a presents the difference between chronic and acute stress. When integrating the total amount of stress over the short (minute) and concise (less than a second) period in time, the surface areas of the two functions can be compared, as shown in Figure 2.1b.

Thermal stress during heatwaves in oceanic waters disrupts the relationship between corals and their algal symbionts (*Symbiodinium spp.*), and this makes the corals lose their colour which is called
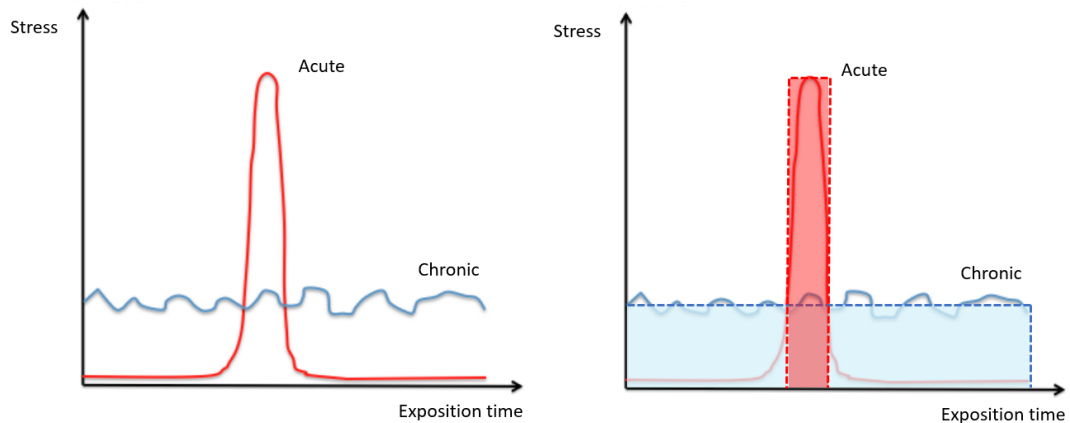
(a) Chronic and Acute exposures to stress (Galante et al., 2014)

(b) Integrated chronic and acute stresses

bleaching (Hughes et al., 2017). Bleached coral have reduced energy input from their symbionts and often lead to high levels of coral mortality. Increasingly, individual reefs are experiencing multiple bleaching attacks, as well as the effects of more chronic local stressors such as pollution and overfishing. Corals can recover from bleaching in case of a sustained absence of thermal stress (Gilmour et al., 2013). Therefore, when stress decreases, corals can restore their symbiotic relationship with algae symbionts and regain strength. Alternatively, when the stress is lasting until a critical value, corals die related to the chronic stress pattern. Similarly, a constant relative low chronic stress is experienced by a coral embryo when flowing through a pipeline.

2.2. Response curves

When relating stressors in a pumping system to the strength of coral embryos, frameworks can help to estimate mortality. A stress-strength relation occurs within many cases, for example, the previously described thermal stress on corals. A useful tool to analyse this interaction is a dose-response curve, which represents the resistance of the species, as a function of exposure duration and intensity (Gough et al., 2011). Figure 2.2 presents an example of a dose-response curve. The dose-response curve is interpretable as the 'strength' of the sensitive receiver. Below, two models are discussed that describe the exceeding of thresholds. First, the Energy budgets model is reviewed and secondly, the toxicological model and one of the two models is chosen to as tool to estimate mortality of embryos in pumping systems.

A Dynamic Energy Budget model (DEB) describes the the health state of an organism (Kooijman, 2010). It describes that the energy flows in the organism depend on the values of its state variables: the amounts of structure and reserve, and the level of maturity. The amount of reserve per volume of the structure is called the energy density and is a good indicator of an individual's condition because better fed individuals have a higher reserve density (Marn et al., 2019). This means that according to this model, an organism can restore energy. However, a problem arises when the model is applied to the mortality of embryos in a pumping system. The pumping time of embryos from the ocean's surface onto the vessel is in the order of minutes. The embryos are not able to restore energy within this period, and this model is therefore not applicable to pumped embryos.

Toxicology is a discipline that involves the study that describes effects after experiencing toxic stresses. A toxicological model describes how the health of organism decline when experiencing constant, often, toxic stresses. Salinity, for example, is the primary environmental factor limiting plant growth and productivity (Allakhverdiev et al., 2002). The earliest response of plants to salinity is a reduction in the rate of leaf surface expansion, followed by a reduction of expansion as the stress intensifies (Parida and Das, 2005). Such a response is also known with thermal stressors on coral, described in Section 2.1, and the response of the organism to constant stresses (pipeline) that result in mortality. The toxicological model is a more suitable model to apply on pumped coral embryos and larvae in comparison to the
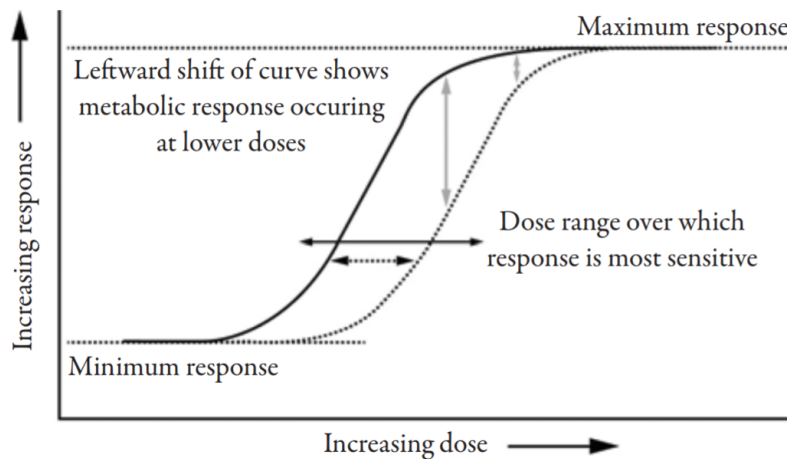
Figure 2.2: Example of a dose-response curve for insulin therapy in diabetes and cancer risk (Gough et al., 2011)

energy budgets model because it works with a maximum value that may not be exceeded and it is supposed that the organism is not able to regain strength.

2.3. Particle count

For simplification, the chosen framework in this research only considers particles that are alive or dead. Dead embryos can't apply cell division anymore and have a different visual form than live embryos. However, coral embryos can split into two equal parts (clones) after experiencing an undefined amount of shear which is called fragmentation (Heyward and Negri, 2012). After this phenomenon, the two separate embryos are still alive and can grow into mature coral. These fragments are selected as living embryos during the calculation of mortality. During the strength tests performed in this research, approximately 30 live coral embryos are selected under a microscope and exposed to stress. Via counting the dead embryos after the experiment, mortality rates are determined. The framework combines mortality rates with exerted stress, and therefore, can be used to estimate mortality rates for other experiments.

2.4. Pumping stressors on coral embryos and larvae

Various pumping systems can be selected to transport coral slick from the ocean surface towards basins on the vessel. Previous research nominates coral embryos and larvae as fragile (Bassim et al., 2003; Berry et al., 2017; Hagedorn et al., 2017). Therefore, the design of the pumping system is of great importance, and low stressors should be present. So far, pumping coral slicks has not been executed before, and its effect is unknown. A paper written by Ulanowicz, (1976) discusses the mechanical effects of water flow on fish eggs and larvae. The three main stressors addressed by the paper that could cause high mortality rates are pressure change, accelerations and shear force and are discussed below. A model has been developed to calculated the stressors and used distinguish between pumps and configurations to optimise for low mortality.

2.4.1. Shear stress and strain

A shear stress or viscous force is present when the velocity of the fluid varies from point to point in space. Also known as a fluid that moves along a solid surface and exerts a viscous drag onto that surface. In Section 4.1, the distribution of shear stress through a pipe is described. A shear within a fluid causes rotation and deformation of the organism. A significant rotational effect would disturb the internal order of the egg, while a deformation would stress both the membrane and the interior. Shear stress is commonly named as force per unit area but in the biological applications, often shear rate s^{-1} is used. The shear rate for Newtonian fluid, such as water, is directly proportional to the shear stress.

"Strain" is a word widely used in biology and geology. In everyday language, strain signifies tightness

and tension, or effort expended against unyielding resistance (Alden, 2019). This is easy to confuse with stress, and indeed, the dictionary definitions of the two words overlap. Physicists and geologists try to use the two terms more carefully. Stress is a force that affects an object, and strain is how the object responds to it. Strain comes in two varieties. Elastic strain is the strain after something stretches that bounces back when the stress is reduced. Elastic strain is easy to appreciate in rubber or metal springs. Objects that undergo elastic strain are not harmed by it, and plastic strain is permanent deformation and organisms do not recover from it.

2.4.2. Pressure fluctuations

The pressure is a force per area and always acts inward normal to any surface and is normal stress. High-pressure changes occur when fluids are pumped over a certain height, are accelerated to a certain speed (in the pump) and near widenings and constrictions. The most destructive pressure is cavitation because vapour bubbles implode at locations where the flowing liquid falls below its vapour pressure. This happens around low-pressure regions where the fluid is accelerated to high velocities. However, because in this pilot research, the embryos and larvae are assumed fragile, the cavitation limit may never be reached. Furthermore, low pressures in the pumping system can cause embryos to expand, which can lead to damage. Therefore, in this research, atmospheric pressure is chosen as minimal pressure. Because the embryos develop on the water surface into larvae, it is known that the embryos can resist this pressure.

2.4.3. Flow accelerations

Acceleration is the time rate of change of velocity and is always accompanied by a force according to Newton's second law of motion. Within a pumping system, multiple ranges of acceleration have been identified. The lower range takes place around the intake and outflow of the system, and the forces usually range from very slight to the order of magnitude of gravitational force. In all likelihood, they are not very damaging. In the intermediate range, accelerations are associated with turbulence around eddies. The particle experiences fast changes in velocity in multiple directions. Such accelerations give forces several times that of gravity and could be damaging. The most destructive stage is accompanied by high magnitude impulse forces, which are due to the impact of particles with solid surfaces. Such forces are usually many times the acceleration of gravity and would probably be fatal.

3

Strength of coral embryos and larvae

When estimating pumping related mortality, the strength of the pumped particle must be known. To the authors knowledge, no validated strength values of coral eggs, embryos and larvae have been developed prior to this study. Therefore, research have been performed on their strength and presented in this chapter.

In Section 3.1 is described how coral strength may vary through the coral life cycle. In the appendix, an introduction of the Great Barrier Reef located in Queensland, Australia is given in Section A.2.1. Section 3.2 describes how the strength of live particles is investigated, and Section 3.3 presents the results of these tests. Furthermore, Section 3.4 presents a framework that relate the strength test results to three randomly chosen pumping systems. Finally, in Section 3.6 conclusions regarding the strength of coral embryos are given.

3.1. Introduction on coral strength

3.1.1. Coral life cycle

The coral considered in this research originates from large spawning events by *Acropora* species that generally occur once a year. The reproductive cycle (Figure 3.1) begins with gametes produced by adult colonies on the reef, followed by a complex sequence of phases which are spatially and temporally separated. Spawning is the release of these gametes from mature coral colonies, positively buoyant membrane-less, egg and sperm bundles, which dissociate at the surface and in the upper water column releasing the eggs and sperm (Babcock et al., 1986). Fertilisation occurs at the surface and in the upper water column, and the initial stages of embryos are formed. Cleavage takes place by progressive formation, and the embryos of most *Acropora* species undergo a relatively unordered, irregular division cycle after the 8-cell stage eventually and after the so-called morula stage comes the prawn-chip stage (Harrison and Wallace, 1990). The embryos then flatten to become a roughly spherical shape, and by 36 h they develop their mobility skill as larvae. The larvae then become progressively elongated and begin searching substrata and eventually settle and undergo metamorphosis into coral polyps (Babcock and Heyward, 1985).

3.1.2. Current knowledge of the strength of coral embryos

To estimate the mortality rate of coral embryos and larvae due to pumping, their critical strength parameters should be known. Coral embryos are not protected by a shell or envelope and thereby are susceptible to stressors (Heyward and Negri, 2012). It has been suggested that abnormal development of embryos may lead to a reduction of viable larvae (Bassim et al., 2003). In a study by Berry et al., (2017) the tolerance of embryos and larvae encountering sediment particles is discussed. They present that larvae are considerably more tolerant than embryos regarding these sediment particles, possibly due to their mobility and the action of their cilia, which would help protect them from close contact with particles. This age-related trend of increasing tolerance may continue into adulthood.

11
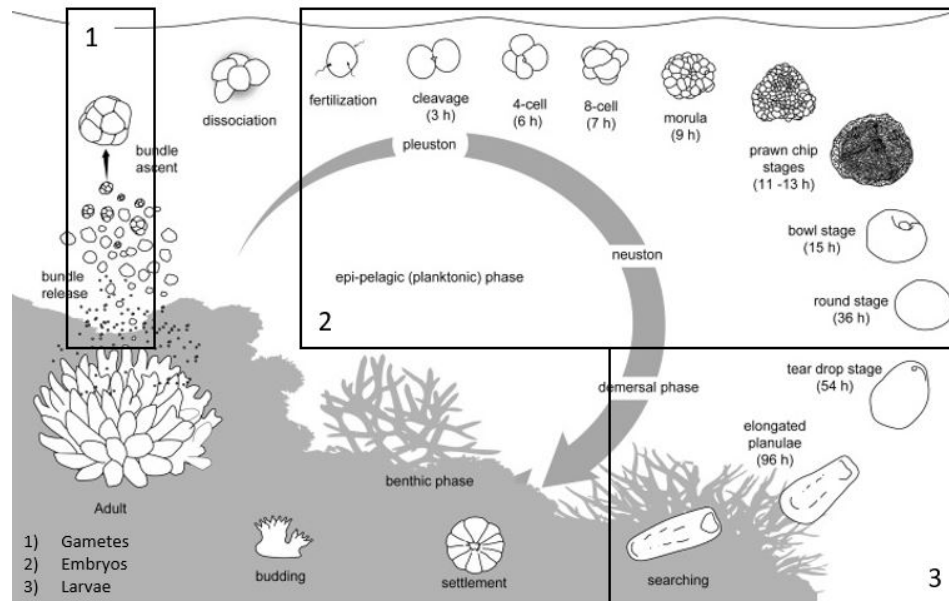
Figure 3.1: A stylised depiction of the reproductive cycle of the broadcast spawning *Acropora* species with indicative timings (adapted from (Jones et al., 2015))

For the different life stages present in coral slicks - eggs, embryos and larvae - the thresholds can be approached by applying different stress levels to the organisms. For example, Heyward and Negri, (2012) executed a study to understand the effect of turbulence onto the embryo stage. By exerting an undefined amount of shear stress onto coral embryos, they found that an embryo can clone into two smaller living fractions. The clones were able to survive after splitting but were more vulnerable to stressors.

3.1.3. Strength development over time
During spawning, gametes are released containing unfertilised eggs and sperm. The eggs are fertilised at the ocean's surface, after which the process of cell division starts as described in the coral cycle in Section 3.1.1. The pumping of slick occurs in this stage, and it is therefore desired to determine the ideal time frame to pump the fragile organisms with the highest chance of survival. Based upon literature it is assumed that particles become stronger over time (Bassim et al., 2003; Berry et al., 2017). Survival rates were assumed to be lower when organisms are weaker and the strength development of the embryos following spawning was investigated. Because this relationship has not been tested empirically for coral embryos and larvae, it is investigated in this research.

To form hypotheses on the strength development of coral embryos, literature on the strength of fish eggs was reviewed. In a paper written by Suga, (1963), a test was executed to investigate the strength of fish eggs in a specific time frame of the fertilisation process. By measuring the indentation of fish eggs after applying a force to them, the toughness of the eggs was related to time. Tests were conducted for eleven days and it was found that after the sixth day of fertilisation, the fish eggs lose their strength gradually with an almost linear decay until the 9th day (see Figure 3.2). Fish eggs, however, are protected by a thick membrane from harmful environments and the study didn't test the inside strength of fish eggs after development. Because coral eggs develops without an external membrane, the properties are different and not directly comparable. However, because there is a noticeable change in strength (regarding fish eggs), the hypothesis was formed that this relationship may also be present for coral embryos and larvae.

The relationship derived by Suga is an excellent example of a functional relationship required for the coral embryo and larvae strength following spawning. The aim of such a relationship is to understand the ideal time frame to pump coral spawn. Because the embryos develop into mobile larvae after around 36h and become negatively buoyant, they start to disperse as shown in Figure 3.1. Therefore,
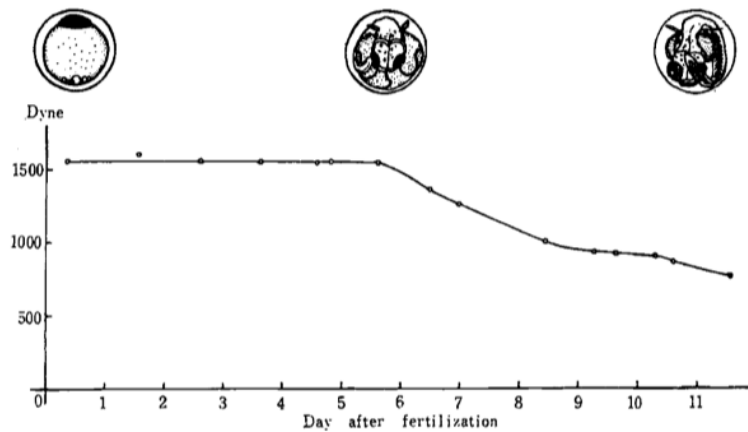
Figure 3.2: Change of the toughness of fish eggs in the days following fertilisation (Suga, 1963).

larvae won't be found in high concentrations on the water surface, and pumping needs to be conducted before this phase. Furthermore, the strength tests are executed between 2 hours and approximately 45 hours following spawning to define the strength development of coral embryos for the possible collection period.

3.1.4. Pressure thresholds of coral embryos

In any pumping system, the role of the pump is to provide sufficient pressure to overcome the operating pressure of the system and move fluid at a required flow rate. Therefore, when pumping live particles (embryos and larvae), they experience changes in pressure in the different parts of the pumping system. Typically, in front of the pump, the pressure is low. The low pressure can cause expansion of the embryos, which can result in critical damage. In the published literature, tests of this phenomena have not yet been described and therefore assumptions have been made. As described in Section 3.1.1, coral embryos naturally develop at the sea surface, and therefore it is known that they can resist atmospheric pressure. Therefore, this value has been used as a minimum pressure for engineering the pumping system, which was a conservative assumption.

The highest pressure in the system is regularly found just after the pump. Because it was unknown what maximum pressure coral embryos and larvae can handle, assumptions have been made for this type of pressure. Because, for example, *Acropora spathulata* grows at depths of up to 10 metres, it is known that the gametes released by the corals can resist the pressure at that depth (approx. 20 kPa). This local pressure has been set as an upper limit within the design criteria for the pumping system to pump embryos and larvae.

3.2. Methodology for determining coral strength

To simulate results of pumping particles through pumps, exerted stressors have been compared with the threshold values of the particles. To find these threshold values for the strength of coral embryos, a Couette-rheometer has been used. This device rotates and exerts the desired shear rate onto particles, after which strength is quantifiable. The particles were rotated in a flow between two cylinders with a set velocity. The resistance of the inner cylinder has been measured and was related to the force executed on the particles.

3.2.1. Taylor-Couette cell

Michels et al., (2010) experimented on microalgae *Chaetoceros muelleri* and applied different shear rates with a Couette-Cell to evaluate the strength of the particles. The shear rate applied in the cylinders is proportional to the rotational speed, and therefore shear sensitivity of the organisms was

measured. The shear rate is given as:

$$\dot{\gamma} = \frac{2 \cdot R_o \cdot R_i \cdot \omega}{R_o^2 - R_i^2} \tag{3.1}$$

Where $\dot{\gamma}$ is the shear rate (s^{-1}), ω the angular velocity of the outer cylinder, R_o is the outer cylinder inner radius (m) and R_i is the inner cylinder outside radius (m) with:

$$\omega = \frac{2 \cdot \pi \cdot n}{60} \tag{3.2}$$

where n is the rotation speed (rps) of the shear cylinder. To link the shear rate to the shear stress, they used the function where the shear stress τ (Pa) divided by the shear rate $\dot{\gamma}$ (s^{-1})is equal to the apparent viscosity η ($pa \cdot s$):

$$\eta = \frac{\tau}{\dot{\gamma}} \tag{3.3}$$

For Newtonian fluids, η is independent of $\dot{\gamma}$ and for non-Newtonian fluids, η depends on $\dot{\gamma}$. The value for the viscosity of seawater is usually close to 1 mPas at 20°C and is a Newtonian fluid. To test the strength of coral embryos and larvae, it was assumed that the same test setup was applicable.

3.2.2. Test setup

The setup used to investigate the critical values of the coral spawn in the period after spawning is presented in Figure 3.3. The white cylinder of the Couette-rheometer fits into the black container that contained fertilised coral eggs to fully developed larvae. Before rotating, approximately 30 living embryos were selected under a microscope for testing in the Couette-rheometer. The cylinder (R = 0.07m) rotates inside the container (R = 0.1m) with a certain speed and therefore a specific shear rate. By multiplying shear rate with duration, the exerted strain has been calculated. After testing, the living embryos were counted, and survival rates calculated. Because the Couette-rheometer rotates with Reynolds numbers between 1500 - 60000 [-] (shear rates ($\frac{du}{dr}$) between 5 and 200 [1/s] with a change in radius of 3mm), the regime was more or less turbulent (when assuming a constant viscosity).

Figure 3.3: Setup of the Couette-rheometer (type: HAAKE VT550) to investigate the strength threshold of coral embryos and larvae.

3.2.3. Test procedure

To investigate the critical values of the coral embryos after spawning, an exact procedure was developed to create usable outcomes:

- Select coral embryos under the microscope for each replicate ($\approx$ 30)
- Insert the embryos into the basin of the Couette-rheometer
- Lower the spinning device into the basin

- Set duration and shear rate

- Run the test

- Remove the coral embryos from the basin into a petri dish

- Count the damaged and undamaged particles under the microscope

3.2.4. Link between Couette test and pumping system

To investigate the strength of coral particles, different shear rates were applied to coral eggs, embryos and larvae with the Couette-rheometer. Because seawater is a very simple Newtonian fluid (viscosity is constant for a constant temperature) with a viscosity close to 1 mPa·s at 20 °, high velocities in the Couette-rheometer were required to reach the shear forces coupled to a pumping system. The setup available at Heron Island Research Station could increase the shear rate up to 200 s^{-1} (shear stress $\approx$ 1Pa) and the duration of the experiments set as desired. For interpretation of the results, strain has been used which couples the duration of the experiment with the shear rate (strain = shear rate * duration) and is dimensionless. Section 4.1.5 describes how strain in pipes of a pumping system can be calculated and how this links to the Couette test.

3.2.5. Discussion of current theory

- The strength of coral eggs, embryos and larvae is unknown from the literature.

- The Taylor-Couette cell is an appropriate instrument to test the strength of coral embryos and larvae.

- The strength of fish eggs declines over time Suga, (1963), and this behaviour should also be known for the life stages of coral spawn.

3.3. Results of coral strength

Tests on fertilised eggs were completed between 2 hours to 12.5 hours following spawning, and on swimming larvae from 43-45 hours following spawning. Within the first period, the eggs (1 cell) were fertilised by sperm cells of other colonies. After 3 hours, cell division was observed, and after 8 hours, the organisms consisted of approximately 60 cells. During this period, tests were executed at varying shear rates from 5 to 200 [1/s], and durations from 5 to 300 seconds.

The strain applied (log scale) on the particles is plotted against time following spawning in hours and shown in Figure 3.4. It is shown that there is a clear trend in the data. Particle survival over developmental time increased independent of increasing strain. Even with higher strain values, the survival of the particles increased (orange vs blue dots). Two hours following spawning, half of the embryos survived strain values of 50. After 7 hours, almost 100% of the embryos survived strain values of 60,000 which is a significant increase (300x) in strain with twice the survival. This indicates that for the given coral species (*Acropora spathulata*) and the strain values applied by the Couette-rheometer, an apparent increase in strength in the early developmental period is found.

When investigating the survival rates of the embryos and larvae against time following spawning, the same trend is found and presented in Figure 3.5. The two Figures 3.4 and 3.5 provide insight into the most important factor of embryo survival in the used Couette-rheometer: time following spawning. Analysis indicates that the most significant effect of shear rate was the developmental stage it was applied (p < 0.001). Proportional survival increased from $\approx$50% at 2-4 hours following spawning, to >95% from 7-44 hours following spawning (Figure 3.5). There was an additive effect of shear rate duration on survival (p = 0.003), with increased duration decreasing survival. Surprisingly, shear rate up to 200 [1/s] did not affect survival (p = 0.865). In the figure, a second order polynomial curve is fitted, which describes the relationship between the survival rate after a certain amount of strain in the period following spawning (R^2 = 0.6). The uncertainty of the estimation regarding the trend-line is represented with the grey band. More data points are required to decrease the uncertainty.
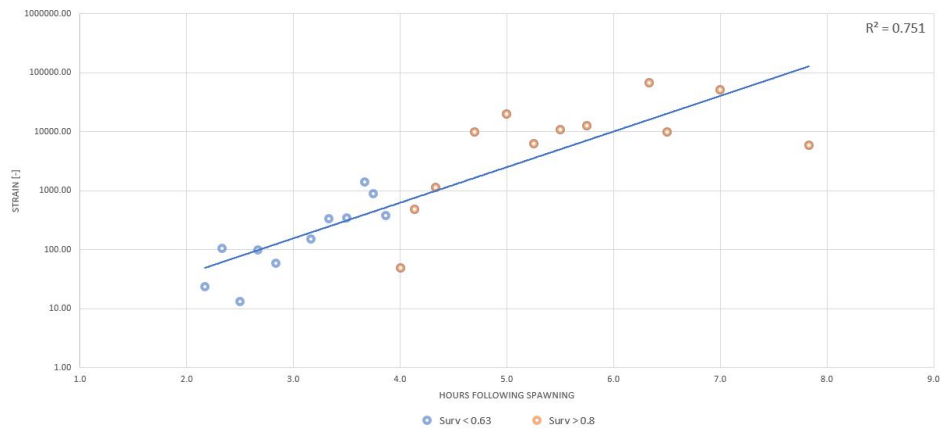
Figure 3.4: Effect of strain on the survival of *Acropora spathulata* embryos throughout early development
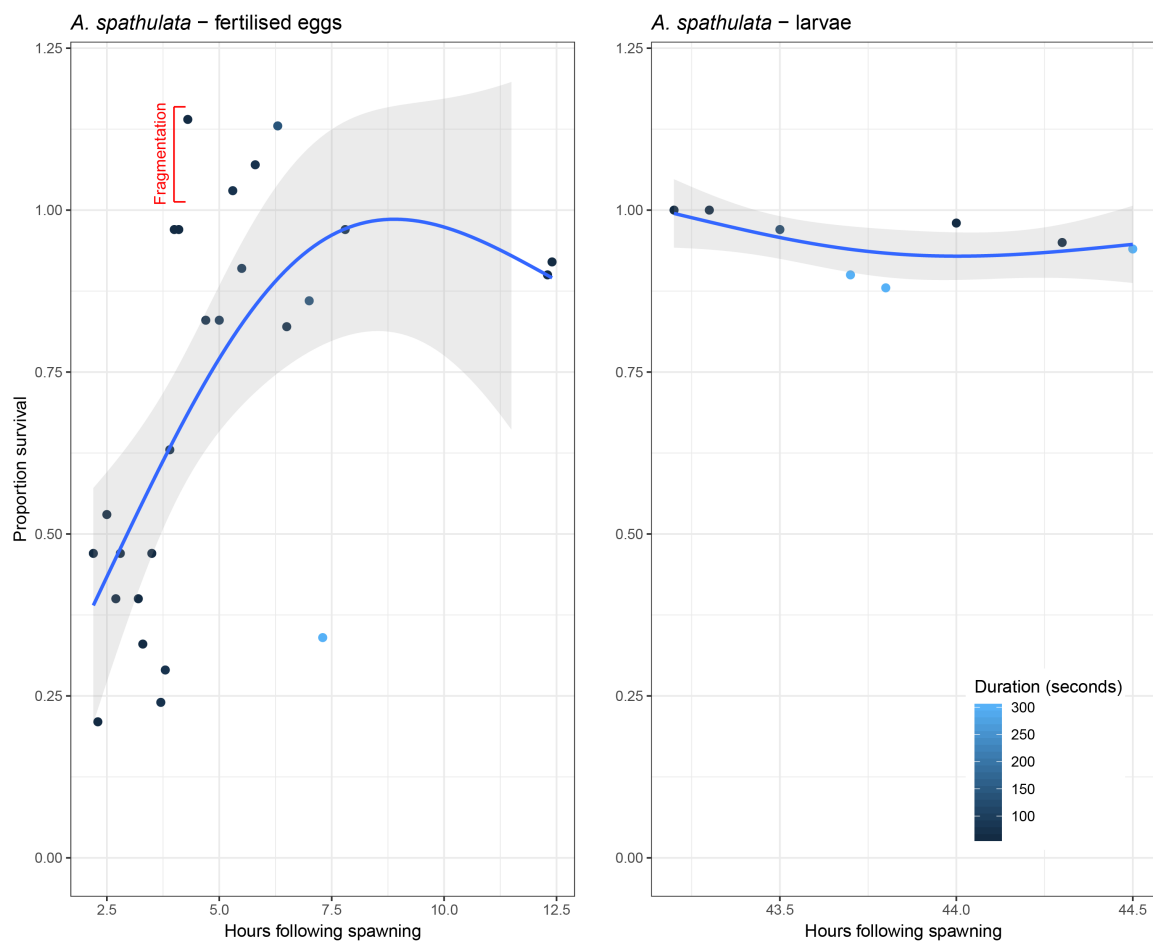
Figure 3.5: The effect of spinning duration on proportional survival over developmental time of *Acropora spathulata* embryos and larvae throughout early development.

3.4. Framework for presenting strength

After plotting strain values applied on coral embryos during 30 tests in the Couette-rheometer on a log-log scale with the shear rate on the y-axis and duration on the x-axis, Figure 3.6 is obtained. The red lines indicate survivability rates < 0.63 and the green lines > 0.8. The particles become stronger over time as shown in Figure 3.4 and Figure 3.5. If the occurring strain in the pumping system is

known, Figure 3.6 can be used to link this value to the threshold values of coral particles. Note that time following spawning is indicated with arrows at the x-axis. If strain in the pipes, for example, is 60,000[-], and pumping begins after 3 hours, there is a high probability that coral embryos will not survive. However, if pumping starts after 7 hours with 60,000 strain in the pipes, the probability of survival is high.
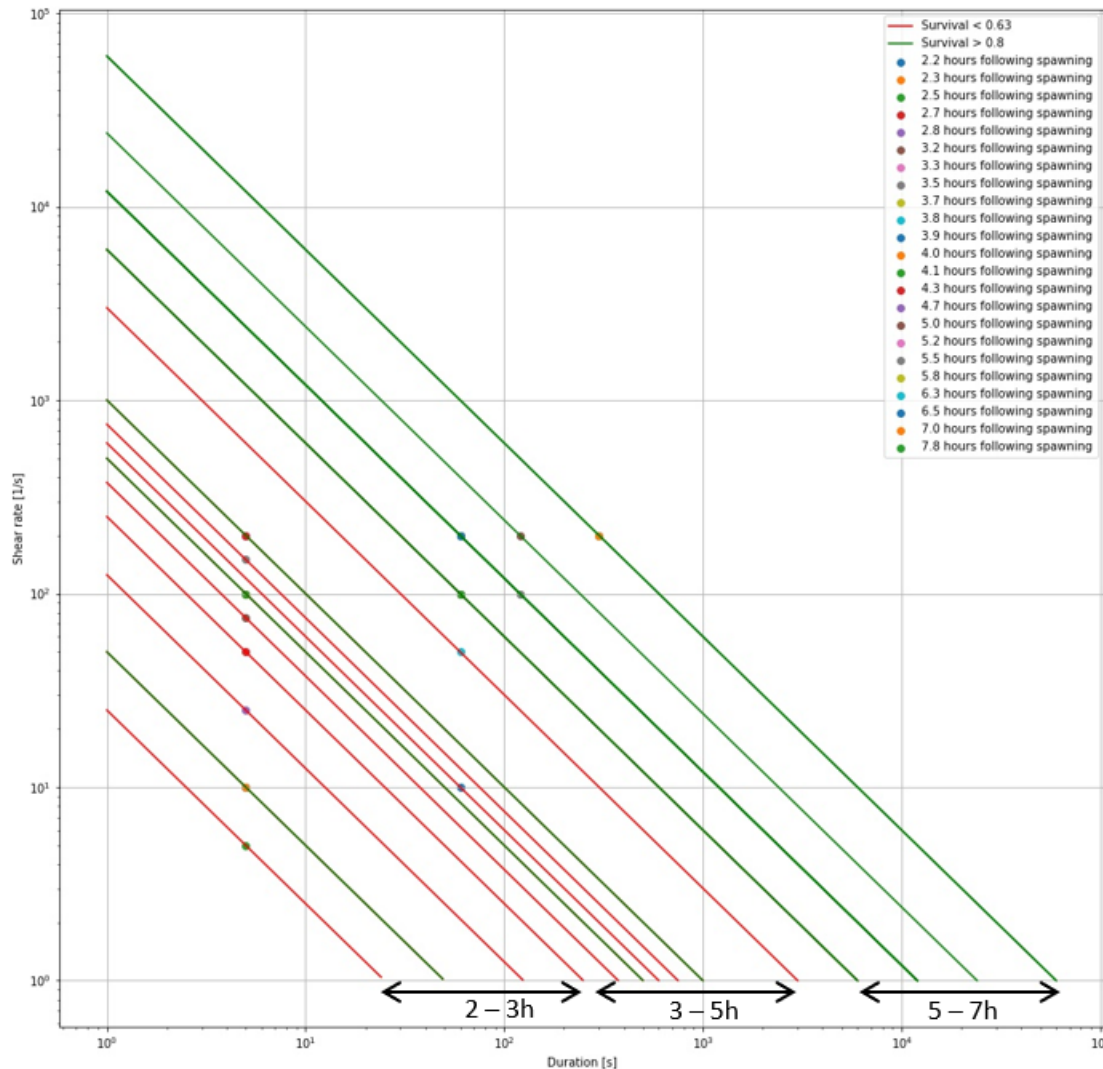
Figure 3.6: Framework that couples strain (shear rate * duration) occurring in the pipes to the threshold strain values of *Acropora spathulata* embryos.

To demonstrate how the plot should be interpreted, three examples are plotted in Figure 3.7. The specific time following spawning is seven hours. Therefore, the last line is plotted from Figure 3.6. The three dots in the plot present three different random pumping systems, all with a unique duration and shear rate. By comparing the dots with the threshold line for that particular time following spawning, an assumption can be made about particle survival. For green dots, strain occurring in the pumping system is lower than the threshold value found with the Couette-rheometer. For the red dots, strain in the system is higher which implies that the user assumes a higher probability of failure of embryos in system 3.

3.5. Discussion for coral strength

In this research, the first known strength estimates of coral embryos and larvae have been executed and show that there is an increase in strength over developmental time. After seven hours, coral
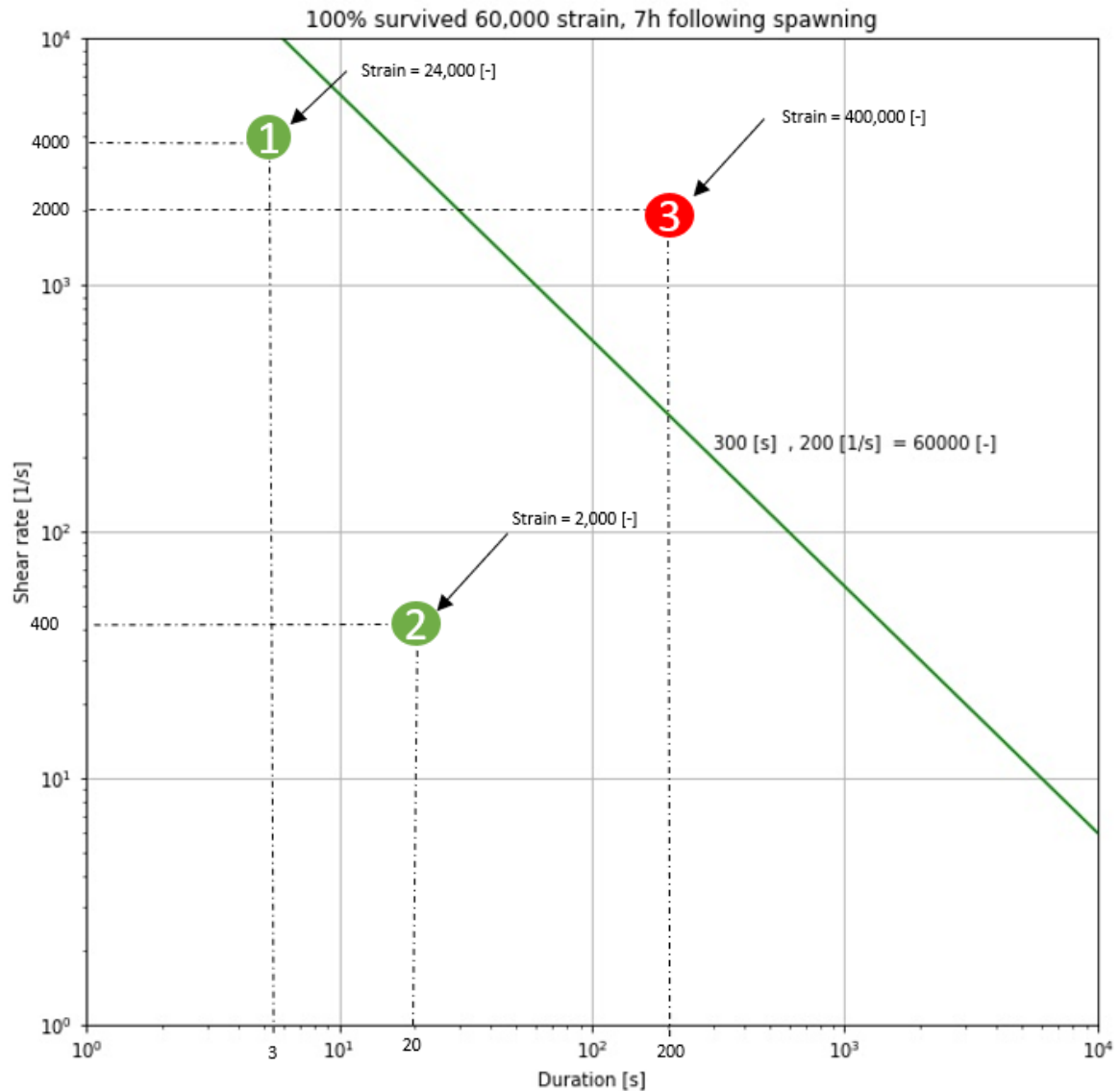
Figure 3.7: Framework that couples the threshold value of seven hours following spawning to three different (arbitrary chosen) pumping systems.

embryos can resist strain values of 60,000[-] but to know the exact strength more research is required.

Before the tests were executed, a change in strength during early development was expected because this has also been documented with fish eggs George et al., (2017) and current literature assumes that coral embryos become stronger over time (Bassim et al., 2003; Berry et al., 2017). For fish eggs, a decay occurs because the external membrane of fish eggs reduce in hardness while the fish embryo must break out of it (Suga, 1963). For coral embryos, this thick membrane is not present, and the embryo is without a protective membrane on the water surface. During the Couette tests the embryos were consisting of four cells after 4h, 16 after 5h and 60 after 7h following spawning. The rapid increase of cell division means that many small cells are occupying the same amount of entire space, rather than just 4 cells. Therefore, the robustness of the embryos probably increases because many tiny things put together are stronger than a single thing of the same size (Galli and Morgan, 2016).

In total, 30 data points are presented in Figure 3.5 of which each test was performed once because the embryos continually develop over time. Ideally, temporal replicates of the tests could be conducted to decrease the variance. To reduce the variability around the predicted functional relationship, the same

experiment should be repeated with a minimum of three Couette-rheometer setups that conduct the same tests at the same development time points after spawning. To investigate the upper limit strength of coral embryos and larvae, higher strains must be applied in the period after spawning. The survival rate became around 100 %, which indicates that they are strong enough to survive pumping. Higher strains can be reached by increasing the viscosity of the medium, increasing the spinning duration or increasing shear rate (Michels et al., 2010). Furthermore, these tests were only executed on *Acropora spathulata* and therefore, the relationship may differ for other species of coral.

During the experiments, coral embryos fragmented in smaller, cloned fractions. When the clones didn't show extensive form loss, they were counted as live embryos. Therefore, survivability can be more than 100%. Fragmentation manly occurred for higher strain values and from the cell division stage where the embryo consisted of 16 cells or more. Further research is required to investigate if fragmentation is more likely to happen and succeed with increasing number of cells.

3.6. Conclusions for coral strength

The hypothesis that a noticeable change in strength may be present during the development stage of coral embryos, is sharpened into: The strength of coral embryos increases over developmental time. The experiment showed that in the first 5 hours, coral embryos are very fragile. After 5-7 hours, coral embryos become stronger and can resist strain values up to 60,000[-] (survival ≈100%). In this stage, coral embryos are still floating on the ocean's surface and therefore easier to collect than after dispersion. The data suggests that pumping should start 7 hours following spawning.

Strain occurring in the Couette-rheometer test is related to strain present in the pumping system, as shown in Figure 3.7. Therefore, the first part of SQ1 can be answered, and it is possible to define a framework where the survivability of embryos is related to the strength of the particles, for now in a generic way. In Chapter 4, the specific strain in the pipeline of a pumping system is added to the framework to conclude which pumping system exceeds the maximal strain for *Acropora spathulata* embryos to stay intact.

4

Stressors in a combined pumping system

From the introduction it became clear that the interaction between a pumping system and coral particles is not known or described in literature and that low mortality rates during pumping are important for reef rehabilitation on an industrial scale. Research that couples the strength of coral embryos to values of occurring strain in pumping systems is presented in Chapter 3. Until now, response strain values were chosen at random. Defining the stressors in system is essential for estimating mortality. Therefore, in this chapter, stressors in a pumping system are calculated and used to design a coral slick pumping system. A mathematical model is built that calculates the shear stress, strain and pressure fluctuations through the pumping system. Threshold values are inserted in the model which may not be exceeded. These values are the minimum pressure, maximum pressure and maximum stress levels. After analysing the outcome of the model, a design is given for a coral slick collection pumping system.

In Section 4.1 background theory is presented to model stressors in a pipeline and in Section 4.2 the modelling of a pump is discussed. Results of the model are depicted in Section 4.3 and used to define a pumping system for the field test in Australia, elaborated in Section 4.4. Finally, a discussion of the stressors in a pumping system are presented in Section 4.5.

4.1. Stressors in the pipeline

To estimate stressors in the system, theoretical knowledge of the interaction between a fluid, pump and pipeline have been used. Below, these theoretical effects are described and used in the model to estimate mortality.

4.1.1. Flow characteristics

The Bernoulli equation quantifies the mechanical energy available in a flow through a pipeline. Supposing that the flow is frictionless, incompressible and steady, Equation 4.1 is constant (Matoušek, 2004).

$$h + \frac{p}{\rho_f \cdot g} + \frac{Q^2}{A^2 \cdot 2 \cdot g} = const. \tag{4.1}$$

Here, h is the position of location elevation above the reference level, p is the pressure at a location on a stream line, Q the discharge, A the surface area of the pipe, ρ_f the density of the fluid and g the gravitational acceleration.

The first term in Equation 4.1 is the potential energy of a control volume per unit gravity force, the second term is the potential energy of the specific volume and the third term the kinetic energy it contains. An important property of the equation is that for two volumes along the same streamline, the sum of the three energies is constant but the magnitudes of individual terms can vary spatially (Matoušek, 2004). The different forms of head in the Bernoulli equation and the difference between

the terms is shown in Figure 4.1. The Bernoulli equation is transformed and used for many aspects in this research.
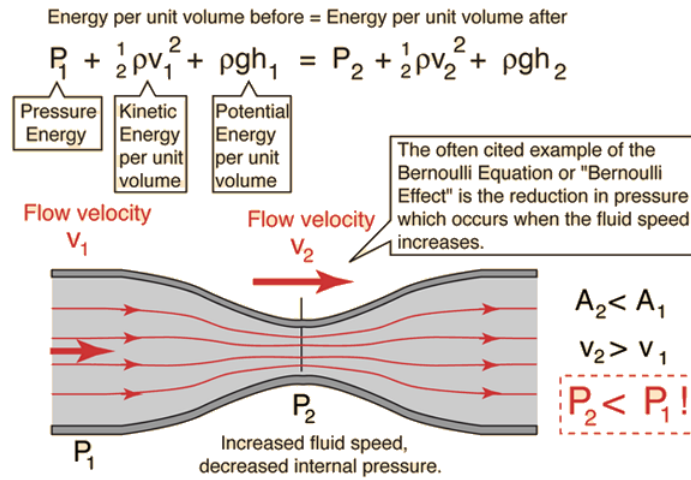
Figure 4.1: Term description of the Bernoulli equation (Matoušek, 2004)

In Figure 4.1 is presented that the flow velocity increases when the flow area reduces. With this, a portion of potential energy is transformed into kinetic energy causing for a drop in pressure along that stream line. For fragile particles, these interactions are of importance.

In Equation 4.1 the media through a pipe is considered frictionless. In reality, it dissipates a portion of mechanical energy is dissipated due to turbulent friction so it has been incorporated in the equation as $H_{totalloss}$. Including this gives:

$$h_1 + \frac{P_1}{\rho_f \cdot g} + \frac{Q_1^2}{A_1^2 \cdot 2 \cdot g} = h_2 + \frac{P_2}{\rho_f \cdot g} + \frac{Q_2^2}{A_2^2 \cdot 2 \cdot g} + H_{totalloss} \tag{4.2}$$

From this equation, the variation in potential, flow and kinetic energy can be described on different locations. In the model, the equation is used to design pump- and system curves and to derive the discharge of the flow. How particles are influenced by pressure changes is so far unknown, but a conservative assumption is made that fluctuations must be minimised.

Energy losses in the pipes have been calculated by integrating the power $P = \rho_f \cdot g \cdot \Delta H \cdot Q$ required to overcome the head losses for a certain section over time as presented in Equation 4.3 with the derivation in appendix B.3.2.

$$E_{losspipe} = \int_a^b P \, dt = \rho \cdot g \cdot \lambda \cdot \frac{L^2}{D^3} \cdot \frac{Q^2}{\frac{1}{2} \cdot \pi \cdot g} \tag{4.3}$$

Another form of energy dissipation is turbulence. Between 1883 and 1892, Osborne Reynolds performed experiments with water flow inside pipes and showed the laminar flow with parabolic velocity profile doesn't persist for higher flow rates (Q. Schiermeier (MIT), 2005). During the experiments, the flow is constantly subjected to small disturbances like the inflow and the roughness of the wall. The disturbances destabilise the flow at a certain flow rate. The fluid viscosity dampens this destabilisation until a certain flow rate where the damping is not strong enough. Turbulent motions appear for Reynolds number approx. > 1000. After Re > 5000, the flow is fully turbulent. Turbulent eddies create fluctuations in velocity which is undesirable as described in 3.2.

Near the wall of a pipe, the flow has a distinct structure called a boundary layer. The velocity of the flow near this layer goes to zero that is called the no-slip condition (the flow matches the boundary velocity). The height of the boundary layer, often noted as δ, describes the distance from the wall where the

flow goes from laminar into turbulent and depends on the flow velocity, viscosity and roughness of the wall and have been calculated with Equation 4.4:

$$\delta = \frac{11.6 \cdot \nu}{u_*} \tag{4.4}$$

Where $u_* = \sqrt{gRi_w}$ and $i_w = \frac{\lambda_f U^2}{8gR}$ (Matoušek, 2004).
Where i_w = the gradient and R the hydraulic radius and λ_f is the flow friction coefficient (calculation of this coefficient can be found in the Appendix, Equation B.15).

Shear stresses develop when a liquid flows through a pipeline. Shear stress is a result of turbulence, and its magnitude is dependent upon the properties of the fluid, the velocity at which it is moving, the internal roughness of the pipe, the length and diameter of pipe. The wall shear stress is correlated with the flow conditions to solve the pressure drop due to friction in pipeline flow. Equation 4.5 describes the shear stress distribution in a cross section of a pipe, both valid for laminar and turbulent flow in which f_f is the Fanning friction factor and U_f the flow velocity.

$$f_f = \frac{\tau_o}{\frac{1}{2}\rho_f U_f^2} \tag{4.5}$$

In a pipe, the shear stress is maximum at the wall and decreases towards the centre of the flow. The shear stress varies with the Reynolds number. Head losses in pipes have been transformed to shear stresses [N/m2] as described in Equation 4.6. The maximum value for shear stress at the wall is not time dependent (like strain). An important conclusion from Equation 4.6 is that an increase in shear stress is related to higher head losses and is negative for coral embryo and survival following pumping.

$$\tau_{wall} = \frac{\rho_f \cdot g \cdot Q \cdot \Delta H_{section}}{U \cdot L \cdot \pi \cdot 2 \cdot r} = \frac{\rho_f \cdot g \cdot \Delta H_{section} \cdot D_{pipe}}{2 \cdot L_{pipe}} \tag{4.6}$$

During transport of fragile particles like coral embryos, the amount of turbulence induced shear stresses should be minimal. Therefore, particle transport through the centre of the flow domain is desired. In Section B.1 is described that floating particles can be directed to the centre of the flow domain by increasing the flow velocity. However, there is a general rule of thumb that the turbulence level increases with the free stream velocity and the laminar sub-layer decreases (Q. Schiermeier (MIT), 2005).

4.1.2. Behaviour of coral embryos in the pipeline

When the force balance (explained in Section B.1), on a coral gamete is made, the resulting force is pointing upwards because the gamete is positively buoyant (Figure 4.2) and travels upwards with 0.00493m/s (Doropoulos et al. unpublished). After splitting into embryos at the oceans surface, bundles become individual cells. Here it is assumed that these cells have the same buoyancy as the bundles. With the exact density of the cells, an approximation of the position in the pipes has been performed. When the density is close to that of water, coral embryos simply follow the streamlines of the water particles (Winer et al., 2014). In current literature, no densities of coral embryos are found. Therefore, fish embryos are investigated to make an assumption. A paper written by (Sundby and Kristiansen, 2015), states that the oil inside of a fish egg has a specific density of 0.926. Assuming that coral embryos contain the same oil, the density is approximate 950kg/m^3.

In the period following spawning, coral embryos disperse through the water column. In the pumping stage (first day following spawning), they are buoyant. However, it is possible that the density of some embryos is equal to that of water. To stay on the safe side, a density of 950kg/m^3 is taken for all embryos. Furthermore, because coral embryos are slightly lighter than water they could tend to flow towards the inside of the bend, as showed by (Fernandes et al., 2010). However, because the density is so close to water, it is assumed that they simply follow the streamlines.
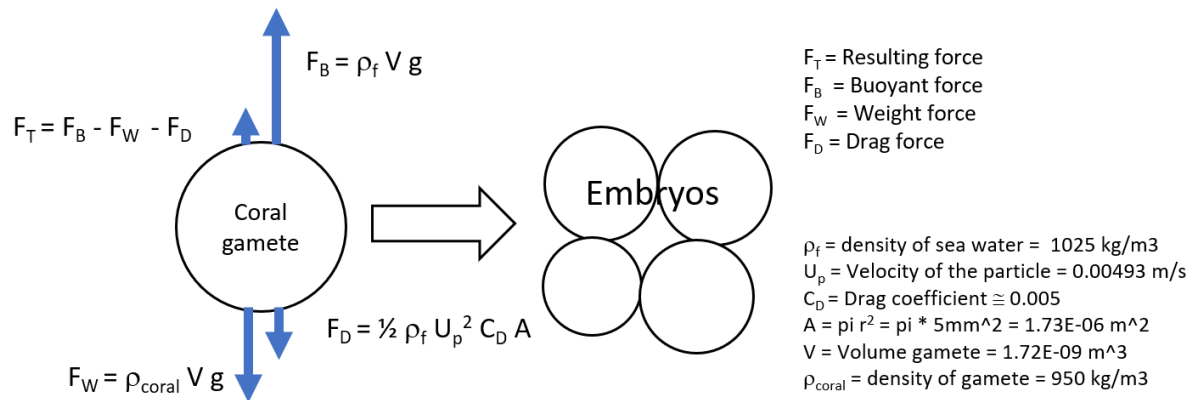
Figure 4.2: Forces working on a coral gamete

4.1.3. Major hydraulic stresses

The frictional head loss for flow of water or mixture in straight pipelines has been determined by using the Darcy-Weisbach (Equation 4.7), which gives a parabolic H-Q curve (Matoušek, 2004).

$$H_{major} = \frac{\lambda_f \cdot L}{D} \cdot \frac{Q^2}{A^2 \cdot 2 \cdot g} \cdot \frac{\rho_m}{\rho_w} \tag{4.7}$$

Here H_{major} represents the head loss due to friction of water in a straight pipe, L represents the length of the pipe and D represents the pipeline diameter. Since the relative density of coral spawn is close to one, $\rho_m/\rho_w = 1$ and can be eliminated from the equation. Furthermore, the position of coral embryos due to the buoyancy in a flow is elaborated in Section 4.1.2.

When the pipeline diameter is increased, the head loss decreases, the system curve become more gradual, and the discharge increases. This can also be seen in the equation of Darcy Weissbach, presented in Equation 4.7. The higher discharge causes for more pressure fluctuations and stresses. If the maximum occurring strain in the pipes (ϵ_{pipe}) is related to the change in diameter, shown in Equation 4.8, the strain decreases to the 1/3 power by increasing the diameter (derivation of the equation can be found in the Appendix B.3.1). When plotting the change in diameter against the strain with a variable discharge, Figure 4.3a is found with the same conclusion as from Equation 4.8. From the Couette-rheometer experiments it is concluded that lower strain values are better for coral embryo survival. Therefore, it was hypothesised that mortality rates decrease with an increase in pipeline diameter (pressure fluctuations should operate between the limits 100kPa - 200kPa).

$$\epsilon_{pipe} = \frac{\rho \cdot \lambda}{\frac{1}{2} \cdot \eta} \cdot \frac{L^2}{D^3} \cdot Q = 12084 \cdot \frac{L^2}{D^3} \cdot Q \tag{4.8}$$

From Equation 4.5, it is furthermore known that the flow velocity should be minimised to minimise the shear stresses. Equation 4.7 shows that when the head losses decrease (with constant length and pump settings) the discharge increases. Equation 4.9 present the relationship between discharge and surface area of the pipes. Figure 4.3b is found after plotting the flow velocity (green line) and the discharge (blue line) against change in diameter. When the diameter is smaller than 0.075m, shear stresses dominate the flow behaviour. Crucial to note is that when increasing the diameter (above 0.075m), the flow velocity drops and the discharge (and therefore production) increases. Furthermore, the production increases with less stress which has a positive effect on mortality rates. The limitations of Figure 4.3b are dependent of the installed pump range and maximum pipe diameter.

$$U = \frac{Q}{A} = \frac{Q}{\frac{1}{4} \cdot D^2 \cdot \pi} \tag{4.9}$$

(a) Change in diameter of the pipe plotted against strain occurring in the pipe

(b) Change in diameter of the pipe plotted against the flow velocity and discharge(NTS)
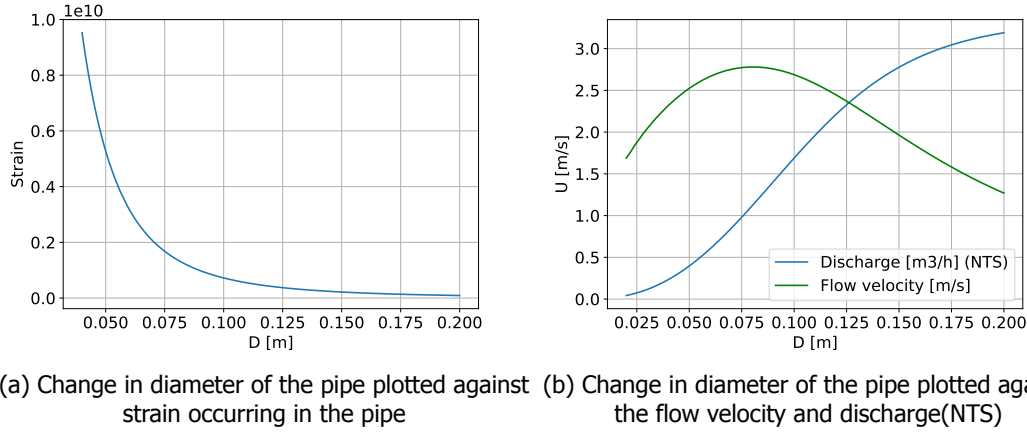
Figure 4.3

If the length of the pipeline section is increased, the head loss increases and the discharge drops (see Equation 4.7). When the flow velocity reduces, the maximum shear stress along the wall becomes smaller and the impact with hard object becomes less significant. The change in strain however, becomes higher when increasing the length of the pipes as can be seen in Equation 4.8 and Figure 4.4. Consequentially an increase in length gives lower flow velocities and therefore less damage, however if the flow velocity is considered constant (by changing pumping settings), the length of the pipes must be minimal to ensure low mortality.
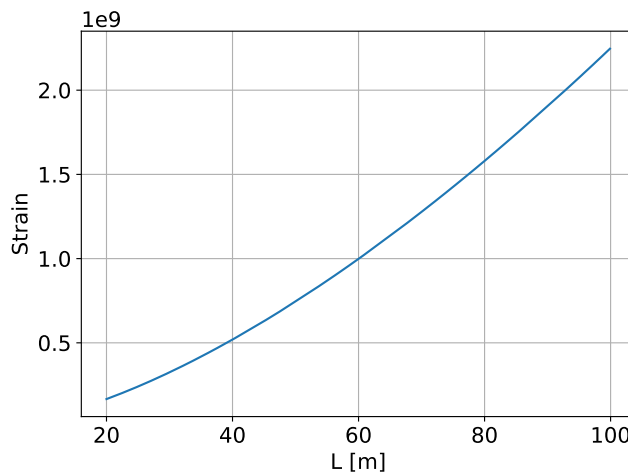
Figure 4.4: Change in length of the pipe plotted against strain occurring in the pipe

4.1.4. Minor hydraulic stresses

Equation 4.10 describes the minor loss component $\sum h_m$ and consists of multiple losses. Each term contributes to a certain value of ξ also known as the minor loss coefficient. This coefficient is multiplied with the velocity head to obtain the head loss through the inlet, outflow, bends, constrictions and widening. The ξ values for different components are presented below.

$$H_{minor} = \sum \xi \cdot \frac{U_f^2}{2 \cdot g} \tag{4.10}$$

For the inflow of the system, streamlines have to adjust which is presented in Figure B.5. The losses that occur with different shapes are described in Figure B.6 and can be calculated with Equation 4.11

where μ is the contraction coefficient.

$$\xi_{inlet} = \left(\frac{1}{\mu} - 1\right)^2 \tag{4.11}$$

The intake section of the pumping system is comparable to a large constriction in the system. The velocity of the fluid builds up to the velocity in the pipes. The more gradually the velocity builds up, the more gradual the pressure drop. A gradually intake ensures that the fluid follows the material and less energy is dissipated. Pumping from the water surface with atmospheric pressure, causes a pressure drop below this threshold because the velocity increases. A suggested solution is to pump from a depth which increases the pressure around the intake as presented in Figure 4.5. The two effects of pressure drop and the formation of eddies could be critical and must be well investigated. A more gradual intake significant below the water surface therefore has a positive effect on mortality.
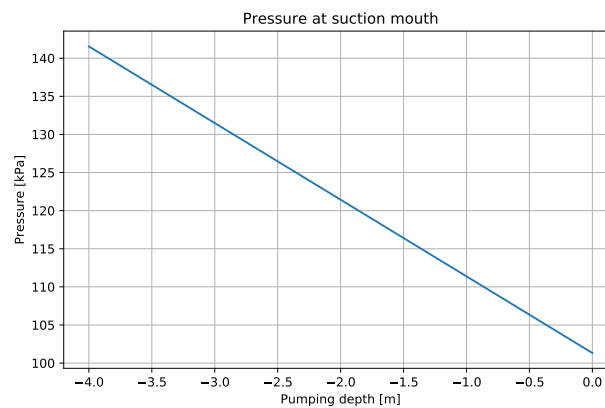
Figure 4.5: Local pressure at different suction depths

When flow encounters bends in the pipeline, streamlines have to adjust, and, energy is dissipated. The degree of dissipation increases with the angle of the bend. When streamlines cannot follow the profile of the bend, turbulent motions originate in the lee side after bends (often with a small radius) which increases the degree of dissipation and shear stress. To calculate ξ in bends Equation 4.12 can be used (Tukker et al., 2010).

$$\xi_{bends} = 0.13 + 0.16 \cdot \left(\frac{D}{r}\right)^{3.5} \tag{4.12}$$

This equation relates the diameter of the pipe and the radius of the bend to the friction coefficient. Other than equations, also some guidelines are available to decide what factor can be applied for certain bends. In Figure B.4, these factors are presented.

In the paper by Ulanowicz, the following is stated: "The most destructive stages are the high magnitude impulse forces which are created due to the impact of the particle with solid surfaces". Such forces could be many times the acceleration of gravity and would probably be fatal (Ulanowicz, 1976). This means, that when a particle doesn't follow the streamlines of water, and encounter a hard surface, they will experience high forces in bends. After calulating the strain occurring in a bend with Equation 4.13, it has been concluded that higher values for ξ, smaller diameters, higher discharges and bends with a smaller radius create more strain. Due to this knowledge the hypotheses is that bends cause higher mortality rates.

$$\epsilon_{bend} = \frac{\rho}{\frac{1}{2} \cdot \pi \cdot \eta} \cdot \xi \cdot \frac{Q \cdot L_{bend}}{D_{bend}^2} \tag{4.13}$$

When a pipeline section widens, streamlines will try to follow the material of the pipe towards the larger diameter. If this goes gradually, almost no energy is dissipated (Matoušek, 2004). However, if

the transition is abrupt, the fluid is not able to follow the surface and eddies can occur which induces stresses, and a higher value for ξ. As shown in formula 4.13, higher values for ξ increases the strain. Therefore, for the widenings in the pumping system the hypotheses is made that they must be avoided in favour of low mortality rates. To calculate the losses, Equation 4.14 and Figure B.8 can be used.

Where the fluid exits the pipe and enters a large reservoir, the velocity is reduced to zero and all of the kinetic energy is dissipated. Therefore, for all geometries, the losses are equal to one velocity head: $\xi_{outflow} = 1$. If the fluid is transported into a basin, the losses can be smaller than 1. The situation can be compared with an expansion of the pipe. Using Formula 4.14 and Figure B.7, the outflow loss coefficient have been calculated for different transitions. By decreasing the flow velocity gradually, and by using a funnel shaped outflow, the outflow loss can further be optimised.

$$\xi_u = \left(1 - \frac{A_1}{A_2}\right)^2 \tag{4.14}$$

4.1.5. Link between pipeline and Couette cell

To couple the shear rates, also known as $\frac{dU}{dr}$, in a Couette-cell to the rates occurring in a pipe of a pumping system, the derivative of Equation 4.15 can be used (Cengel and Cimbala, 2004). The derivative is presented in 4.16. When plotting the equation for a pipe section with a diameter of 0.1m Figure 4.6 is obtained. Crucial to note is that the higher shear rates occur along the pipe wall and decrease towards the centre of the flow. In Figure B.10 the linear distribution of shear stress through a pipe is presented. This linearity is not found for the distribution of shear rate towards the wall as viscosity isn't present in Equation 4.16 while that's eliminated and where $U_* = \sqrt{\frac{\lambda}{8} \cdot U}$ (Matoušek, 2004) which is the friction velocity.

$$\frac{U_{max} - U}{U_*} = 2.5 \cdot ln\left(\frac{R}{R - r}\right) \tag{4.15}$$

$$\frac{dU}{dr} = U_* \cdot 2.5 \cdot \frac{1}{R - r} \tag{4.16}$$
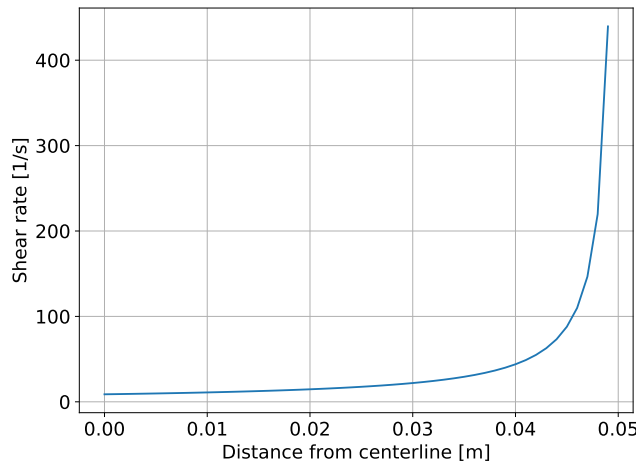
Figure 4.6: Shear rate variation from the pipe wall (D = 0.1m) to the centre of the flow

4.2. Stressors in the pump

To find the interaction between pump and coral particles, calculations have been performed to gain insight in the head losses and stresses in the pump. The pump is the driving force of the system

and the only input of energy. Therefore, it is assumed that the pump is a significant factor regarding the mortality rates of particles. A multi-criteria analyses (Figure 4.9) is created to make a division between 17 pumps. In Figure B.4, the explanation of the grading for the Hidrostal, the Centrifugal, the Diaphragm and the Archimedes screw are presented.

4.2.1. Stressors in the pump

When the hydraulic power $P_{hyd} = \rho \cdot g \cdot \Delta H_{system} \cdot Q$ and efficiency curves are known for different setups, the shaft power and the power loss of the pump can be calculated with Equation 4.17 and Equation 4.18. This loss have been transformed to the total shear stress in the pump with Equation 4.19. Since Q and $P_{loss,pump}$ both depend on many factors, it cannot be concluded that with higher discharges the shear stress in the pump becomes lower (which Equation 4.19 initiate).

$$P_{shaft} = \frac{P_{hyd}}{\eta_{pump}} \tag{4.17}$$

$$P_{loss,pump} = P_{shaft} \cdot \left(1 - \eta_{pump}\right) \tag{4.18}$$

$$\tau_{pump} = \frac{P_{loss,pump}}{Q} \tag{4.19}$$

When the rotational speed of the pump is adjustable, the user can adjust the power input and therefore the discharge and pressure head. When the discharge increases, the flow increases in the pipeline which result in higher shear stresses. Inside the pump, the stresses have been estimated by using the affinity law which relate the rotational speed to pressure head in Equation B.4. To derive an equation for the influence of the rotational speed on stresses in the pump, Equation 4.17, 4.18 and 4.19 are used which results in Figure 4.7. The efficiency is kept constant (= 0.8) because only the influence of the rotational speed on stresses in the pump is investigated. From Figure 4.7 it is concluded that the stresses in the pump increases exponential with an increase in rotational speed.
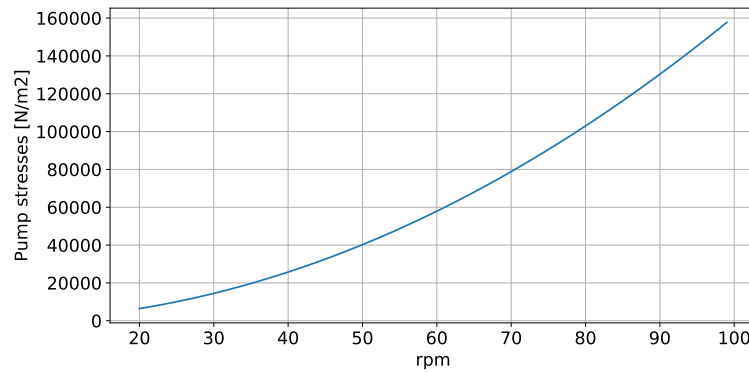
Figure 4.7: Total shear stress in the pump due to the increase of rpm with a constant pump efficiency

When the pump efficiency is 100%, zero stresses are exerted to the particles in the pump. However, the efficiency of the pump is never equal to 100 % and therefore stresses are present. Because the shaft power is multiplied by $1 - \eta$, to get the pump losses, the P_{shaft} should be minimal and η_{pump} optimal. However, if a certain system requires less power but doesn't work in its optimal point, it can still exert lower stresses onto the particles. For example, if the efficiency curves of the D100S Hidrostal pump (Figure B.3) are compared considering head losses, it can be concluded that with 584 rpm P_{hyd584} will be in the order of 0.2 kW and $P_{hyd1460}$ around 3 kW. When the efficiency point regarding P_{hyd584} is far from ideal (say $\eta = 0.5$), the energy loss is 0.1 kW. Comparing with an ideal efficiency point for the 1460 rpm setup ($\eta_{max} = 0.73$), the energy loss is equal to 1 kW. Therefore, higher efficiency's don't directly result in lower damage. Figure 4.8 shows that a lower required discharge results in a lower pump efficiency and a lower power loss and therefore lower shear stresses for the D100S Hidrostal pump. It is therefore not directly desired to optimise the pumping system regarding the best efficiency

point (BEP) which is normally done for dredging operations.
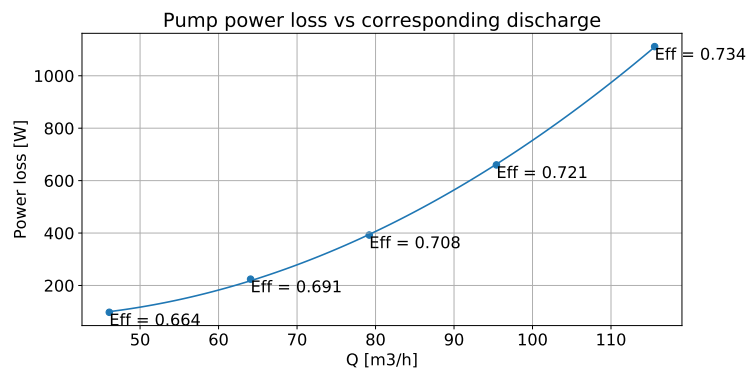
Figure 4.8: With an higher rpm, the pump will work in a more efficient point with an higher discharge but also more power loss and higher stresses.

When pumping over a certain height, energy is added to the flow by the pump. Because the local pressure will fluctuate significantly when pumping over heights, the pressure difference must be investigated. Low pressures can cause coral embryos to expand and it's unknown what their response is to expansion. To stay on the safe side, the atmospheric pressure is assumed as the threshold pressure and pressure fluctuations should be minimised. Increasing the pumping distance requires more pump power what will increase the head losses. For low mortality rates the head difference should be minimised.

4.2.2. Pump selection

To make a choice between different pumping systems they are evaluated based on theoretical and practical criteria. Existing literature and in-house knowledge of Van Oord is used to select the best pump. First, the theoretical selection criteria will be disused after which, the practical criteria are presented.

From literature, the 3 main criteria of Ulanowicz, (1976) have been selected to criticise the pumping systems. They are:

- Pressure change

- Flow accelerations

- Shear stress

Not only damage of the pumped particles can cause failure of the project. If the desired pumping system with low exerted stresses is not available in the field, the project will fail as well. Therefore, four practical selection criteria are selected to criticise the different pumps namely:

- Pump priming

- Availability of the pumping system in Australia

- Handling of the system

- The scalability of the system

These criteria are only focusing on the pump because the pump configuration is assumed to be the same for all the pumping systems.

Worst 1 - 5 Best Scenario			Criteria									Total
			Low shear forces	Turbulence	Pressure differences	Self priming	Low local flow accelerations	Hydraulic head capacity	Scalability	Availability	Handling	
		Weight →	1	1	1	1	1	1	1	3	2	
		Pump type ↓										
Archimedes	Jackscrew	Archimedes	4	5	5	5	4	4	5	1	2	39
Positive displacement pump	continu	Worm	3	3	3	5	2	5	4	1	4	36
		Gear	2	3	2	1	1	3	4	4	3	34
		Flexible vane	2	3	2	1	1	3	4	4	3	34
		Bulkhead pomp	2	3	2	1	1	3	4	4	3	34
		Nutating	3	3	3	1	3	2	3	2	3	30
		Lobe	3	4	3	1	2	1	1	3	3	30
	discontinu	Piston	2	3	2	1	1	4	2	4	4	35
		Peristaltic	2	3	3	3	3	1	1	3	3	31
		Diaphragm	3	2	2	5	2	4	2	5	4	43
Centrifugal	Radiaal	Peripheral	1	1	1	1	1	3	2	3	3	25
		Centrifugal	1	1	1	1	1	4	4	3	4	30
	Ejecteur	Hidrostal (half axiaal)	3	3	3	2	4	4	4	5	4	46
	Axiaal	Propeller and mixed flow	2	2	3	1	2	3	4	3	4	34
Injection	Injection	Venturi (dyson idee)	1	1	1	3	1	3	4	1	3	23
Airlift	Airlift	Airlift	4	3	4	1	2	1	2	1	2	24
Bucket chain	Bucket chain	Bucket chain	3	2	4	5	3	3	1	1	1	26

Figure 4.9: Multi criteria analysis on 17 different pumps, criticised on the criteria set-up for this research

From this analyses, the top 3 pumps are:

- The Hidrostal pump
- The Archimedes screw
- The Diaphragm pump

Another pump is added to the top three, which is not the right pump for pumping fragile particles, but because it is common and well known at the dredging department of Van Oord, it has been investigated:

- Centrifugal pump

The hypothesis concluded from the multi-criteria analyses states that the top three are the right pumps to pump coral embryos. This is further elaborated and validated in Chapter 5.

4.2.3. Behaviour of coral embryos in a Hidrostal pump

The shear stress along the edge of a pipe wall follows from Equation 4.5. A relation does not exist to calculate the local shear stresses along the edge of the pump. Because friction is related to the velocity squared, the velocity has a large influence on the shear stress. When investigating the velocities inside of a Hidrostal pump (Figure B.13), it is known that the velocity at the wall is higher than at the centre of the pump ($U = \frac{L}{t}$) where t is constant for all the streamlines because of the assumption that Q is constant. Therefore, the shear stresses towards the centre of the pump are assumed lower. In Figure 4.10 the assumed distribution of shear stresses towards the centre of the pump for a random setup is presented. Concluded from the figure, it is important to note the position of particles inside of the pump. Because coral embryos float and are therefore lighter than water, they tend to be directed inwards towards the centre of the pump. This is assumed positive for the survivability of coral embryos following pumping.
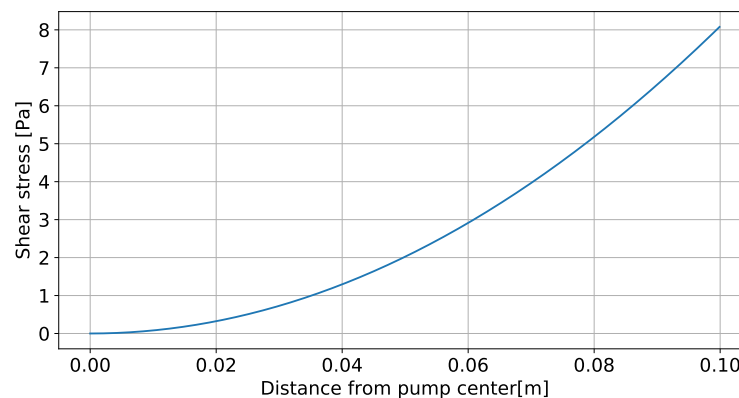
Figure 4.10: The distribution of shear stress towards the wall of the pump house (Free passage = 0.1m)

4.3. Model outcome

The relations mentioned in this chapter are used to build a model that calculates the shear stress in the system, the strain in the pipes, the head losses and the pressure fluctuations. By modelling different pumping sections, the total energy loss, friction losses and pressure differences have been calculated for a given setup based on the relations presented in this chapter. In Figure 4.11, an overview is given of the different values for the criteria considered for the different pumping setups. The first row indicates which pump system parameter is varied and in the second row the quantity. The green cells indicate an positive effect on pumping coral embryos and the red cells a negative effect. By combining the setups of the green cells, an optimal pumping system has been designed.

Test scheme															
Only vary:	L [m]					D [m]					RPM				
	5	10	15	20	25	0.05	0.063	0.075	0.1	0.15	584	800	1000	1200	1460
Total E loss [kJ]	1.64	3.26	5.8	9.09	13.02	17.51	14.62	12.51	9.09	4.84	5.25	7.23	9.09	11	13.52
Total friction loss [mwc]	4.89	5.08	5.3	5.54	5.75	13.5	10	7.88	5.54	5.76	2.03	3.65	5.54	7.83	11.36
Min Pressure [kPa]	80	79	78	78	77	65	68	70	78	91	93	86	78	67	51
Max Pressure [kPa]	108	112	114	116	118	129	126	123	116	107	106	111	116	123	133
U [m/s]	4.57	4.09	3.74	3.48	3.27	3.36	3.55	3.62	3.48	2.59	2.04	2.79	3.48	4.17	5.07
Q [m3/s]	129.29	115.57	105.79	98.31	92.34	23.78	39.86	57.53	98.31	164.69	57.73	78.81	98.31	117.96	143.31
n	0.57	0.64	0.68	0.7	0.7	0.47	0.58	0.67	0.7	0.28	0.66	0.68	0.7	0.7	0.72
nmax	0.71	0.71	0.71	0.71	0.71	0.71	0.71	0.71	0.71	0.71	0.66	0.69	0.71	0.72	0.73
Only vary:	# Bends					h2 [m]					Pump & h1 location [m]				
	0	1	2	4	8	0	1	2	3	4	-3	-2	-1	0	1
Total E loss [kJ]	9.09	8.93	8.8	8.61	8.4	9.09	9.13	9.24	9.41	9.66	9.41	9.24	9.13	9.09	9.13
Total friction loss [mwc]	5.54	5.67	5.81	6.05	6.5	5.54	5.54	5.55	5.56	5.57	5.56	5.55	5.54	5.54	5.54
Min Pressure [kPa]	78	75	73	70	65	78	78	78	71	61	101	98	88	78	68
Max Pressure [kPa]	116	115	114	113	110	116	126	116	117	117	147	137	126	116	106
U [m/s]	3.48	3.34	3.22	3.02	2.71	3.48	3.47	3.47	3.46	3.44	3.46	3.47	3.47	3.48	3.47
Q [m3/s]	98.31	94.44	91.02	85.25	76.55	98.31	98.25	98.05	97.73	97.31	97.73	98.05	98.25	98.31	98.25
n	0.7	0.7	0.7	0.7	0.71	0.7	0.7	0.7	0.7	0.7	0.7	0.7	0.7	0.7	0.7
nmax	0.71	0.71	0.71	0.71	0.71	0.71	0.71	0.71	0.71	0.71	0.71	0.71	0.71	0.71	0.71

Figure 4.11: In this overview, different quantities are calculated for multiple pumping system setups, the green cells indicate positive setups for pumping coral embryos with low mortality.

4.3.1. Designing the system

By using the relations in this chapter, the most influencing parameters on low mortality of coral embryos are investigated.

(a) Strain vs Length   (b) Strain vs Diameter   (c) Stress vs rpm
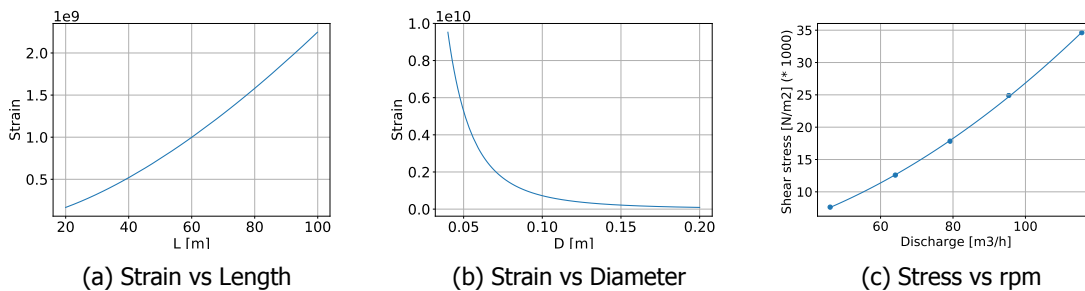
Figure 4.12: Influence of length, diameter and rpm on stressors

Figure 4.12 shows that for low stresses on the particles, it is required to have a minimal pipe length, maximum diameter and low rpm. Figure 4.13 depicts that the pipe length must be minimal, the diameter maximal or high rpm to have a high production. Therefore, the user must decide which parameter is critical: discharge or survival.

When designing a pumping system, often the length of the pipelines and the production are set. By keeping the rotational speed constant and varying the diameter of the pipes, a sweet spot can be found which optimises strain in the pipes, stresses in the system or the production. When the strain in the pipes, the shear stress in the pump and the corresponding production are plotted again, Figure 4.14 is obtained. Both the discharge and strain stagnate when the diameter reaches 0.15m, and when it

(a) Length vs dicharge   (b) Diameter vs discharge   (c) Rpm vs discharge
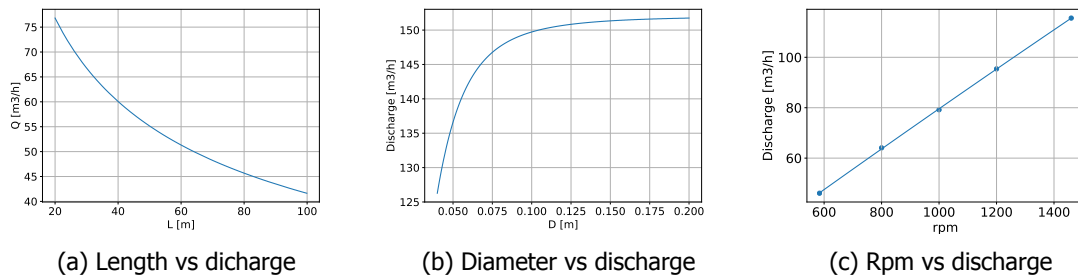
Figure 4.13: The influence of the pipe length and diameter and pump RPM on the production

reaches 0.175m, almost no change can be detected. Please note that, the discharge line and shear stress in the pump are not to scale and only the trend of the line must be interpreted.
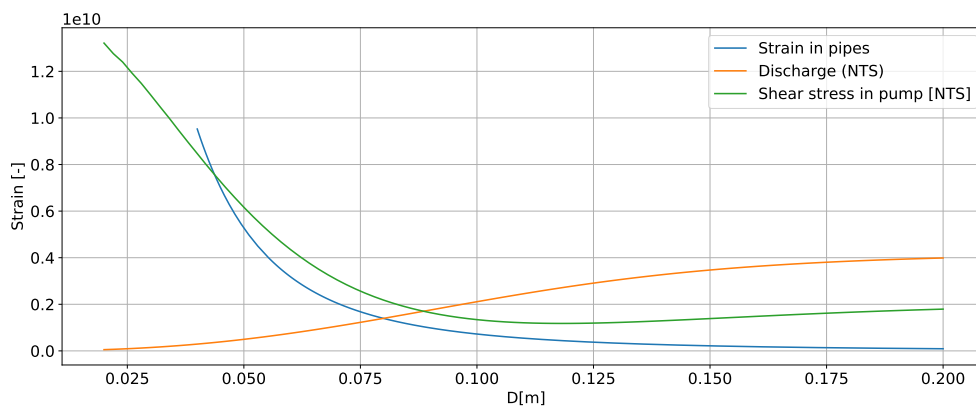
Figure 4.14: The relation between strain in the pipes, pump stresses, discharge and pipe diameter

Figure 4.14 helps to optimise the pumping system with constant rpm by varying the diameter of the pipe. Zooming in on the minimum pump shear stresses Figure 4.15 is obtained. If the user wants to optimise towards minimal shear stress in the pump, the dotted line in Figure 4.15 can be used. Furthermore, if the user wants to optimise towards maximum production or minimal strain in the pipes, a diameter must be chosen which is maximal for the pump.
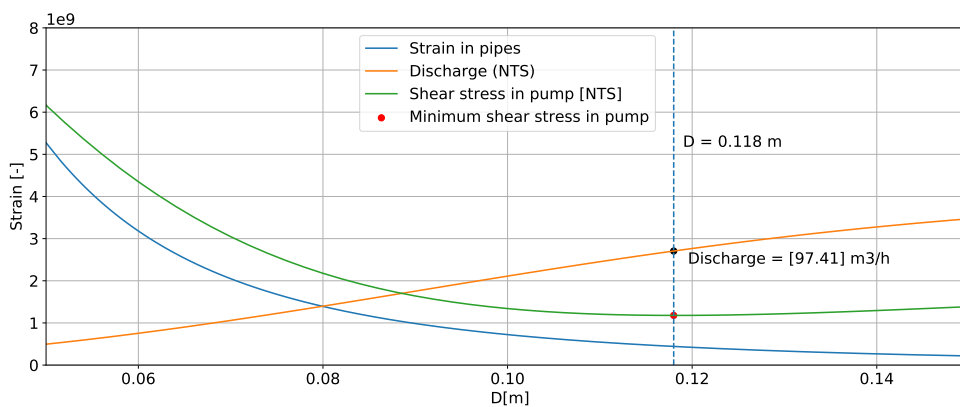
Figure 4.15: The sweet spot when optimising towards minimal shear stresses occurring in the pump

4.4. Case study, Australia

After applying the relations outlined in Chapters 3 and 4, an ideal pumping system has been obtained. Before designing a pumping system, all the requirements had to be known. As a final goal of this research, Van Oord and CSIRO wanted to pump 14,000m^3 containing > 230 embryos L^{-1}. With the assumption that pumping starts after 7 hours and the time frame exists of 12 hours (sun rise to sun set), a production of approximately 1,000m^3/h must be reached. Because the D100S Hidrostal in this research cannot reach these quantities, this case has been evaluated on scale with the model. For the test case scale, coral slick must be pumped within two hours from the water surface into the basins on board of the tugboat onto which an aquaculture facility was built with a capacity of 60m^3.

4.4.1. Requirements

- Low pump related mortality of coral embryos

- Required discharge is 30 m^3/h

- Slicks must be pumped from water surface into basins on a rehabilitation vessel

- System must be workable and available in Australia

4.4.2. Optimal system drawings

To design an ideal pumping system which can pump coral embryos with low mortality, the model is used to test different setups on shear stress, energy loss and strain and the most ideal setup is shown in this section. An impression of a system that exceeds the threshold values is presented in Appendix Section C.2.

First, a two dimensional drawing is presented in Figure 4.16 to give insight in the shape of the system. Both the inflow and the pump are positioned one meter below the water surface. This depth ensures that the pressure at the inflow is higher than atmospheric. The outflow is positioned at the 0m level, so a pipeline must be constructed through the hull of the ship which positions the outflow in the basin on the vessel. The whole systems is around 7m in length and the diameter of the pipes is consistent 0.1m. The pump rotational speed is set on 584 which results in a flow velocity of 2.55 m/s and a discharge of 70m^3/h.
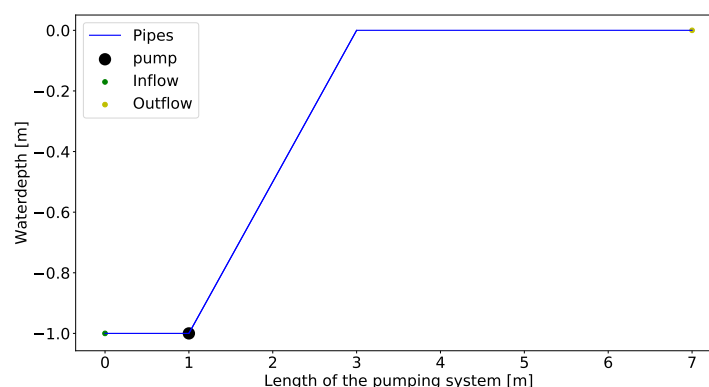
Figure 4.16: Two dimensional presentation of the pumping system

In Figure 4.17a the head losses and in Figure 4.17b the energy losses over the length of the system can be found. The pump has the most significant role considering the local head losses. Looking at the energy losses, the duration for which the particle is flowing through the object becomes important and therefore the pipes play a more significant role.

While the suction mouth is positioned under the water surface and the height difference and flow velocities are low, the local pressure will not be less than atmospheric, which is one of the requirements. In Figure 4.18 the local pressure variation over the pumping system is presented.

(a) Head losses over the pumping system

(b) Energy losses over the pumping system
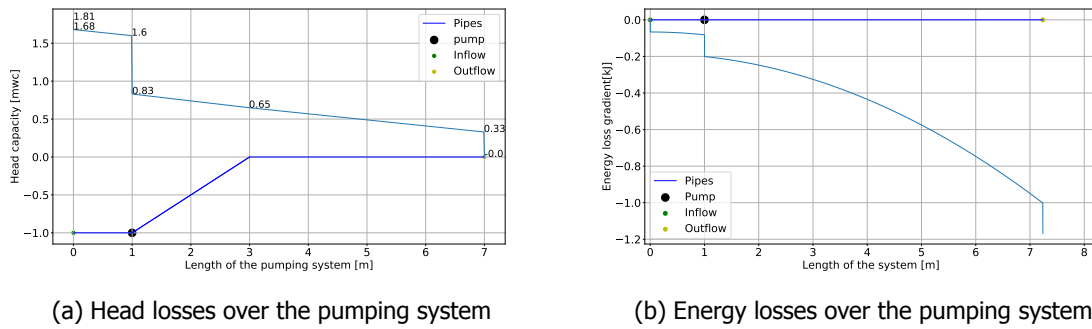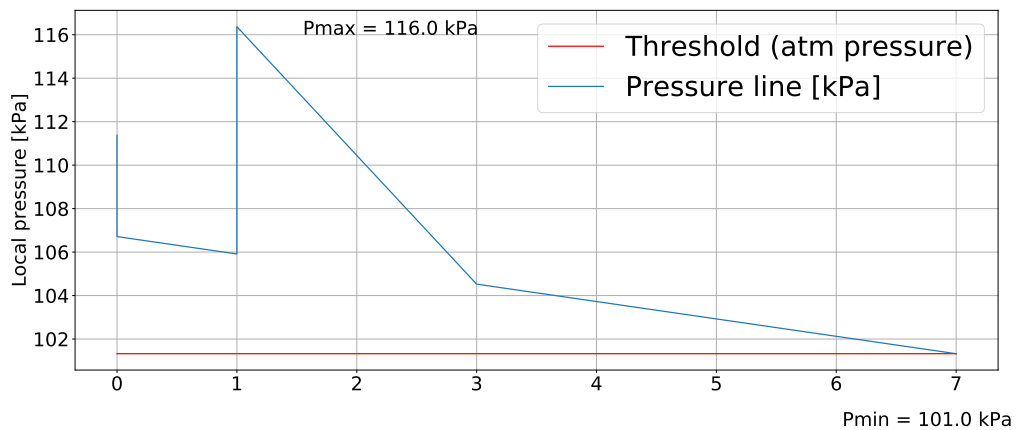
Figure 4.17

Figure 4.18: Local pressure variation over the pumping system

4.5. Discussion

To ensure low mortality rates of coral embryos due to pumping, pressure fluctuations, flow accelerations and shear stresses should be minimised (Ulanowicz, 1976). From the experiments, indeed a fluctuation in the criteria resulted in more damage (hydrogel balls) and mortality (coral embryos). By modelling the system and plotting the three criteria over the system, critical pumping sections have been detected and adjusted during the development. The best scoring pumping systems are Diaphragm or Hidrostal pump with low flow velocity, minimal hard surfaces to encounter (e.g. bends), constant diameters, low head differences and significant suction depth.

Two important factors determine the value of the mathematical model namely: the precision of stress calculation but more importantly the precision of the threshold values of coral embryos. As described in Chapter 3, further research is required to describe the exact strength of coral embryos and larvae. When this strength is known more exact, the survivability can be better estimated. Moreover, a minimal pressure of 101.325 kPa (atmospheric pressure) and maximum pressure of 200 kPa are assumed as thresholds regarding the pressure fluctuations in the system. Especially lower pressures are assumed as critical but are still just assumptions. To further investigate this threshold value, one could apply low pressures on coral embryos in a vacuum chamber in the period following spawning. By investigating the ability of cell division after experiencing certain low pressures, more precise conclusions can be done regarding this threshold.

In the current model, only the Hidrostal pump is modelled. It is therefore recommended to investigate if it is necessary to model more pumps when they are described as low shear pumps. From the multi criteria analysis, the Archimedes screw looked promising. The screw can be attached to the side of the

vessel and literally lifts the embryos onto the deck. However, during the field test in Australia, embryos survived the Hidrostal pump and described as promising coral slick harvest pump. An important factor to considered is the priming of the pump for good workability. One could design a system in which the suction mouth is positioned a significant distance under water with a minimal suction pipe which has multiple advantages: no priming issues, increase local pressure at the suction mouth and increase the local pressure in front of the pump. By minimising the suction pipe, the pump increases the pressure in an early stage which is beneficial for the whole system.

The flow in the model is assumed constant which is not the case for the diaphragm pump. It is advised to model noncontinuous flows to better estimate mortality. Furthermore, the shear rate and shear stresses are decreasing from the pipe wall towards the centre of the pipe. This phenomena is so far not considered in the model and therefore a potential error in estimation of the survival could be present. A more accurate estimation of the coral embryos and larvae in a flow would help the user to better estimate the operating stressors. Moreover, the optimisation required for an optimal system are not suggested and presented by the model. The user must interpreted the lines and make conclusions. The next step is to make the model parametric which directly designs the optimal solution for the given case.

If the threshold values of the coral particles can be determined with higher precision, the model can be used to estimate the mortality rate of embryos in certain pumping systems. Without these precise values, the model can be used to indicate critical sections for the mortality of coral embryos.

5

Experimental validation of stresses and the pumping system

To validate the hypotheses and results given in the previous chapters, laboratory tests were executed in Steenbergen, the Netherlands and at a field test in Australia. The objective of the laboratory tests was to determine the damage inflicted on proxies considering different pumps and pumping systems. Furthermore, the aim was to identify potential practical problems. After the laboratory tests, two pumping systems were selected and used during the field test that was executed to determine the mortality rate of coral embryos and larvae using these pumping systems. The results of the laboratory tests are given in Section 5.1 and these of the field test in Section 5.2 and discussed in Section 5.3.

5.1. Laboratory tests

Laboratory tests have been performed in collaboration with Aqua Unique, a specialist in the construction of swimming pools and ponds, to investigate the effect of pumping systems in different setups on pumping of coral embryos and larvae. At first, different proxies such as hydrogel balls, berries, fish eggs and peas were used to estimate the damage. However, after multiple tests, the hydrogel balls came out as the most promising and reliable proxy because they are easy to count and the damage can easily be recognised. Therefore, from here, only hydrogel balls are mentioned as proxy.

5.1.1. Test setup

During the tests, different configurations were used to study the damage caused to the hydrogel balls. For all configurations, tests were done in sixfold. Per test, sixty particles were brought into the system and collected at the outflow. If more particles are brought into the system, the result will be more reliable. Because time was limited, sixty particles were chosen because the particles were counted by hand per test. After pumping, the number of broken particles was counted, and the damage percentage calculated. Five different pumps were used: Hidrostal pump ($35m^3$/h), Hidrostal pump ($170m^3$/h), Diaphragm pump ($15m^3$/h), Centrifugal pump ($28m^3$/h), and the Centrifugal pump ($90m^3$/h). The pumps were connected to the same configuration to investigate the influence of the pumps. After selecting the pump causing least damage to the hydrogel balls, different setups for the configuration have been tested while using the same pump (for contingency) but it was not possible to set a constant discharge for the systems, and thus varies per configuration. To evaluate the damage induced by just the pump, a similar pump (turned off) was installed in series and the difference in damage was analysed. The tested configurations varied in; the number of bends: 1,2,4 and 8, discharge pipeline lengths: 2.8m, 5.6m and 16m; suction pipeline length: 2.8m, 5.6m and 13.2m; and diameters of the pipeline: 50mm, 63mm, 75mm and 90mm. These lengths and diameter were chosen because Aqua Unique already possessed corresponding pipeline sections and therefore a economical advantage. For the outflow, a dropdown distance of 0cm, 50cm and 100cm (at random) above the surface of the water was used. The inflow was not tested regarding damage. Figure 5.1 depicts a schematic set-up of the laboratory tests.
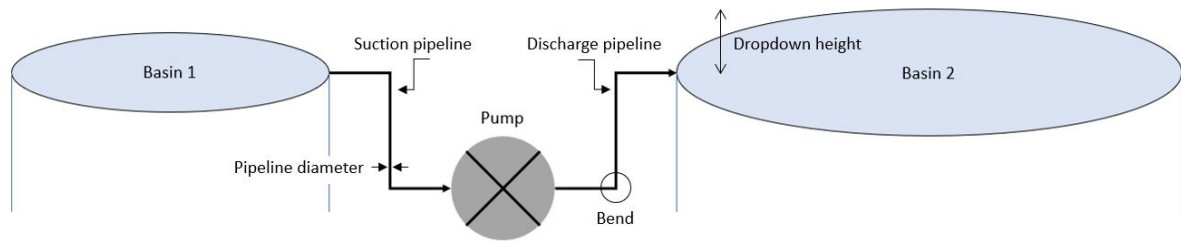
Figure 5.1: Laboratory set-up in Steenbergen

5.1.2. Laboratory test results

Concluded from the multi-criteria analysis in Figure 4.9, the three most promising pumps to pump coral spawn are the Hidrostal pump, the Diaphragm pump and the Archimedean screw. Because the Archimedean screw was not available during testing, it is not considered further in this research. The centrifugal pump is added a negative control in the preliminary pump testing.

Figure 5.2: Three different tested pumps: Diaphragm (4.5m3/h), Hidrostal(30m3/h) and centrifugal(30m3/h)

Test results are presented in the overview in Figure 5.3. Least damage was caused by the bigger Hidrostal pump (170 m^3 h^{-1}) followed by the Diaphragm pump. Both centrifugal pumps caused high damage to hydrogel balls. The difference in damage rates between pumps have been assigned to the pumps themselves as the configuration was kept constant. An example of tests results of hydrogel balls following pumping is presented in Figure 5.4.

Pump	Discharge [m3/h]	Test #	Substrate	Number of particles in	Number of unbroken particles	Number of broken particles	Percentage broken particles	Broken average	Standard deviation	Remarks
Hidrostal	30	1	Hydrogel balls	60	53	7	11.67%	10.00%	1.49%	*Medium damage percentage
		2	Hydrogel balls	60	54	6	10.00%			*Good workability
		3	Hydrogel balls	60	55	5	8.33%			*High flow velocity
		4	Hydrogel balls	60	54	6	10.00%			*Not self priming
		5	Hydrogel balls	60	53	7	11.67%			
		6	Hydrogel balls	60	55	5	8.33%			
Hidrostal	90	1	Hydrogel balls	60	59	1	1.67%	1.39%	1.25%	*Almost no damage
		2	Hydrogel balls	60	59	1	1.67%			*Big setup, crane needed
		3	Hydrogel balls	60	60	0	0.00%			*Highest discharge
		4	Hydrogel balls	60	59	1	1.67%			*Not self priming
		5	Hydrogel balls	60	60	0	0.00%			
		6	Hydrogel balls	60	58	2	3.33%			
Diaphragm	4.5	1	Hydrogel balls	60	55	5	8.33%	5.28%	1.95%	*Low damage percentage
		2	Hydrogel balls	60	58	2	3.33%			*Medium workability due to pulsing flow
		3	Hydrogel balls	60	56	4	6.67%			*Lowest discharge and velocity (six times
		4	Hydrogel balls	60	58	2	3.33%			lower than small Hidrostal pump)
		5	Hydrogel balls	60	57	3	5.00%			*Self priming
		6	Hydrogel balls	60	57	3	5.00%			
Centrifugal	17	1	Hydrogel balls	60	0	60	100.00%	100.00%	0.00%	*Highest damage percentage (100%)
		2	Hydrogel balls	60	0	60	100.00%			*Good workability
		3	Hydrogel balls	60	0	60	100.00%			*Medium discharge and velocity
		4	Hydrogel balls	60	0	60	100.00%			*Medium self priming
		5	Hydrogel balls	60	0	60	100.00%			
		6	Hydrogel balls	60	0	60	100.00%			
Centrifugal	30	1	Hydrogel balls	60	20	40	66.67%	80.83%	8.48%	*High damage percentage
		2	Hydrogel balls	60	14	46	76.67%			*Medium workability
		3	Hydrogel balls	60	5	55	91.67%			*High flow velocity
		4	Hydrogel balls	60	10	50	83.33%			*Medium self priming
		5	Hydrogel balls	60	11	49	81.67%			
		6	Hydrogel balls	60	9	51	85.00%			

Figure 5.3: Damage rate of hydrogel ball particles after pumping with different pumps

Figure 5.4: Example of the damage to hydrogel balls following pumping for six tests. The balls are soaked over night with the same duration and therefore have the same dimensions and properties.

After pump selection validation, the pumping configuration is validated. In the model, longer pipes result in more friction and higher energy losses and lower flow velocities. These energy losses are due to shear stress that is experienced by the particles. The maximum shear stress at the wall of the pipe, however, is related to the flow velocity squared and is, therefore, more significant with higher velocities. In Chapter 4 is stated that an increase in pipeline length is coupled to a lower mortality because the maximum shear stress decreases. To validate this, six setups are investigated and presented in Figure 5.5 with a inverse exponential trend (discharge increases exponentially with an decrease in pipeline length). From the figure, it has been concluded that indeed damage decreases with an increase in pipeline length, because the discharge decreases with an increase in pipeline length. The result on the damage is counter intuitive because when the time in the pipes increases, logic reasoning suggests that the particle collapse is higher. However, because the flow velocity decreases with an increase in pipeline length, the maximum shear stress at the wall becomes smaller and the damage therefore lower.
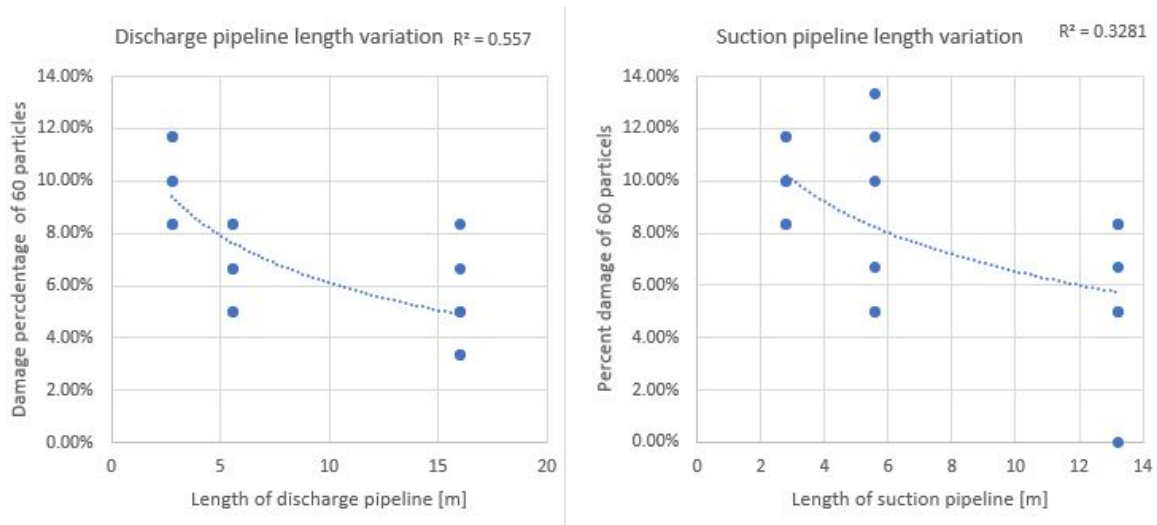
Figure 5.5: Correlation between the length of the suction- and discharge pipeline and the damage percentage of hydrogel balls

During the laboratory tests, a maximum of eight hard bends were included in the system. Figure 5.6 depicts that an increase in bends is associated with an increase in damage. The data follows a polynomial trend and implies that the the damage stagnates with an increase in the number of bends. This is explained due to the fact that the discharge decreases due an increase in head losses and therefore the impact force decreases. Furthermore, the figure shows the damage percentage related to changing the pipeline diameter. From the model was concluded that a larger pipeline diameter results in higher discharges because the losses reduce. The configuration was equipped with a constant suction pipeline diameter and different diameters for the discharge pipeline. After increasing the discharge pipeline diameter, the discharge increases and therefore, the flow velocity in the suction pipeline increases. Figure 5.6 depicts that the tests done with different diameters are associated with an exponential increase in damage which is counter intuitive. However, due to the higher flow velocities, the maximum shear stress in the suction pipeline increases and therefore the damage increases.
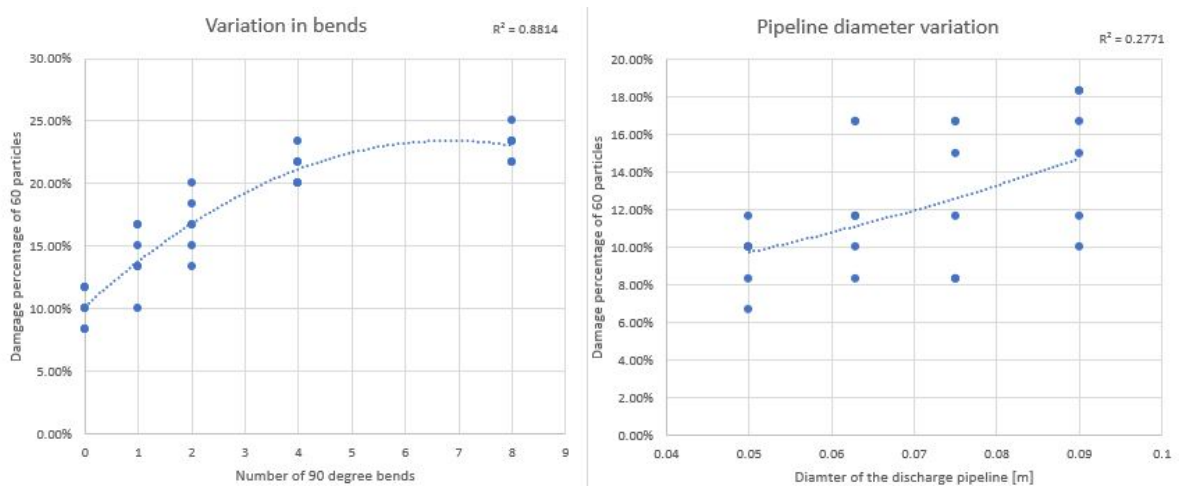
Figure 5.6: Correlation between number of 90 degree bends and pipeline diameter vs the damage percentage of hydrogel balls

Releasing particles from a certain height onto the water surface increases the impact force on the particles during outflow. This is not part of the mathematical model, but experiments verified the theoretical hypothesis. As presented in Figure 5.7, the damage rate increases with increasing release height.
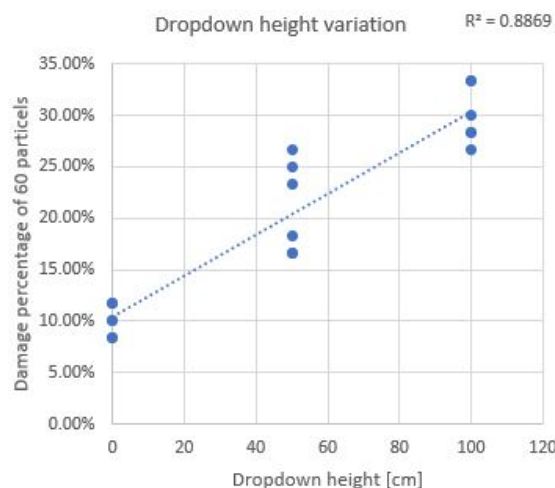
Figure 5.7: Correlation between the drop-down height and the damage percentage of hydrogel balls

5.1.3. Laboratory test conclusions

- An increase in bends in the system results in an increase in damage to the hydrogel balls.
- Longer pipeline (suction and discharge) results in less damage, probably as a result of the reduction in flow velocity due to an increase of the friction length.
- A larger diameter results in more damage, probably due to the higher velocity. Also, change in diameter at the the connection between 50mm(pump) and 100mm (pipeline) can result in higher stresses.
- Underwater release of the particles results in lower damage compared to dropping them on the water surface.
- Close to the suction mouth, vortices arise due to the suction of water close to air. These vortices must be avoided as they cause high shear stresses.
- Near joints and sharp edges, the streamline should be parallel which results in a smaller probability that particles hit those obstacles and collapse.
- More connections in the system result in higher damage.

5.2. Field test in Australia

The selected pumps and configuration were used during field tests in Australia around the Capricorn bunker at the Heron-Wistari reef to investigate if coral-spawn slicks can be pumped in large quantities with high survival. The project was timed around the mass spawning event after the full moon of November 23, 2018. The mass spawning at this location generally takes place between the 6th and the 8th day after full moon of the hottest month in the southern part of the Great Barrier Reef (Martyn, 2018). It was decided to work around Heron island because of high coral densities in the area (AIMS, 2018). Other parts of the Great Barrier Reef, affected by crown-of-thorns starfish, cyclones and bleaching, have recently encountered sever coral reductions (Hughes et al., 2017). The chance of finding coral slicks, which was critical for the project, is higher around (large) healthy reefs because there is a generally higher production of gametes.

The pumps were used to pump coral-spawn and seawater into twelve large ($5m^3$) tanks set up on the back deck of the vessel. Tanks used to store the pumped mixture were of either steel or plastic and fitted with flow-through seawater, aeration and a central stand-pipe that filtered the water, for cultivation.

5.2.1. Objective

The objective of the field test was to determine the possibility to pump coral embryos on board of a vessel where they can grow into competent larvae and later-on be deployed over a degraded reef, at an industrial scale. The results are used to validate the mathematical model, built as a design tool for a coral-spawn pumping system. The two key processes investigated in this research are:

- Ability to collect coral slick at high quantities.
- The effects of the pump types used on the survival of embryos and larvae for both 1) surface to deck and 2) deck to deck pumping.

5.2.2. General approach and test set-up

One of the major challenges for the RECRUIT project was whether pumping fragile coral gametes could occur without causing them major damage. As described in Chapter 3, coral embryos are delicate, and therefore, a gentle pumping system was required. Furthermore, the strength of the coral particles increases over time. Especially within the first 5 to 7 hours, the coral embryos are very fragile. Because these results were found after the field test was completed, the optimal pumping schedule to pump coral particles could not be used during this field test. From the previously described tests, the Diaphragm and Hidrostal were selected for harvesting coral-spawn slicks during the field test.

Following pump selection, the configuration of the intake and outflow of the pipeline was defined. In Chapter 4 it is concluded that low flow velocities, large pipeline diameters and relative short pipes without bends are positive for coral embryos survival. In practise it is difficult to use the optimal

configuration because of the stiffness and the weight of the pipeline (the used pipelines filled with water are around 10kg/m), the route to the different tanks was far from straight, and the priming of the hidrostal was more difficult than expected.

The final set up of the system to pump coral slick from the sea surface into basins is presented in Figure 5.8 (1). To pump coral slicks from the ocean surface into a basin on board of the rehabilitation vessels, the slicks first needed to be located. This has been done by using a helicopter which launched from Heron Island. After locating the slicks, the vessel positioned next to the slick and the skimmer with suction pipeline was positioned into the slick. The outflow of the discharge pipeline discharged underwater in one of the twelve basins. When a basin was full, the discharge pipeline was switched to a next one. In total, four basins have been filled this way.

A contingency plan was made to exclude the effects of the weather (e.g. waves and currents on the workability of the skimmer) on the probability of pumping. Tanks on deck were filled with coral colonies (Figure C.5) from which the eggs and embryos were collected and pumped from deck to deck as is presented in Figure 5.8 (2). To increase the number of embryos that were available to pump from deck to deck, buckets with coral spawn have been collected from the oceans surface. To pump the coral spawn from deck to deck, the intake of the suction pipeline was kept underwater by hand and a water and spawn mixture inside of the buckets was poured from a bucket into the system. This was repeated 8 times.

The same set-up was used for both tests except for the head difference. When pumping with the deck to deck principle the head difference was approximately 0m and pumping from the water surface around 2.5m. The critical factors of the intake system were found to be the skimmer, the priming of the pump and the air/water mixture pumped by the pumps.
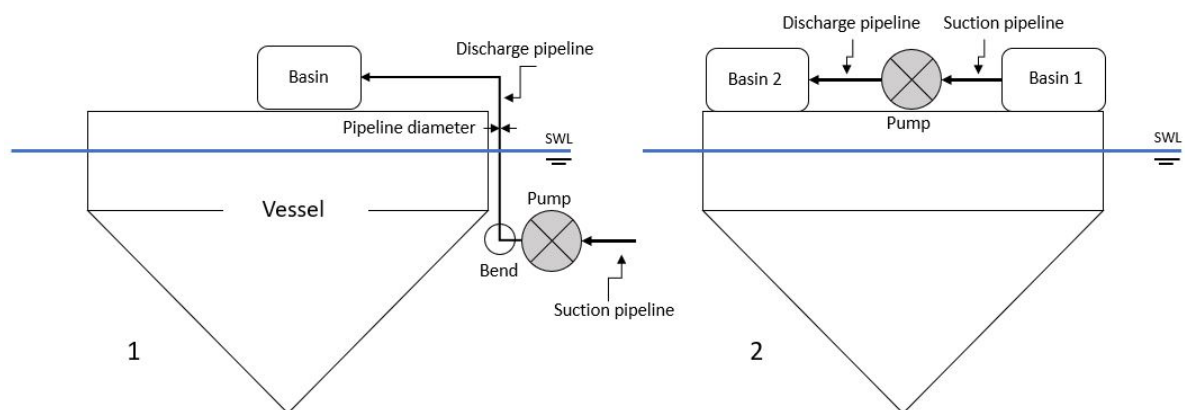
Figure 5.8: Set-up to pump coral spawn from ocean surface (1) and from another basin (2) into a basin on the rehabilitation vessel

5.2.3. Model approximations
The two pumping system setups have been used as input for the model to know how the pumped embryos react on the system. In Figure 5.9, the drawings of the different setups are presented in detail.

In Figure 5.10, the modelled head losses in the different sections are presented. The head losses in the pump for both systems are interesting to compare (2.65 [mwc] in (a) vs 1.72 [mwc] (b)). Both systems end with a 0 head, and proof conservation of energy. Furthermore, the head losses at the entrance most depend on the flow velocity in the system. The head losses increase with pipeline length, and the losses in the pipes are greater with higher flow velocities.

Figure 5.11 depicts the energy losses over the system. When calculating the energy losses, the time needed for the flow to pass through the system plays a significant role. Therefore, the energy losses in

the pump are relative small compared to the losses in the pipes ($t_{pump} = 0.14[s]$ and $t_{pipes} = 10[s]$). While energy losses can be seen as stresses in the system, this again pleads for a short system.

In Figure 5.12, the pressure fluctuations through the systems are presented. Pumping with a larger head difference (a) requires more pump power. More power results in higher stresses as described in Section 4.2.1. Furthermore, the maximum pressure is much higher and the minimum pressure lower in (a). In both systems, the pressure is below 1 Atm. which has been recommended to not exceed. Because this hypothesis was thought of later in the process, this threshold was not considered during the tests in Australia.

In Table 5.1 the values for different parameters are presented for the two systems (a) and (b). The discharge of the systems is approximately equal, so especially the higher rpm, length of the pipeline and height differences of system (a) cause the differences.

Description	Value	Unit	Description	Value	Unit
Suction length	9	m	Suction length	3	m
Discharge length	23	m	Discharge length	20	m
Total length	32	m	Total length	23	m
Pipeline diameter	0.1	m	Pipeline diameter	0.1	m
Pump rpm	1200	rpm	Pump rpm	1000	rpm
Discharge	91	m3/h	Discharge	94	m3/h
Flow velocity	3.21	m/s	Flow velocity	3.34	m/s
Max shear in pipe	31	pa	Max shear in pipe	34	pa
Total shear in pump	26000	pa	Total shear in pump	17000	pa
Pump efficiency	72	%	Pump efficiency	70	%
Total strain in pipes	300,000	-	Total strain in pipes	220,000	-
Total head loss	7.76	mwc	Total head loss	5.67	mwc
Total energy loss	21.06	kJ	Total energy loss	11.53	kJ
Max local pressure	168	kPa	Max local pressure	139	kPa
Min local pressure	89	kPa	Min local pressure	96	kPa

(a) Surface pumping   (b) Deck to deck pumping

Table 5.1: Model outcome for the two setups
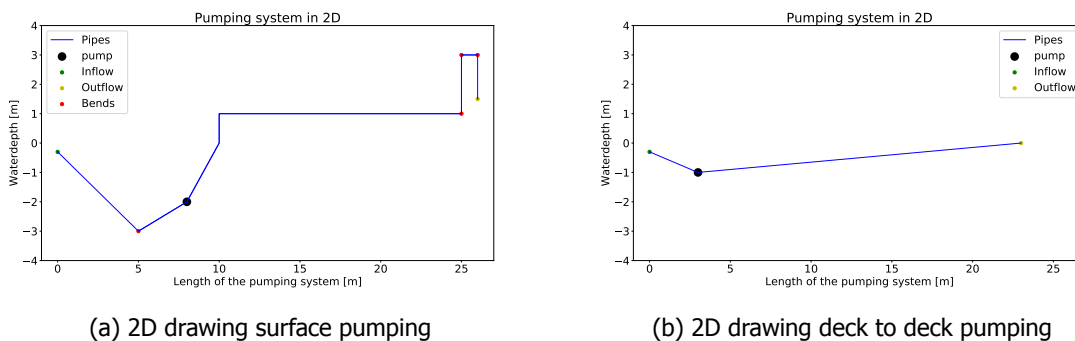
(a) 2D drawing surface pumping   (b) 2D drawing deck to deck pumping

Figure 5.9
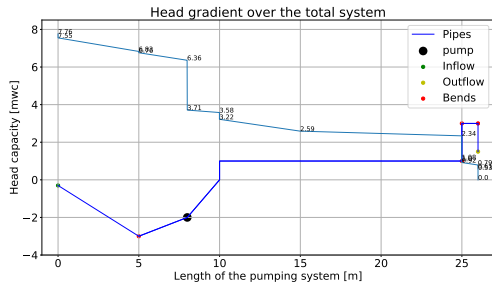
(a) Head losses during surface pumping
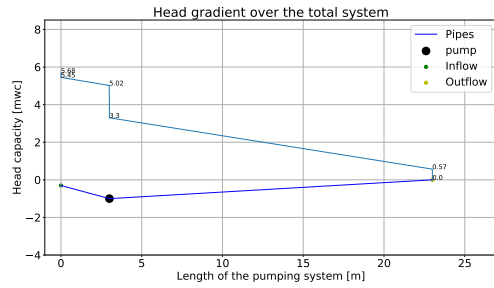
(b) Head losses during deck to deck pumping

Figure 5.10
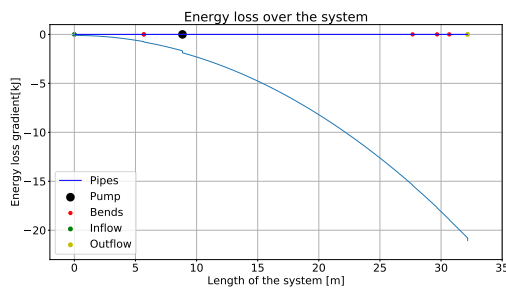
(a) Energy losses during surface pumping
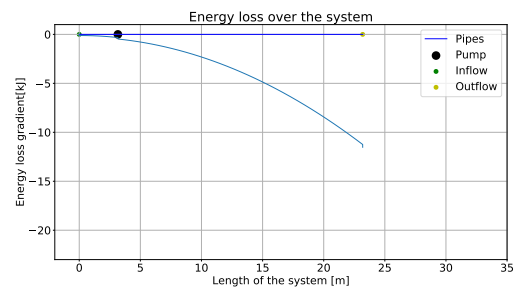
(b) Energy losses during deck to deck pumping

Figure 5.11
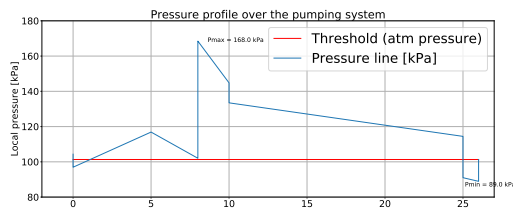
(a) Pressure gradient during surface pumping
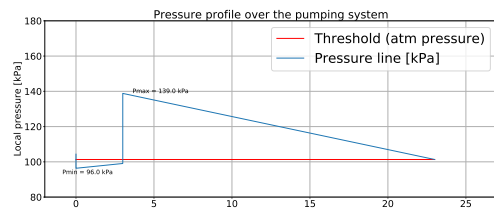
(b) Pressure gradient during deck to deck pumping

Figure 5.12

5.2.4. Field test results

As described in Section 5.2.2 in total, twelve tanks were filled with coral spawn. In Figure 5.13 the details and results are presented per tank. The layout of the tanks in the figure is equal to the setup on board of the vessel with tank number 1 on the bow side and tanks number 3 and 12 on the stern side of the vessel. The survival after pumping deck to deck is known because the initial density of the eggs and embryos entering the system had been measured. For the sea to deck tests the initial density of the slick could not be determined prior to pumping.

Tank #	Material	Slick	Pump	Discharge	Survival rate	Amount larvae	Survival after 4 days:
1	Plastic	Wild	D | H	N/A %	N/A	N/A	N/A
2	Plastic	IBC	Diaphragm	43 m3/h	119 %	995.992	23 %
3	Plastic	Bucket	Hidrostal	58 m3/h	150 %	3.537.119	23 %
4	Plastic	Wild	Diaphragm	24 m3/h	N/A %	260.424	N/A
5	Plastic	IBC	Hidrostal	128 m3/h	46 %	248.362	52 %
6	Plastic	Bucket	Diaphragm	68 m3/h	77 %	4.340.258	36 %
7	Steel	IBC	Diaphragm	34 m3/h	142 %	1.158.839	3.9 %
8	Steel	Bucket	Hidrostal	78 m3/h	170 %	3.914.398	33 %
9	Steel	Wild	Diaphragm	N/A	N/A %	41.650	N/A
10	Steel	Wild	Diaphragm	16 m3/h	N/A %	53.984	N/A
11	Steel	IBC	Hidrostal	112 m3/h	198 %	906.385	6.6 %
12	Steel	Bucket	Diaphragm	45 m3/h	138 %	12.214.512	16 %

Figure 5.13: Situation sketch of the twelve tanks on-board the rehabilitation vessels which have been filled with pumped coral-spawn slicks with deck to deck pumping (tanks 2,3,5,6,7,8,11,12) and by pumping form the ocean surface (tanks 1,4,9,10)

In Figure 5.14 the survival rates per tank during the first days following pumping are presented. In the legend, H is standing for Hidrostal and the D for Diaphragm pump and the indicated red arrow indicates stress induced fragmentation. The grey IBC control tank line, is the survival trend that un-pumped embryos follow in the first days following spawning which was also considered in Doropoulos et al., (2019). The grey IBC trend however, also shows fragmentation which is likely the result of having them in a tank where they stick to the wall and have been exposed to shear stresses due to aeration and water inflow. Note that the plots most of of the pumped particles follow the same trend as the un-pumped ones. This could mean that pumping doesn't affect the survival of the embryos over time.
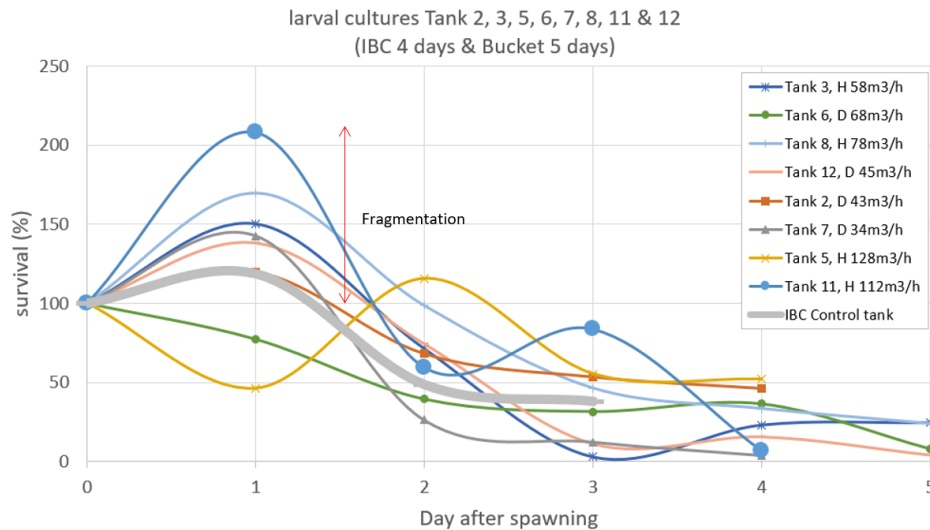
Figure 5.14: The survival trends in the days following spawning after pumping from deck to deck.

In Figure 5.15a and Figure 5.15b the survival in the days following pumping are presented for the Hidrostal and Diaphragm pump. After initially higher fragmentation, the final survival becomes lower for both pumps. The overall survival after 4 days is higher for the Hidrostal (29%) than for the Diaphragm (26%). However, the discharges are not the same for the two pumps (AvgHidrostal = 94m^3/h and AvgDiaphragm = 47.5 m^3/h) and therefore difficult to compare (note that the calculated discharge and the averaged measured one are equal). Because the configuration is the same, the flow velocity of the Hidrostal is significantly higher and one would expect higher mortality. Most of the survival trends of both pumps are following the un-pumped trend like Figure 5.14.
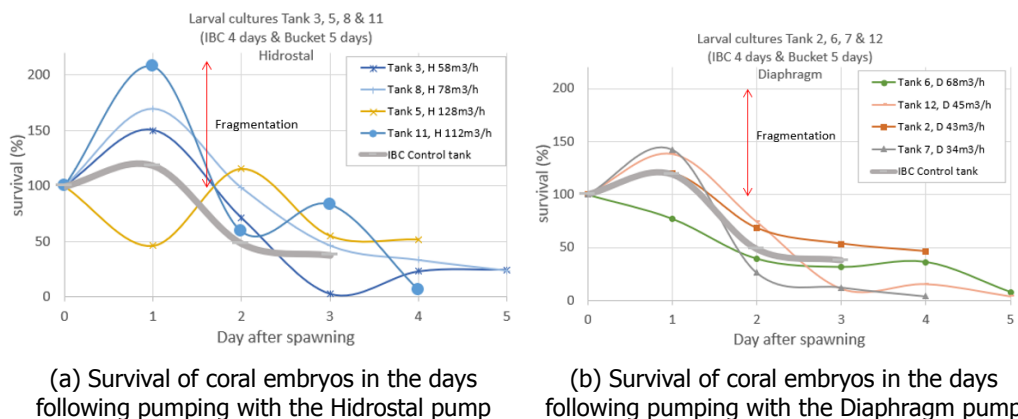
(a) Survival of coral embryos in the days following pumping with the Hidrostal pump

(b) Survival of coral embryos in the days following pumping with the Diaphragm pump

Figure 5.15

The deployment of competent larvae onto a degraded reef is not part of this research. However,

because the field test in Australia went beyond expectations, extra tests were executed to investigate the possibility to pump them. Deploying competent larvae using pumps, decreases the limitations regarding, for example, the draught of the vessel. Shallow reefs can easily be reached with a pipeline but is impossible with a hopper. The experiment was executed using the deck to deck pumping technique and resulted in high survival rates ($\approx$ 88%). That the survival rates following pumping are higher for larvae in comparison with embryos was also expected from Figure 3.5.

5.2.5. Field test conclusions

- It is showed for the first time that it is possible to successfully pump live coral embryos and (competent) larvae with positive survival rates.
- After pumping, embryos can grow into competent larvae and settle (see Figure C.6).
- No real difference regarding mortality is found between the Hidrostal and diaphragm pump.
- Higher survival is found for deck to deck pumping compare to pumping from the oceans surface.
- Fluctuations in pressure likely result in more damage.
- More energy losses likely result in more damage.
- Higher head losses likely result in more damage.
- The pressure gradient around the used suction mouth was too small to take in a large surface of embryos.
- Due to currents and wave action, it was hard to place the skimmer in its preferred position for optimal intake.
- Applying a setup designed upon a theoretical model in practise is difficult.
- Priming of the pumps is an important practical feature with possible issues when designing a pumping system to pump coral-spawn from the surface.

5.3. Discussion

For this research, laboratory and field tests have been executed to investigate the possibility of pumping live coral embryos and larvae. Furthermore, a theoretical framework was derived which can act as design tool for a coral harvesting pumping system. The discussion of the results and conclusions of the tests are described below.

5.3.1. Laboratory tests

The laboratory tests showed that the Diaphragm pump and the bigger Hidrostal pump (90 m^3 h^{-1}) are capable of pumping hydrogel balls with low damage percentage. As previously described, the discharge was not equal for the different pump tests. Therefore, the flow velocity and shear stresses in the pumps was different for each test but are directly compared. Therefore, an error is present between this comparison.

From the calculations presented in Chapter 4 is concluded that a short system, with a large diameter, is favourable for low damage. From Chapter 5, the optimal configuration for low damage percentage includes longer pipes with a small diameter (opposite as Chapter 4), low head difference, no bends or sharp edges and underwater release. The contradiction is likely because during the tests in the laboratory, the shaft power wasn't controllable and therefore the discharge varied with a different configuration. Large diameters and long pipes are coupled to lower discharges and therefore probably lower damage rates. The results from the laboratory tests, therefore, should be interpreted that lower flow velocities are favourable for lower damage.

The Hidrostal pump is scalable towards high discharges ($\approx$ 2000 m^3/h). The biggest diaphragm pump available on the market reaches 100 m^3/h. Therefore, if the diaphragm pump is chosen to pump large quantities of coral slick, approximately 140 hours is required to fill a hopper (14.000m^3). Because the time frame to pump slicks is 36h following spawning, in minimum of 5 diaphragm pumping systems are required to fill the hopper in time which may result in extra practical and workability issues. The type of vessel used will determine the pumping configuration. Therefore, the most optimal possible configuration must be designed tailor made for the vessel.

5.3.2. Field tests Australia

It is now for the first time demonstrated that it is possible to pump live coral embryos and (competent) larvae with positive survival rates.

During the field test in Australia, several practical issues had to be overcome. The flexible pipes used on the vessel could only be positioned when they were empty. The priming of the Hidrostal pump appeared difficult, and alterations for this problem are proposed in Section 4.5. During the positioning of the suction mouth, it was noticed that the combination between positioning the vessel and the skimmer at the same time was difficult.

In Figure 3.5, is presented that the strength of coral embryos increases during the developmental time and it is advised to begin pumping after 5-7 hours following spawning. However, the dispersion through the water column is not considered in this assumption. Because the embryos become less buoyant over time and mobile after 36h following spawning, an optimal moment in time can be found in which the embryos developed their strength significantly but are still in high concentrations found at the surface. Because the coral-slicks are easier to spot on the ocean surface during daylight, the proposed time frame is on the first day following spawning from sun-rise to sun-set. The spawning often begins between 20.00 - 22.00 pm. and therefore sun-rise is approximately 7h following spawning and matches the results from the Couette-rheometer. Further research is required to sharpen the exact sweet spot.

In Figure 5.14, the yellow line follows a non consist trend which could be due to observer errors. Six different scientists counted and graded embryos in seize, livability and form. Because it is impossible to exactly grade the embryos in the same way, errors are probably present.

The strength tests on coral larvae show that approximately all larvae survived the tests and that strain up to 60,000[-] is not enough to damage the larvae (Figure 3.5). During the field test in Australia, 5-day old larvae are pumped with the Hidrostal and Diaphragm pump, which showed 88% survival. This means that it is possible to pump the larvae over a certain distance after which they can be deployed by pumping over a degraded reef where they can settle. However, the specific weight of coral larvae is not specified but because they can swim to the bottom of the ocean, it is assumed, that it is greater than water ($\rho_{larvae} > \rho_f$). Therefore, the particles can likely be pushed towards the outer edges in bends and in the pump which can cause higher mortality. However, further research is required to validate this assumption. For coral embryos ($\rho_{embryo} < \rho_f$) it is concluded that they follow the streamlines through the system because the relative specific weight is approximately 1.

5.3.3. Framework

After to the validation of the model and hypotheses presented in Section 5.1 and 5.2 sufficient information is available to complete the framework. The goal of the framework is to connect the strength of the coral embryos to the stresses in the pumping system. While the exerted stress in the Couette cell is described in strain, the stresses in the pumping system also have been transformed to strain. In Chapter 4, it is discussed how this was done for pipes. For pumps this is not described because a simple transformation is not possible due to non linear effects. The strain in the pump is beyond the scope of this research and is recommended for further research. Therefore, the framework will only couple the pipe length and diameter combination with constant rpm to the mortality of the embryos.

Chapter 3 presents that the strength of coral embryos develop through time and that after seven hours following spawning coral embryos can resist strain levels up to 60,000. In Figure 5.16, the framework is presented with different pipeline length and pipeline diameter combinations for a Hidrostal pump with 1000 rpm. As described in Section 3.2.1, shear rates in the pipes have been linked to the shear rates in the Couette-rheometer. Because Equation 5.1 is used to calculate the local shear rates in the pipes, the flow velocity in combination with the boundary layer r, the local shear rate is determined just outside the boundary layer (Cengel and Cimbala, 2004). The shear rates are only valid for the location of r from the wall. Positions closer to the centre of the flow are coupled to significant lower shear rates.

$$\frac{du}{dr} = u_* \cdot 2.5 \cdot \frac{1}{R - r} \tag{5.1}$$
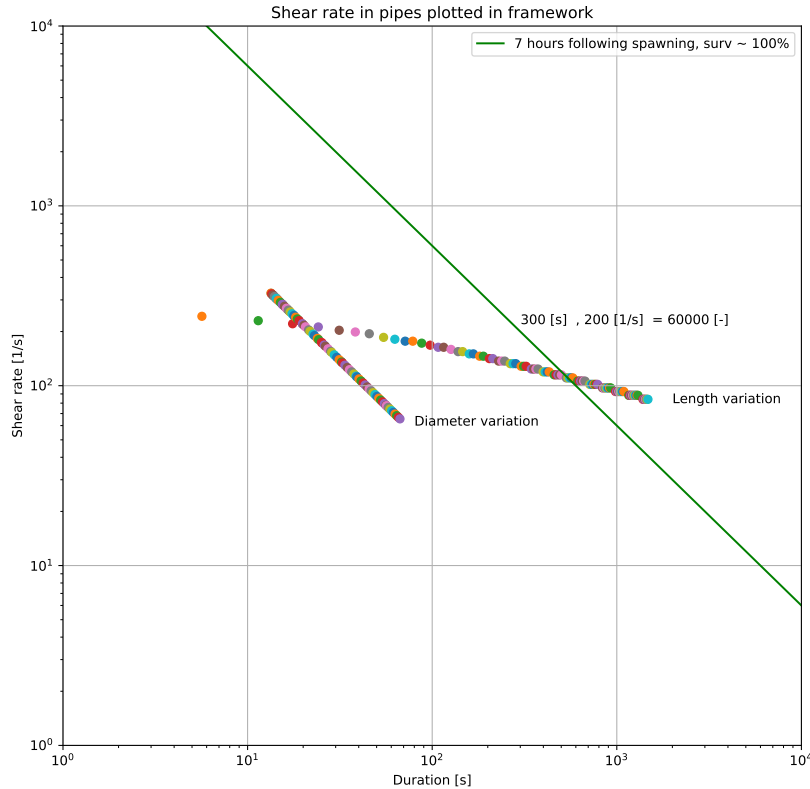
Figure 5.16: Framework which couples strength of the embryos seven hours following spawning to the strain values in the pipes for varying length and diameter. An increase in pipeline length and diameter is coupled to a longer duration. The shear rate, calculated with Equation 5.1 is plotted against the duration of the particles in the system on log scale.

Previous, it has been concluded that the variation in diameter is one of the most critical actions considering mortality because it has a large influence on the flow velocity and head loss. In Figure 5.16 however, the diameter doesn't increase the strain in the system (the line is nearly linear in log scale). This indicates that when using Equation 5.1, the pipeline length has more influence on the strain because it significantly increases the time in the system and pleads again for a short system. Because in Figure 5.16 the strain in the pump is not implemented and only valid for the distance just after the boundary condition (r = 0.001m) the framework is not advised to use as main design tool and further discussed below.

The objective of the theoretical framework is to relate the strength of the embryos 7 hours following spawning (threshold) to the stressors (shear rate) in the pipeline system. The shear rate is calculated at a certain distance from the pipeline wall with Equation 5.1. The main parameter that influences the shear rate due to this equation is the friction velocity and is related to the flow velocity. Two main concerns arise by using this equation.

1. The shear rate is only calculated at that specific distance from the pipeline wall and decreases significantly when that distance is increased (see Figure 4.6). When the particles are travelling through the pipeline at another distance, the shear rate is not calculated right and the exceedance of the threshold will be incorrectly estimated.

2. By decreasing flow velocity (decreasing pipeline diameter), the shear rate appears to decrease, however, the discharge decreases due to an increases in friction. As previously mentioned, friction (or energy loss) is experienced as shear stress by the particles and shear stress is related to the shear rate. Therefore, further research should investigate if Equation 5.1 is the right equation to calculate the shear rate in a pipeline system.

Furthermore, the shear rate variation by changing the pipeline characteristics are calculated without the influence of the pump. The time that the embryos are flowing through the pump is very limited, however, the flow velocities in the pump are much higher than in the pipeline and therefore the strain can be significant. Especially in shorter pumping systems, the influence of the pump becomes relatively higher because the time in the pipeline decreases with shorter pipes. The shear rate in the pump is so far not calculated and is crucial to investigate when using a framework to define if a pumping system is exceeding a threshold.

The trend defining the strength of coral embryos 7 hours following spawning indicates that 100% of the embryos survived this value of strain (60,000[-]). Because all particles survived, it therefore doesn't indicate the strength upper limit of coral embryos. However, it can be assumed that if the pumping system in total exerts less strain than 60,000[-], coral embryos survive the system. If the threshold value is calculated more exact, optimisations regarding the production of pumping coral embryos can be executed in further research.

6

Discussion, Conclusion & Recommendations

The focus of this study is the possibility of pumping coral embryos and larvae from the water surface onto a vessel for reef rehabilitation on an industrial scale. This chapter aims to answer the main research question: "How can a pumping system be designed best to maximise the number of embryos and larvae pumped from coral-spawn slicks (Q > 30m3/h), into a vessel based container or hopper with maximal survival rates (surv > 0)?" The discussion is given in Section 6.1 and the conclusions given Section 6.2. In the process of answering the research questions, various additional aspects were observed, which are interesting to assess in further research. These specific aspects are discussed in the recommendations in Section 6.3.

6.1. Discussion

Tests to harvest coral embryos and larvae for reef rehabilitation on an industrial scale using a pumping system showed positive results. Prior to the test, considerations done by Doropoulos et al., (2019), regarding pumping related mortality required confirmation. In their paper, a mortality of coral embryos of 20-30% due to pumping is considered and a final mortality (until reaching full competency) of 75-79% after 5 days following spawning. By using a tug vessel with a culturing facility and different pumping systems, the RECRUIT project team showed during their field test in Australia that it is possible to locate and pump coral slicks. The survival rates of the embryos and larvae directly after pumping varied between 50-210% which is a wider range than Doropoulos et al., (2019) suggested probably due to unexpected rates of fragmentation. However, 4 day after spawning the survival rates were 29% for the Hidrostal and 26% for the diaphragm pump and almost matches their suggestion. The harvested embryos and larvae can be transported over large distances after which competent larvae can be deployed onto a degraded reef. It is showed that the coral eggs and embryos can handle the stressors in a pumping system and can be developed into competent larvae in both steel and plastic basins. In total, 60 m^3 was available for storage and approximately 29 million embryos were pumped from which 19% developed into competent larvae. These outcomes suggest that harvesting slick is a feasible method for reef rehabilitation and further upscaling to an industrial scale should be explored.

The first objective was to locate the slicks after spawning. For this a helicopter was used. Within 15 minutes, multiple wild slicks were located that contained orders of magnitude and higher concentrations of coral embryos than described in literature. This suggests that if the coral-spawn slicks can be located, they contain highly abundant volumes of eggs and embryos that can be used for reef restoration. Before, 230 embryos L^{-1} was the maximum detected concentration of coral embryos in slicks (Oliver and Willis, 1987). Due to the relative calm weather conditions during the field test, the slicks kept their density and the tug vessel could be placed next to the slicks in order to position the skimmer into the slick. Further research should investigate the localisation of the slicks in other weather conditions.

After concentrating the slicks, the pumping system pumped the wild coral eggs, embryos and larvae

onto the tug vessel. A skimmer has been designed with the purpose to pump surface water from the sea-surface with high concentrations of eggs, embryos and larvae. Because the surface layer was relatively thin, the pumping system often pumped air into the systems. This was not undesirable as air in the pipeline creates turbulence and decreases the efficiency of the pump which results in increasing energy losses (Q. Schiermeier (MIT), 2005). Furthermore, the pressure gradient around the intake was not significant enough to collect large amounts of coral-slick. For future research, another intake system is recommended that directs the spawn towards the suction mouth (e.g. by using fish pot shape constructions) and pumps the spawn from further below the water surface. Both the Hidrostal and diaphragm pump were able to pump the particles with a survival rate of over 100%, an indication of fragmentation of the embryos (Heyward and Negri, 2012). However, the embryos were still capable of growing into competent larvae. This abnormal development of embryos into larvae was questionalble for Bassim et al., (2003). When it is required to upscale the intake volume, the Hidrostal pump possibly has more potential because discharges of 2000 m^3 h^{-1} can easily be reached and therefore can fill a hopper($14,000m^3$) in 7 hours. Regarding the diaphragm pump, only 100 m^3 h^{-1} pumps are available on the market. Hence, 140 hours are required in order to fill a hopper with a single pump.

For *Acropora spathulata* strain values up to 60,000 [-] 7 hours following spawning resulted in 100% survival. Therefore, higher strain values should be applied to find the upper strength. When the upper strength limit of the coral particles is known, the pumping system can be optimised. The pumping system designer should decide whether a higher production with lower survival or a lower production with higher survival is required. Further research should be executed on the strength of the embryos for different species, and the optimal time frame for harvesting wild slicks should be defined. Because coral-spawn slicks always contain different species, this information is crucial. The Couette-Rheometer setup used in this research can be applied to test the strength of the embryos as also suggested for algae in Michels et al., (2010).

After coral embryos develop into competent larvae, they can be deployed onto a degraded reef. The deployment of the larvae is made possible by pumping. During the field test, 88% of the pumped competent larvae survived the stressors in the system. If bottom doors of a hopper are used to deploy the larvae onto the reef, the draught of the vessel including the extra draught due to the bottom doors, cause limitations for reef selection. Therefore, an alternative approach such as pumping the larvae from the deck onto the reef with a pipeline system may be a better solution with shallow reefs. However, deployment was not part of the scope of the RECRUIT project, and further research should focus on deployment. It is yet unknown what percentage of competent larvae as deployed from a vessel actually settle on a reef and grow into mature colonies. When this percentage is known, a more precise analysis can be executed to validate that 140.000 mature colonies can develop onto a degraded reef by pumping approximately 3 billion embryos using the proposed method (Doropoulos et al., 2019). Developing and moving this number of embryos is not possible with the conventional approaches and harvesting embryos is therefore a promising rehabilitation method.

6.2. Conclusions

SQ1: What are the basic elements of a theoretical framework, that can act as a design tool, where the survivability of coral embryos and larvae is related to the strength of the particles and stresses occurring in the pumping system?

The basic elements of the framework are the strength of the particles and the stressors in the pumping system such as pressure fluctuations, shear stress and flow accelerations. Strain in the pipeline of a pumping system is a stressor that can be related to the strength of coral embryos and larvae. However, for strain in the pump this relation is not yet found and requires further investigation. When the relationship between the strength of the particles (or threshold) is presented on a log scale plot and the strain (or shear rate and the duration) in a pumping system are known, the user can make an estimation on the survival of coral embryos and larvae. Different pumping systems setups can be compared to define setups that doesn't exceed the threshold values.

SQ2: What is the strength of live coral embryos and larvae in the 48 hours following spawning in

relation to shear stress?

From the Couette-Rheometer tests, the strength of coral embryos appears very low during the first couple of hours following spawning. After $5 - 7$ hours, the strength increases and high survival rates (0.83 - 1) are found for strain between $500 - 60,000$. Hence, a significant strength development over time is detected. The minimum and maximum pressure thresholds for disruption of the embryos were not tested during the Couette test. Before testing, atmospheric pressure at the seawater surface is assumed as being the minimum threshold for designing a coral harvesting pumping system. During the field test in Australia, live embryos have been detected which were pumped with pressures decreasing towards 88kPa. Therefore, the minimum pressure threshold should be further investigated. The maximum pressure limit is set on 200kPa before testing. This limit is not exceeded.

SQ3: Which pumping systems are able to pump coral embryos and larvae with maximal survival rates?

Criteria that should be included in a selection of a coral harvest pumping system are low-pressure changes, low flow accelerations and low shear stresses. The influence of these parameters within the system is most significant around pumps, pipes, head differences, widening, constrictions the inflow and the outflow of the system. From the multi-criteria analysis for pumps it has been concluded that the Hidrostal, Archimedes and Diaphragm pumps are suitable for harvesting coral slick. After field tests with the Hidrostal and Diaphragm pump in Australia, it is concluded that both can pump coral embryos with little mortality. This mortality can be estimated by calculating the major and minor head losses, for all sections in the system. These losses can be contributed to higher shear stresses at more significant head losses. Therefore, higher mortality rates are expected in systems with more significant head losses.

It is observed that mortality rates increase with higher pressure fluctuations. Regarding flow accelerations, it is concluded that for the hydrogel balls ($\rho_{balls} > \rho_f$) positive or negative accelerations are linked to higher damage (for example in bends). For the coral embryos ($\rho_{coral} \approx \rho_f$), this effect is also expected to occur because accelerations are coupled linked to variances in pressure. However, as it is likely that the embryos will follow the streamlines almost precisely, they will not be damaged by hitting hard surfaces. Considering shear stresses, it is concluded that for both the hydrogel balls ($\rho_{balls} > \rho_f$) and coral embryos ($\rho_{coral} \approx \rho_f$) higher losses are linked to higher mortality rates. The shear stress in the pump is relatively high compared to the stress occurring in pipes. As the embryos will follow the streamlines due to comparable densities, lower mortality rates than the damage rates of the hydrogel balls are expected to occur.

SQ4: Is it possible to pump coral embryos and larvae during a prototype scale test, and how can the pumping system be optimised?

The pumping systems showed that they can pump coral embryos (survival $\approx$ 19%) and larvae (survival $\approx$ 88%). During the deck to deck pumping test, a maximum shear stress of 35 Pa was calculated for the pipes as well as a maximum strain of 300,000. This value is five times the applied strain in the Couette-Rheometer while a significant number of embryos survived. This means that the embryos are stronger than concluded from the Couette tests. To increase the efficient collection of coral embryos, a solution to increase the concentration of the embryos around the suction mouth should be found. Furthermore, based upon the modelling results, the optimal pumping system should contain low flow velocities, minimal hard surfaces, constant diameters, low head differences and significant suction depth.

MQ: How can a pumping system (discharge $> 30 \ m^3 h^{-1}$) be designed to maximise the amount of embryos and larvae pumped from coral-spawn slicks, into a vessel based container or hopper with maximal survival rates (number of survivors > 0)?

The combination of sub-questions shows that it is possible to design a pumping system to harvest coral-spawn slicks with positive survival by using a Hidrostal or Diaphragm pump. This can be done by using an intake that concentrates the slick towards the suction mouth, with minimal pipe length,

minimal surface to encounter (e.g. bends and connections), low rpm and flow velocities and significant submerged outflow. Furthermore, pumping should be taking place after 5-7 hours following the mass spawning as the strength of coral embryos increases over time. Because the embryos and larvae disperse through the water column over time, it is advised to finish the pumping process before 36h following spawning. After dispersion it becomes difficult to find high concentrations of eggs, embryos and larvae on the surface.

6.3. Recommendations

To better estimate the mortality of coral embryos and larvae in a pumping system, their strength threshold should be known with more precision. In current research the survival rate was around 100 %, which indicates that they are strong enough to survive. To investigate the actual strength of coral embryos and larvae, higher strains must be applied in the period after spawning. Higher strains can be applied by increasing the viscosity of the medium, increasing the spinning duration or increasing shear rate. Furthermore, until now, the strength tests have only been applied to *Acropora spathulata* and it is recommended to also determine the strength of other dominant species. The lower pressure limit for coral embryos and larvae is assumed and set on atmospheric pressure. This condition is very limiting when designing a pumping system because the pressure decreases until the pump. Therefore, in the design, the pump has to be connected close to the intake. To exemplify, it is therefore not possible to construct the pump on deck of the vessel. It is advised to further investigate this threshold value by applying different pressures onto the particles. A vacuum chamber can be used to decrease the pressure experienced by coral embryos. Note that the lower pressure may never reach the vapour pressure because destructive cavitation will occur. After applying different vacuum pressures onto the particles, one can investigate if the embryos survive and a more precise threshold will be found.

Bucketing (scooping with buckets) coral embryos of the water surface seemed more promising than pumping as a bucket is easier to position than the suction mouth. During bucketing one could make sure that only the top layer of the water column is collected, making this a promising harvesting technique for the future. When the buckets are emptied in a main vessel or barge, the bucketed embryos can still develop into mature larvae and be transported. However, a very dense slick is required to reach the ecologically significant rates in combination with many buckets and personal on the vessels. If the concentration of coral slicks can be optimised, the rehabilitation can process a lot more surface water in a small time frame. A possible method could be to use large fish pots that are positioned on the reef and use the currents to fill automatically. Furthermore, the helicopter in this research can be replaced by multiple drones to reduce costs.

The deployment of the competent larvae onto the reef was not part of the scope of this research and should be investigated further. A proposed method of deployment is using pumps to transport them from the vessel towards degraded reefs by using a long pipeline in order to reach shallow reefs. Other possible ways to deploy them onto a degraded reef are given below but require further research:

- By using bottom doors of a hopper, competent larvae can be released in front of a shallow reef and, in combination with the currents be deployed onto the reef.
- After concentrating the competent larvae, smaller basins on-board of small vessels can be used to transport them towards coral reefs. These smaller basins can accurately be placed on shallow and deeper reefs. After opening the basins at the desired location, the competent larvae have a high probability of reaching the targeted reef.

Because the field test has been executed during calm weather conditions, it is not investigated if the used harvesting approach also functions during other conditions. It is assumed that higher waves will influence locating, concentration and the collection of the coral embryos and larvae. When larger vessels will be used to collect the coral-spawn, the maneuverability will decrease, and adaptions to the collections system are required. Hence, for example, a larger funnel with a beam of 10m, which directs the embryos underwater towards the suction mouth, could make this process more optimal. Moreover, pumps that are able to collect 1000 m^3 h^{-1} are much heavier than the pumps used during the field trial and the pipes are no longer movable. Therefore, despite the success of the RECRUIT team, a robust system should be designed that is operational under all weather conditions.

Bibliography

AIMS (2018). Annual summary report on coral reef condition for 2017/18. pages 1–5.

Alden, A. (2019). What is Geological Strain ? pages 1–2. URL https://www.thoughtco.com/what-is-strain-1440849.

Allakhverdiev, S. I., Sakamoto, A., Nishiyama, Y., Inaba, M., and Murata, N. (2002). Ionic and Osmotic Effects of NaCl-Induced Inactivation of Photosystems I and II in Synechococcus sp. . *Plant Physiology*, 123(3):1047–1056.

Anderson, G., Barr, R., and Benvenga, R. (2007). Minor losses. volume 2, pages 1–6. URL http://fluidmechanics.datechengvn.net/FMEP/Appendix/MinorLosses.pdf.

Australian, G. (2009). Water Quality Guidelines for the Great Barrier Reef Marine Park. page 107.

Babcock, R. C., Bull, G. D., Harrison, P. L., Heyward, A. J., Oliver, J. K., Wallace, C. C., and Willis, B. L. (1986). Synchronous spawnings of 105 scleractinian coral species on the Great Barrier Reef. *Marine Biology*, 90(3):379–394.

Babcock, R. C. and Heyward, A. J. (1985). Larval development of certain gamete-spawning scleractinian corals. pages 1–6. URL papers2://publication/uuid/55F0320E-10DA-407F-8DC4-700F6ECF3452.

Bassim, K., Sammarco, P., and Snell, T. (2003). Effects of temperature on success of (self and non-self) fertilization and embryogenesis in Diploria strigosa (Cnidaria, Scleractinia). *Marine Biology*, 140(3):479–488.

Berry, K. L., Hoogenboom, M. O., Brinkman, D. L., Burns, K. A., and Negri, A. P. (2017). Effects of coal contamination on early life history processes of a reef-building coral, Acropora tenuis. *Marine Pollution Bulletin*, 114(1):505–514. URL http://dx.doi.org/10.1016/j.marpolbul.2016.10.011.

Cengel, Y. A. and Cimbala, J. M. (2004). Flow in Pipes. *Fluid Mechanics: Fundamentals and Applications*, pages 347–437. URL https://www.uio.no/studier/emner/matnat/math/MEK4450/h11/undervisningsmateriale/modul-5/Pipeflow_intro.pdf.

Cicchetti, D. (2010). Resilience under conditions of extreme stress: a multilevel perspective. *World Psychiatry 2010*, pages 15–18.

Connell, J. H., Hughes, T. P., and Wallace, C. C. (2010). A 30-Year Study of Coral Abundance , Recruitment , and Disturbance at Several Scales in Space and Time Published by : Ecological Society of America. *America*, 67(4):461–488.

De'ath, G., Fabricius, K. E., Sweatman, H., and Puotinen, M. (2012). The 27-year decline of coral cover on the Great Barrier Reef and its causes. *Proceedings of the National Academy of Sciences*, 109(44):17995–17999. URL http://www.pnas.org/cgi/doi/10.1073/pnas.1208909109.

Doropoulos, C., Elzinga, J., ter Hofstede, R., van Koningsveld, M., and Babcock, R. C. (2019). Optimizing industrial-scale coral reef restoration: comparing harvesting wild coral spawn slicks and transplanting gravid adult colonies. *Restoration Ecology*, pages 1–10.

Doropoulos, C., Roff, G., Bozec, Y.-M., Zupan, M., Werminghausen, J., and Mumby, P. J. (2015). Characterising the ecological trade-offs throughout the early ontogeny of coral recruitment. *Ecological Monographs*, 86(1):15–0668. URL http://doi.wiley.com/10.1890/15-0668.1.

Engineering360. Centrifugal Pumps Information. URL https://www.globalspec.com/learnmore/flow_transfer_control/pumps/centrifugal_pumps.

Fernandes, V., Buchlin, J., and Kourakos, V. (2010). Experimental study of a 90 degree elbow bend effect in a two-phae bubbly flow. page 1.

Galante, E. B. F., Lima, A. L. S., Franca, T. C. C., and Haddad, A. N. (2014). Exposure limits and its applications in chemical warfare. *Revista Virtual de Quimica*, 6(3):591–600.

Galli, M. and Morgan, D. O. (2016). Cell Size Determines the Strength of the Spindle Assembly Checkpoint during Embryonic Development. *Developmental Cell*, 36(3):344–352. URL https://linkinghub.elsevier.com/retrieve/pii/S153458071600037X.

Garrett, G. (2018). Science , solutions and the future: The Great Barrier Reef in a time of change final synthesis stakeholder report.

George, E. M., Stott, W., Young, B. P., Karboski, C. T., Crabtree, D. L., Roseman, E. F., and Rudstam, L. G. (2017). Confirmation of cisco spawning in Chaumont Bay, Lake Ontario using an egg pumping device. *Journal of Great Lakes Research*, 43(3):204–208. URL http://dx.doi.org/10.1016/j.jglr.2017.03.024.

Gilmour, J. P., Smith, L. D., Heyward, A. J., Baird, A. H., and Pratchett, M. S. (2013). Recovery of an isolated coral reef system following severe disturbance. *Science (New York, N.Y.)*, 340(6128):69–71. URL http://www.ncbi.nlm.nih.gov/pubmed/23559247.

Gough, S. C., Belda-Iniesta, C., Poole, C., Weber, M., Russell-Jones, D., Hansen, B. F., Mannucci, E., and Tuomilehto, J. (2011). Insulin therapy in diabetes and cancer risk: Current understanding and implications for future study. *Advances in Therapy*, 28(SUPPL. 5):1–18.

Hagedorn, M., Carter, V. L., Henley, E. M., Van Oppen, M. J., Hobbs, R., and Spindler, R. E. (2017). Producing Coral Offspring with Cryopreserved Sperm: A Tool for Coral Reef Restoration. *Scientific Reports*, 7(1):1–9. URL http://dx.doi.org/10.1038/s41598-017-14644-x.

Harrison, P., Babcock, R. C., Oliver, J. K., Wallace, C. C., and Willis, B. L. (1983). Mass spawning in tropical reef corals.

Harrison, P. and Wallace, C. (1990). Reproduction, dispersal and recruitment of scleractinian corals. In: Dubinsky Z (ed) Ecosystems of the world: coral reefs. Elsevier, Amsterdam,. *Coral Reefs*, (January):133–207.

Heyward, A. J. and Negri, A. P. (2012). Turbulence, Cleavage, and the Naked Embryo: A Case for Coral Clones. *Science*, 335(6072):1064–1064. URL http://www.sciencemag.org/cgi/doi/10.1126/science.1216055.

Hidrostal (2018). Screw centrifugal pumps. URL http://www.hidrostalpumps.com/dox/bro-hves.pdf.

Hughes, T. P., Kerry, J. T., Álvarez-Noriega, M., Álvarez-Romero, J. G., Anderson, K. D., Baird, A. H., Babcock, R. C., Beger, M., Bellwood, D. R., Berkelmans, R., Bridge, T. C., Butler, I. R., Byrne, M., Cantin, N. E., Comeau, S., Connolly, S. R., Cumming, G. S., Dalton, S. J., Diaz-Pulido, G., Eakin, C. M., Figueira, W. F., Gilmour, J. P., Harrison, H. B., Heron, S. F., Hoey, A. S., Hobbs, J. P. A., Hoogenboom, M. O., Kennedy, E. V., Kuo, C. Y., Lough, J. M., Lowe, R. J., Liu, G., McCulloch, M. T., Malcolm, H. A., McWilliam, M. J., Pandolfi, J. M., Pears, R. J., Pratchett, M. S., Schoepf, V., Simpson, T., Skirving, W. J., Sommer, B., Torda, G., Wachenfeld, D. R., Willis, B. L., and Wilson, S. K. (2017). Global warming and recurrent mass bleaching of corals. *Nature*, 543(7645):373–377.

Hughes, T. P., Kerry, J. T., Baird, A. H., Connolly, S. R., Dietzel, A., Eakin, C. M., Heron, S. F., Hoey, A. S., Hoogenboom, M. O., Liu, G., McWilliam, M. J., Pears, R. J., Pratchett, M. S., Skirving, W. J., Stella, J. S., and Torda, G. (2018). Global warming transforms coral reef assemblages. *Nature*, 556(7702):492–496.

Jones, R., Ricardo, G. F., and Negri, A. P. (2015). Effects of sediments on the reproductive cycle of corals. *Marine Pollution Bulletin*, 100(1):13–33. URL http://dx.doi.org/10.1016/j.marpolbul.2015.08.021.

Kooijman, S. A. (2010). *Dynamic Energy Budget Theory for Metabolic Organisation*. Cambridge University Press.

KSB (2017). Archimedes screw pump. URL https://www.ksb.com/centrifugal-pump-lexicon/archimedean-screw-pump/191708/.

Manshanden, G. (2018). The fish friendly screw pump. URL http://fishflowinnovations.nl/en/innovations/screwpump/.

Marn, N., Jusup, M., Catteau, S., Kooijman, S. A., and Klanjšček, T. (2019). Comparative physiological energetics of Mediterranean and North Atlantic loggerhead turtles. *Journal of Sea Research*, 143(December 2017):100–118.

Martyn, P. (2018). SmallBusiness Innovation Research presentation. URL https://advance.qld.gov.au/sites/default/files/sbir-boosting-coral-abundance-gbr-information-session.pdf.

Matoušek, D. i. V. (2004). Dredge pumps and slurry transport. (September):518.

Mellin, C., Thompson, A., Jonker, M. J., and Emslie, M. J. (2019). Cross-Shelf Variation in Coral Community Response to Disturbance on the Great Barrier Reef. *Diversity*, 11(3):38.

Michels, M. H., Van Der Goot, A. J., Norsker, N. H., and Wijffels, R. H. (2010). Effects of shear stress on the microalgae Chaetoceros muelleri. *Bioprocess and Biosystems Engineering*, 33(8):921–927.

Oliver, J. K. and Willis, B. L. (1987). Coral-spawn slicks in the Great Barrier Reef: preliminary observations. *Marine Biology*, 94(4):521–529. URL http://link.springer.com/10.1007/BF00431398.

Parida, A. K. and Das, A. B. (2005). Salt tolerance and salinity effects on plants: a review. *Ecotoxicology and environmental safety*, 60(3):324–49. URL http://www.ncbi.nlm.nih.gov/pubmed/15590011.

Paull, J. M. (1984). The origin and basis of threshold limit values. *American Journal of Industrial Medicine*, 5(3):227–238.

Power, N. Relative Roughness of Pipe. URL https://www.nuclear-power.net/nuclear-engineering/fluid-dynamics/major-head-loss-friction-loss/relative-roughness-of-pipe/.

Q. Schiermeier (MIT) (2005). Basics of Turbulent Flow. pages 1–10.

Schiermeier, Q. (2018). Great Barrier Reef saw huge losses from 2016 heatwave. *Nature*, 556(7701):281–282.

Sikopump (2009). Tech. Information for the QBY Diaphragm Pump(AODD Pump). URL http://www.sikopump.com/En/QBY-Diaphragm-Pump-Tech.html.

Suga, N. (1963). Change of the toughness of the chorion of fish eggs. 8(1):63–74.

Sundby, S. and Kristiansen, T. (2015). The principles of buoyancy in Marine Fish Eggs and their vertical distributions across the World Oceans. *PLoS ONE*, 10(10):1–23.

Tukker, M. J., Kooij, C., and Pothof, I. W. M. (2010). Hydraulisch ontwerp en beheer van afvalwaterpersleidingen; CAPWAT Handboek. 2010(24 June):CAPWAT webpage \nHandbook and dissemination progra. URL http://capwat.deltares.nl.

Ulanowicz, R. E. (1976). The mechanical effects of water flow on fish eggs and larvae. *Fisheries and energy production: a symposium*, 1(593):77–87. URL http://aquaticcommons.org/id/eprint/1986.

Van Koningsveld, M., ter Hofstede, R., Elzinga, J., Smolders, T., Schutter, M., and Osinga, R. (2017). ReefGuard: A scientific approach to active reef rehabilitation. *Terra et Aqua*, (147):5–16.

Weber, E. D., Borthwick, S. M., and Helfrich, L. A. (2004). Plasma Cortisol Stress Response of Juvenile Chinook Salmon to Passage through Archimedes Lifts and a Hidrostal Pump. *North American Journal of Fisheries Management*, 22(2):563–570.

Winer, M. H., Ahmadi, A., and Cheung, K. C. (2014). Effects of Density Difference Between Particles and Fluid on Inertial Focusing Positions in Transient Micro- Flows. pages 2462–2464.

A
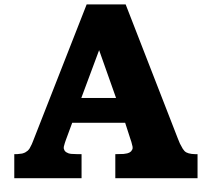
Appendix - Introduction

A.1. Project time table
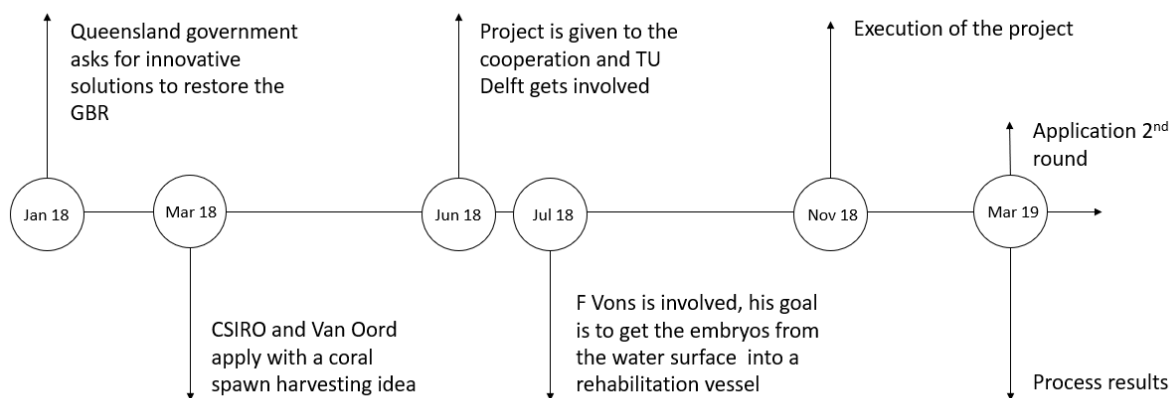
Figure A.1: Project time table

A.2. Introduction to the Great Barrier Reef

A.2.1. Research location

The Great Barrier Reef is the largest coral reef system in the world and extends for over 2300 km along Queensland. It consists of over 2900 reefs and covers an area of approximately 344 000 km2 (Australian, 2009). The Great Barrier Reef was declared a World Heritage Area in 1981, and internationally recognised by the World Heritage Committee for its Outstanding Universal Value. It remains one of only a small number nominated for all four natural criteria under the World Heritage Operational Guidelines:

- Exceptional natural beauty and aesthetic importance

- Significant geomorphic or physiographic features

- Significant ecological and biological processes

- Significant natural habitats for biological diversity

The Great Barrier Reef's diversity reflects the maturity of the ecosystem, which has evolved over hundreds of thousands of years. It is the world's most extensive coral reef system and is one of the world's richest areas in terms of faunal diversity. A majority of its reefs are situated on the midand

outer-continental shelf, and are located 40 to 150 km from the mainland. Individual reefs range in size from less than one hectare to more than 100 000 hectares, and in shape from flat platform reefs to elongated ribbon reefs. Great Barrier Reef industries such as tourism, recreational and commercial fishing are highly dependent on the marine environment. These valuable reef-based activities rely on a healthy reef ecosystem (Australian, 2009).

Current bleaching events have changed the Great Barrier Reef faster than expected. About half of the coral died in 2016 and 2017 because of extreme heat; a result of climate change driven by greenhouse gas emissions, researchers found out (Schiermeier, 2018). When coral dies, there can be a lack of new larvae supply to those areas and this could degrade the reef further. Intact reefs often have plenty of coral spawn, which develop into larvae and disperse from the natal reefs to surrounding reefs up to 1000 km away, as well as a portion that recolonise the reef of origin.

The Australian and Queensland governments, working with scientists, stakeholders and the community, have initiated a number of key plans and strategies aimed at halting and reversing the decline in the quality of waters entering the Great Barrier Reef. Key initiatives include (Australian, 2009):

- The Australian Government's Reef Rescue Plan, targeting improved farm management practices and supporting water quality monitoring programs

- The Australian and Queensland Government's Reef Water Quality Protection Plan 2003 (Reef Plan)

- The Australian Government's Coastal Catchments Initiative (CCI)

- The Australian Government's National Water Quality Management Strategy (NWQMS) 2

- The Queensland Wetlands Program

- The Queensland Environmental Protection (Water) Policy 1997.

These guidelines were developed to support those initiatives, and in particular, to compile the currently available scientific information to provide environmentally-based values for water quality contaminants that, if reached, will trigger management actions (Australian, 2009).

B

Appendix - Pumping system

B.1. Particle motion through a fluid

When a particle is flowing through a fluid, different forces are working on it namely: buoyancy force, drag force and lift force (Matoušek, 2004). If flow is turbulent, also the turbulent diffusive force can play a roll. In this research, the particles transported by the fluid are positively buoyant. To understand behaviour of coral spawn in a fluid, the different forces working on the particle are described in this section.

Gravitational and buoyancy force

The body force due to gravitational acceleration is determined from the volume and density of the particle. The gravitational force on a spherical particle can be determined with formula B.1 (Matoušek, 2004):

$$F_{Gp} = \rho_s \cdot g \frac{\pi * d^3}{6} \tag{B.1}$$

Archimedes describes immersed particles in fluids and concludes that the weight of the particle is reduced due to buoyancy effects. For a spherical particle the submerged weight is determined by expression B.2:

$$F_{Wp} = (\rho_s - \rho_f) \cdot g \cdot \frac{\pi \cdot d^3}{6} \tag{B.2}$$

Where $F_{Gp}[N]$ is the gravitational force on a spherical particle, $F_{Wp}[N]$ is the submerged weight, ρ_s the density of the particle, ρ_f the density of the fluid and d the diameter of the particle(Matoušek, 2004). While ρ_s is smaller than ρ_f, the submerged weight is negative and the vector will work in the negative direction of the gravity.

Drag

The drag force is a force exerted to the particle in the negative direction of the velocity so it slows down the particle. It can be described with Equation B.3.

$$F_D = 0.5 \cdot \rho \cdot U^2 \cdot C_D \cdot A \tag{B.3}$$

Where the drag coefficient C_D depends on the Reynolds number. In the laminar regime, C_D is asymptotically proportional to Re^{-1} and in the turbulent regime (till Re $\approx$ 400,000) the C_D coefficient is more or less constant. The relation between Re and C_D can be seen in Figure B.1.

The balance between the buoyancy, gravitational and drag forces on the submerged solid body, determines a settling velocity (Matoušek, 2004). Because coral particles float in the medium, the settling velocity is probably negative. This is a new phenomena in dredging because normally, particles which are pumped through the system sink.
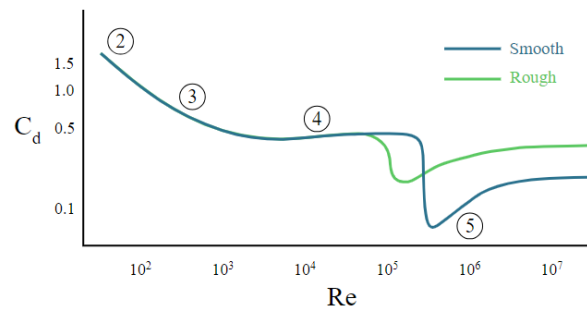
Figure B.1: Drag coefficient of a sphere versus Reynolds number

Fall velocity

When pumping particles through pipes, they normally fall in the direction of gravity until reaching the bottom part of the pipe. While the coral particles float, they will move towards the upper part of the pipe. When the particles touch the wall of the pipe, they experience higher shear stresses. To avoid this, the flow velocity can be increased to keep the particles in the centre of the flow. However, when the velocity is to high, high stress can be exerted by solid obstructions and will probably be fatal (Ulanowicz, 1976).

Lift

Simultaneous slip and rotation results in a lower hydrodynamic pressure in flow above the particle relative to the flow below the particle. Due to this pressure difference, lift F_L is generated. The lift force is most active near a pipeline wall where the velocity gradient is high. However, often does the lift force play a minor role in the majority of mixture flow regimes (Matoušek, 2004).

B.2. Pumping literature

In this section, literature is presented regarding pumping systems and the corresponding stressors.

B.2.1. Pumpings system curves and losses

Pump H-Q curve

A pump adds mechanical energy to the medium flowing through a pump. Therefore, a pressure difference occurs between the inlet and the outlet of a pump. The energy head or pressure added to the medium, depends on the principle of the pump, the speed of the pump and the flow rate of the medium trough the pump. This relationship is often described by pump curve or Q-H curves (Matoušek, 2004). These curves are specific for each pump and relates the revolutions per minute of the impeller n, the head H (which is a measure of mechanical energy of a flowing liquid per unit gravity force(Matoušek, 2004)) and the discharge Q to another. The "pump characteristics" are usually available with the pump manufacturer. An example of the pump characteristics of a Hidrostal pump can be found in appendix A Figure B.3. The affinity Equations B.4 enable to produce the pump curves for different frequencies (Matoušek, 2004).

$$\frac{Q_1}{Q_2} = \frac{n_1}{n_2}, \frac{H_1}{H_2} = \left(\frac{n_1}{n_2}\right)^2 \tag{B.4}$$

For the model, the pump H-Q curve is essential to investigate the interaction between the system and the pump. With this interaction, the expected discharge as well as the flow velocities can be calculated. In this report, the pump curves are delivered by the manufacturer and will not be calculated.

System H-Q curve

Next to the pump H-Q curve, the system H-Q curve gives the amount of energy that the pipeline requires maintaining a certain flow rate in a pump-pipeline system (Matoušek, 2004). These two graphs are often plotted in the same figure and at the intersection point of these curves give the discharge and head for that specific setup. When the pipe diameter is adjusted, the system curve will change (not

the pump curve) and therefore the head and discharge. In Equation B.7 is presented how the curve can be constructed which is obtained by using conservation of energy B.5 and B.6:

$$z_1 + \frac{P_1}{\rho \cdot g} + \frac{U_1^2}{2 \cdot g} = z_2 + \frac{P_2}{\rho \cdot g} + \frac{U_2^2}{2 \cdot g} \tag{B.5}$$

If one adds the pump head h_p on the left side and the major h_L and minor $\sum h_M$ losses on the right side, the following results:

$$z_1 + \frac{P_1}{\rho \cdot g} + \frac{U_1^2}{2 \cdot g} + h_p = z_2 + \frac{P_2}{\rho \cdot g} + \frac{U_2^2}{2 \cdot g} + h_L + \sum h_m \tag{B.6}$$

For now, it is assumed that the starting and ending points are open air reservoirs were essentially the flow is at rest and the pressures are even. This results that U_1, U_2, P_1 and P_2 can be cancelled out. After rewriting the final formula for the H-Q system curve is obtained:

$$h_p = z_2 - z_1 + h_L + \sum h_m \tag{B.7}$$

Working point
When all the ingredients to produce a H-Q curve for both the pump and the system are known they can be plotted in graph. The intersection point between the two lines describes the velocity of transported medium in the pump-pipeline system (Figure B.2). The point gives the velocity at which a balance is found between the energy provided to a system by a pump and the energy required to overcome a flow resistance in a pipeline and a change in a geodetic height between the pipeline inlet en outflow (Matoušek, 2004). In other words, when both the system and pump curve are known, the flow discharge can be read from the graph. When one adjusts the frequency of the pump from n_A to n_B, the pump curve will change and the new discharge Q_2 can be pulled out of the graph.

For dredging operations it is common that the fluid/solid mixture varies in density. This fluctuation might produce a fluctuation in the velocity, even if all the other parameters are constant(Matoušek, 2004). However, in this research it is assumed that the density will not vary considering water with coral slick mixture.
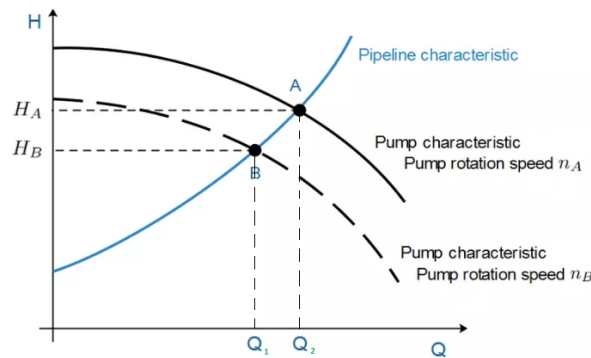
Figure B.2: Pump and system curves with the corresponding working points

Every pump is built with a certain working point where the efficiency is highest namely: the optimal working point. If a system is designed with a working point deviated far from this point, high vibrations in the pump can occur. These vibrations can cause turbulence's in the pump and must be avoided.

D100-S01

Project:	Notitie Pompvermogen P inclusief mechanische seal wrijving en lagerstoel verlies ingelopen lagerstoel.
Klant:	
Project nr.: Order nr.: Datum:	Pomptest overeenkomstig ISO 9906:2012-3B
	Toerental: 584 - 1460 t.p.m. D = 100 mm
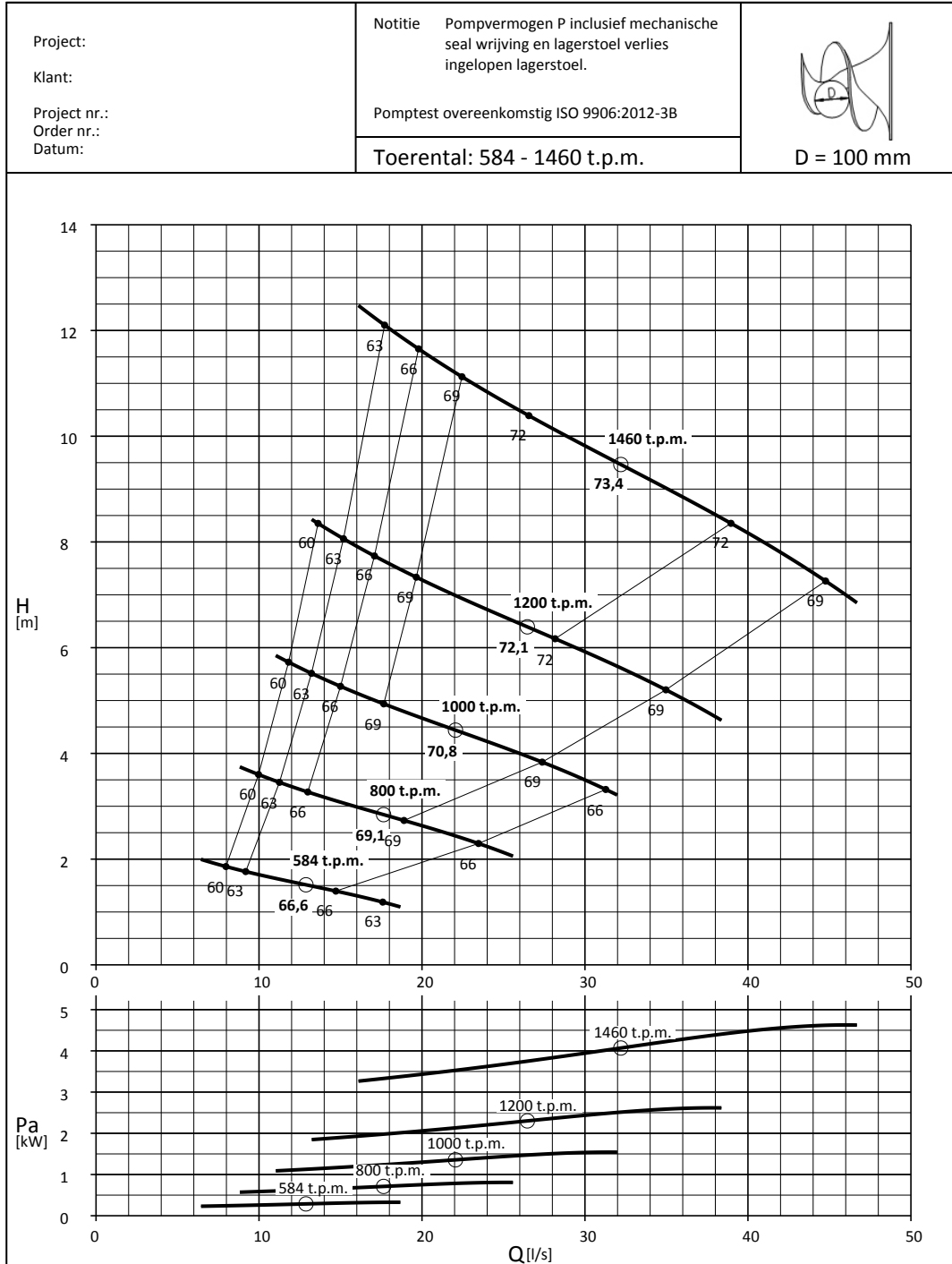
Figure B.3: QH and power curves for the D100-S Hidrostal pump at different rpm

Minor losses - flow through bends ξ_{bends}

	ξ-waarden: bocht α in °					
r/D	15°	22,5°	30°	45°	60°	90°
1,5	0,03	0,050	0,085	0,13	0,17	0,20
2	0,03	0,045	0,060	0,09	0,12	0,13
3	0,03	0,045	0,055	0,08	0,10	0,13
5	0,03	0,045	0,050	0,07	0,08	0,11
10	0,03	0,045	0,050	0,07	0,07	0,11
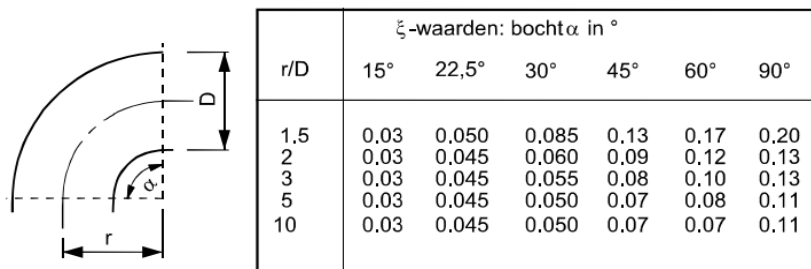
Figure B.4: Coefficients of minor losses in bends (Tukker et al., 2010)

Minor losses - inlet ξ_{inlet}
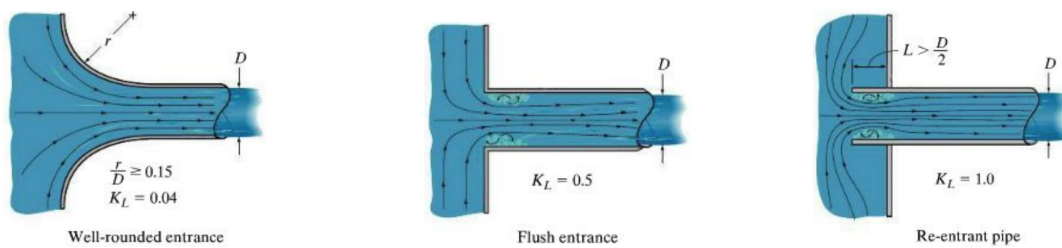
Figure B.5: Well rounded, flush and re-entrance pipe entrance (Anderson et al., 2007)

Minor losses - outflow $\xi_{outflow}$
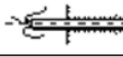
Type of entrance	ξ	μ
	0.4 ... 0.5	0.58...0.61
	0.8 ... 1.0	0.5...0.53
	0.2 ... 0.3	0.65...0.69
	0.1	0.75
	0	1
	0.5 + 0.32 cos α + 0.2 cos²α	
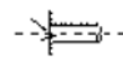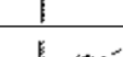
Figure B.6: Coefficients of minor losses at the inflow
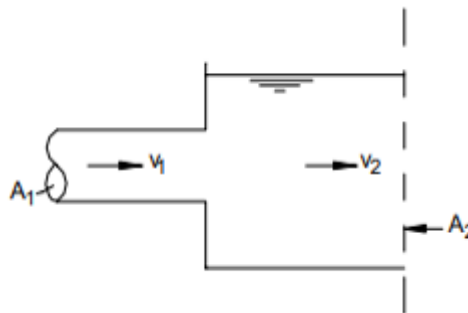
Figure B.7: Outflow into a basin

Minor losses - dilation $\xi_{widening}$
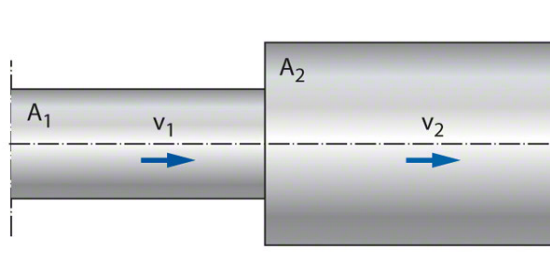
Figure B.8: Dilation in a pipe section (Matoušek, 2004)

B.2.2. Shear stress, turbulence and pressure changes

:

$$-\frac{dP}{dx} = \tau \frac{2}{r} \tag{B.8}$$

The predicted Reynolds regime in this research is >5000 so turbulent flow. In a fully developed turbulent flow, the turbulent core usually occupies almost the entire pipe cross section, excepting
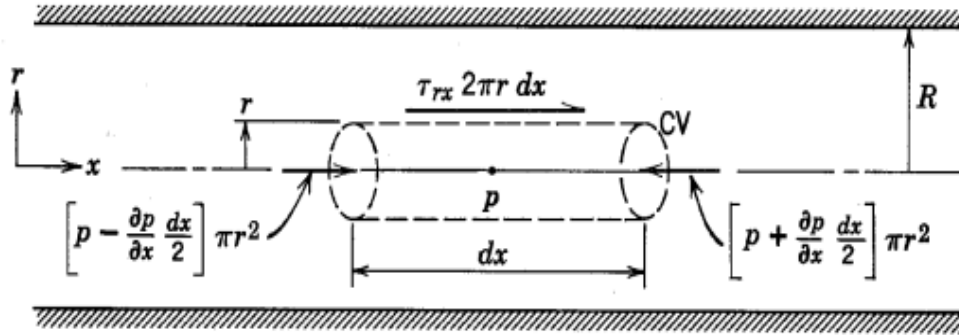
Figure B.9: Control volume for analysis of force balance in flow in a circular pipe (Matoušek, 2004)
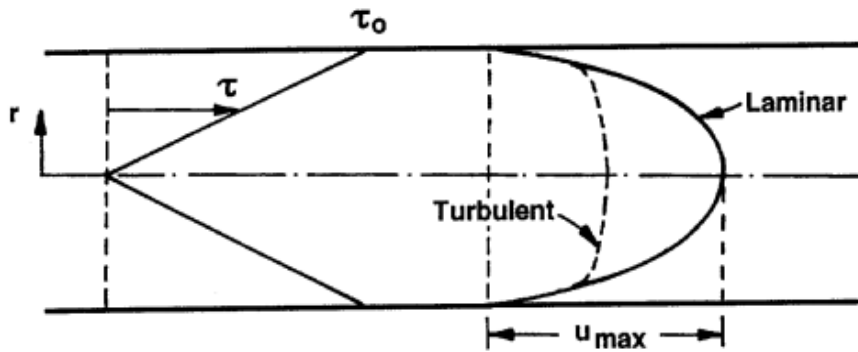
Figure B.10: Stress and velocity distribution in pipe flow of liquid (Matoušek, 2004)

only the near-wall region or boundary layer (Matoušek, 2004). Matousek is using the following analysis to describe the shear stress. A function

$$\tau_0 = fn(\rho_f, U_f, \mu_f, D, k) \tag{B.9}$$

is assumed which provides a relation between dimensionless groups:

$$\frac{\tau_o}{\frac{1}{2}\rho_f U_f^2} = fn\left(Re, \frac{k}{D}\right) \tag{B.10}$$

Dimensionless group Re relates the inertial and viscous forces in the pipeline flow:

$$Re = \frac{U_f D \rho_f}{\mu_f} = \frac{U_f D}{\nu_f} \tag{B.11}$$

The left part of Equation B.10 is called the friction factor and is the ratio between shear stress and kinetic energy of the liquid in a control volume in a pipeline:

$$f_f = \frac{\tau_o}{\frac{1}{2}\rho_f U_f^2} \tag{B.12}$$

The parameter f_f is known as Fanning friction factor. Which can be related to the Darcy-Weisbach friction coefficient: $\lambda_f = 4f_f$. The Darcy-Weisbach friction coefficient, combined with the integrated linear momentum equation of pipeline flow, gives the equation first published by Weisbach in 1850 (Matoušek, 2004):

$$-\frac{dP}{dx} = \frac{\lambda_f}{D} \frac{\rho_f U_f^2}{2} \tag{B.13}$$

Which can be written as

$$P_1 = P_2 + \frac{\lambda_f}{D} \frac{\rho_f U_f^2}{2} L \tag{B.14}$$

Which again is the equation for determination of the frictional head loss in liquid flow, as already seen in Section B.2.1 to calculate the major loss in a pipeline. P_1 and $P_2[pa]$ are the absolute pressures at beginning and end of the pipe section. Unknown so far is the value for λ_f. White-Colebrook states that for a turbulent flow the following equation can be used:

$$\frac{1}{\sqrt{\lambda_f}} = -2 \log \left(0.27 \frac{k}{D} + \frac{2.5}{Re\sqrt{\lambda_f}} \right) \tag{B.15}$$

Where the factor k stands for the roughness of the pipe material. For this factor, different values are given in Appendix A Figure B.11. The function must be iterative approached which is done in the mathematical model.
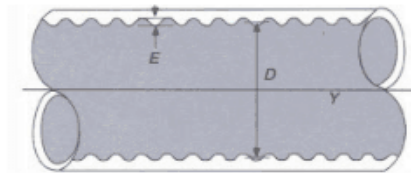
Material	Absolute Roughness (mm)
Copper, Lead, Brass, Aluminum (new)	0.001 - 0.002
PVC and Plastic Pipes	0.0015 - 0.007
Flexible Rubber Tubing - Smooth	0.006-0.07
Stainless Steel	0.0015
Steel Commercial Pipe	0.045 - 0.09
Weld Steel	0.045
Carbon Steel (New)	0.02-0.05
Carbon Steel (Slightly Corroded)	0.05-0.15
Carbon Steel (Moderately Corroded)	0.15-1
Carbon Steel (Badly Corroded)	1-3
Asphalted Cast Iron	0.1-1
New Cast Iron	0.25 - 0.8
Worn Cast Iron	0.8 - 1.5
Rusty Cast Iron	1.5 - 2.5
Galvanized Iron	0.025-0.15
Wood Stave	0.18-0.91
Wood Stave, used	0.25-1
Smoothed Cement	0.3
Ordinary Concrete	0.3 - 1
Concrete – Rough, Form Marks	0.8-3

Figure B.11: Roughness k of different pipe material (Power,)

B.3. Derivation of equations

B.3.1. Derivation of the strain in pipes

$Strain = shearrate * duration = \gamma * t$

$shearrate = \frac{Shearstress}{Dynamicviscosity} => \gamma = \frac{\tau}{\eta}$

$Shearstress = \tau = \frac{\Delta P_{lossPipes}}{Q} = \rho * g * \Delta H$

$Shearrate = \frac{\rho*g*\Delta H_{pipes}}{\eta}$

$Strain = \frac{\rho*g*\Delta H_{pipes}}{\eta} * t$

$\Delta H_{pipes} = \lambda * \frac{L}{D} * \frac{U^2}{2g}$

$Strain = \frac{\rho*g}{\eta} * \lambda * \frac{L}{D} * \frac{U^2}{2g} * t$

$t = \frac{L}{U} = \frac{L \cdot A}{Q}$

$Strain = \frac{\rho*g}{\eta} * \lambda * \frac{L}{D} * \frac{U^2}{2g} * \frac{L \cdot A}{Q}$

$Strain = \frac{\rho*g}{\eta} * \lambda * \frac{L}{D} * \frac{Q^2}{2gA^2} * \frac{L \cdot A}{Q}$

$Strain = \frac{\rho*g}{\eta} * \lambda * \frac{L^2}{D} * \frac{Q}{2gA}$

$Strain = \frac{\rho*g}{\eta} * \lambda * \frac{L^2}{D^3} * \frac{Q}{2*g*0.25*pi}$

$Strain = \frac{\rho*\lambda}{\eta*0.5*pi} * \frac{L^2}{D^3} * Q$

$Strain = 12084 \frac{L^2}{D^3} * Q$

B.3.2. Derivation of energy loss in pipe sections

$P = \rho g H Q$

$H = \lambda \frac{L}{D} \frac{U^2}{2g} = \lambda \frac{L}{D} \frac{Q^2}{2gA^2}$

$P = \rho g \lambda \frac{L}{D} \frac{Q^2}{2gA^2} Q$

$P = \rho g \lambda \frac{L}{D} \cdot \frac{Q^3}{2gA^2}$

$E_{loss} = \int_a^b P dt$

$E_{loss} = \int_a^b \rho g \lambda \frac{L}{D} \cdot \frac{Q^3}{2gA^2} dt$

$E_{loss} = \rho g \lambda \frac{L}{D} \cdot \frac{Q^3}{2gA^2} t$

$t = \frac{L}{U} = \frac{L \cdot A}{Q}$

$E_{loss} = \rho \lambda \frac{L^2}{D^3} \frac{Q^2}{\frac{1}{4} \cdot \pi}$

B.4. Pump selection

From the multi criteria analysis, three pumps remain which are probably the most promising with an addition of a centrifugal pump. That pump is not the right pump for pumping fragile particles but because it is a very common pump at Van Oord, it is interesting to see what such a pump will do in practise to fragile particles. Below, the four pumps are described in detail and the score of the MCA is clarified.

Archimedes screw

Archimedean water screw pumps (or lifts) are a special type of volumetric pumps and can be seen in Figure B.12. It is often used for constant-pressure lifting of a fluid to a given geodetic height with the aid of a rotating screw which works on the principle of Archimedes (KSB, 2017). At each turn the screw, usually made of sheet metal and can have up to three flight or starts, scoops up a limited volume of water. This volume is dependent on the inclination angle, the diameter of the screw, the speed of the screw and how much the screw is submerged. The principle presupposes that the screw is constantly

submerged in the liquid to at least half the diameter of its leading screw passage and that the clearance gap width between the screw and the sheet steel of concrete trough is not to large (KSB, 2017). The pressure differences and flow accelerations are low and because the diameter is scalable from 0.3m to 4m with different frequencies, the discharge can vary from 1m3/h to 15000m3/h or more. Typical applications of the Archimedes water screw are waste water treatment, fish migration, drainage and irrigation and generally whenever water has to be lifted.
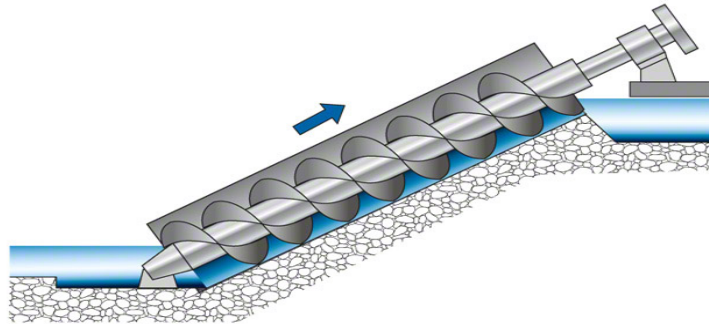
Figure B.12: Archimedes screw pump (KSB, 2017)

The pump is reviewed on the requirements given in section B.12 and in more detail below:

- Low shear forces **4**
  The parts where the particles will experience high shear forces will be around the inlet of the screw where it "hits" the water and along the skin of the screw. While the flow velocity is low, the diameter respectively large and the wet surface small, the particles encounter low shear forces.

- Turbulence **5**
  Fish Flow innovations executed, together with the TU Delft, experiments regarding turbulence which resulted in very low turbulence (Manshanden, 2018).

- Pressure differences **5**
  The pump functions without a pressure difference. The screw is open and "lifts" the fluid. (KSB, 2017).

- Self priming **5**
  Due to the open fabrication of the screw, it is totally self priming.

- Low local flow accelerations **4**
  While the screw turns with a constant frequency over the whole length of the system, the local flow velocities are small. Only around the entrance, where the water is scooped out, and at the outflow accelerations occur.

- Hydraulic head capacity **4**
  The screw opperates best under an angle of 30 degree, so, the hydraulic head capacity is not limited. However, when a height of, for example, 30m must overcome, the system have got a length which is not workable anymore.

- Scalability **5**
  When the diameter, the speed or the submerge depth are adjusted, the discharge can be easily modified. As described above, the discharge can vary from 1 to more than 15000 m3/h.

- Availability **1**
  Because the screw is often made from heavy steel and is customized for every project, the screws availability is very low. To built a screw takes around two months (Manshanden, 2018) and especially for the pilot project, time and budget were limited.

- Handling **2**
  Because the system is rigid, when chosen, it must be constructed directly to the ships hull.

Furthermore, its not possible to move the suction mouth so the vessel must direct the mouth towards the coral slicks. Also, the outflow cannot be directly positioned in the desired basin.

- Costs **..** For the pilot project, it was not possible to find a screw that was affordable which also was available in Australia. However, FishFlow innovations was willing to built a screw with the specific specifications out of fibers for 20.000,-(Manshanden, 2018).

Conclusion of the Archimedes screw pump: If the pump would be available in Australia, made out of light weight materials and a solution of the handling would be presented, the pump can be very promising.

Hidrostal pump

Hidrostal's submersible/immersible pumps are a range of screw centrifugal non clog pumps. They are capable of pumping general effluent and industrial waste water that includes solids, rags and other common materials. Viscous pumping and even gentle handling are also possible with this type of pump. The submersible motor is cooled by conducting heat from the motor to the liquid in which it is submerged (Hidrostal, 2018). The pump is often used for fish migration and multiple experiments have been executed. The centrifugal screw impeller in Figure B.13 with open channels is designed to combine clog free features of a vortex pump with the high efficiency of a centrifugal pump (Hidrostal, 2018).
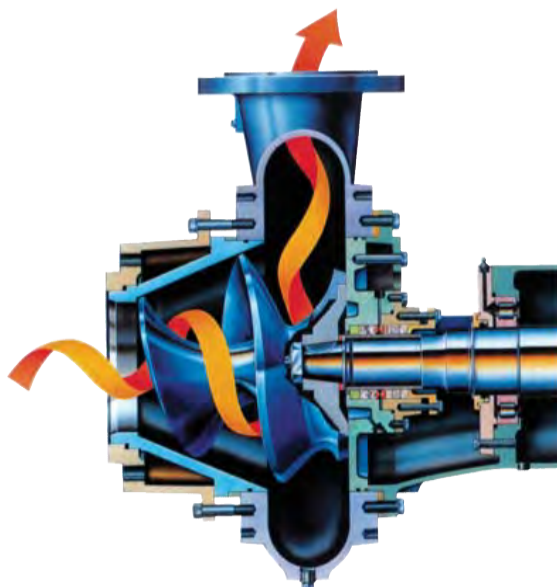
Figure B.13: Archimedes screw pump (Hidrostal, 2018)

The pump is reviewed on the requirements given in section B.12 and in more detail below:

- Low shear forces **3**
  The hidrostal pump is often operating with high frequency which creates a curvature flow in front of the pump. When the particles are hitting the wall of the pump, high shear can occur. However, because the particles are not facing a bladed impeller, the shear forces will be much lower than with a normal centrifugal pump.

- Turbulence **3**
  Due to the curvature from and the pressure difference over the pump, turbulence will occur where the streamlines cannot follow the pump housing. This depends to the manufacturing of the pump screw-impeller.

- Pressure differences **3**
  Due to pressure difference created by accelerations of the fluid, the medium is transported, so pressure differences will be present.

- Self priming **2**
  The pump must be immerged so is not self priming but, most of the pumps are equipped with a cooling system that allows the pump to pump some air.
- Low local flow accelerations **4**
  While the screw rotates with a constant frequency the outflow of the pump is constant. Because the fluid must encounter an spinning screw impeller, accelerations in the pump are present.
- Hydraulic head capacity **4**
  Hidrostal pumps can pump up to 20+ meters in height difference (Hidrostal, 2018).
- Scalability **4**
  By adjusting the size of the pump, high discharges can be reached. The smallest hidrostal pump pumps with 38 m3/h and the larger pumps around 3000 m3/h.
- Availability **5**
  In Brisbane there is a Hidrostal manufacture which is able to built the desired pump.
- Handling **4**
  The system works with an immersed pump and hoses which can be directed in any desired position.
- Costs **..** For the pilot project, Hidrostal Australia offered to loan the desired pump for the investigation. The transportation and maintenance costs are around 3000euro for a single pump.

Conclusion of the Hidrostal pump: Its concept is proven during transportation of fish. While the pilot project is focusing on transporting living fragile particles, this pomp is promising. Because the coral slick particles are far supposed to be more fragile than fish, the frequency of the pump must be adjustable and set minimum. The handling and the cost are very positive, which are major benefits. (Weber et al., 2004)

Diaphragm pump

A diaphragm pump or membrane pump B.14 is a positive displacement pump that uses valves and vacuums to transport a fluid. Due to pressure differences in the chambers created by the movement of valves, a fluid is drawn into the pump. When the chamber is full, the valve closes on the other side and the fluid is pump trough a discharge pipe. The pump has good lift characteristics and can handle sludge's and slurry's with relatively high amount of content. The pump is self-priming due to the vacuum created in the chambers. Because the chambers open en closes over time, the flow pulses through the system. In 2017, Ellen M. George et al. executed an experiment where they pumped fish eggs of: *Coregonus artedi* with a small diaphragm pump (George et al., 2017). The pump collected eggs, silt, mall rocks, vegetation and other invertebrates but the eggs remained undamaged and the majority of the embryos were still alive and often observed moving under the microscope (George et al., 2017).

- Low shear forces **3**
  The diaphragm pump transports the fluid through small passages due to valves that open and closes. The streamlines around these valves are automatically not straight lines so the accelerations and small openings will cause shear forces. However, these will be lower than a fast rotating impeller in a centrifugal pump.
- Turbulence **2**
  Because the fluid is pulsing through the system, the probability of turbulence is high. Also it is hard for the streamline to follow the profile within the pump which is often built out of pipes with bends.
- Pressure differences **2**
  Due to pressure difference created by vacuums in the chambers, the medium is transported.
- Self priming **5**
  The pump works with vacuum and is self priming.
- Low local flow accelerations **2**
  As described above, the pump pulses the fluid trough the system.
- Hydraulic head capacity **4**
  Diaphragm pumps are able to pump over multiple meters in height.
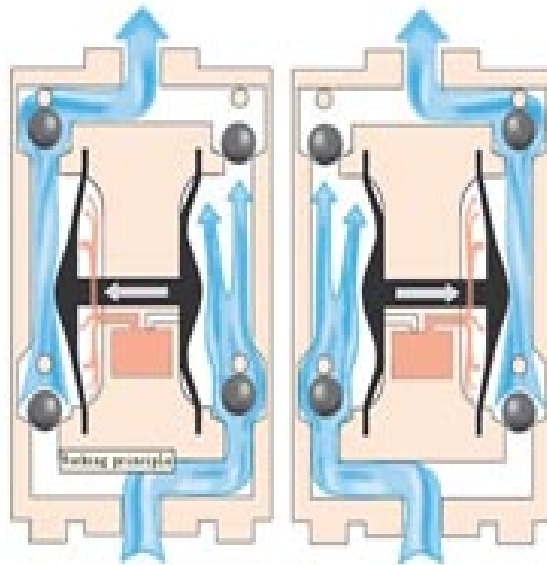
Figure B.14: Diaphragm pump principle (Sikopump, 2009)

- Scalability **2**
  By adjusting the size of the pump, higher discharges can be reached. The largest diaphragm pump available on the regular market have got a free passage of 100mm and a discharge of 70m3/h. To use this pump on a hopper, multiple small ones must encounter the demand in discharge.
- Availability **5**
  All over the world, diaphragm pumps are good accessible.
- Handling **4**
  The system works with an self priming pump and hoses which can be directed in any desired position. The pulsations of the pump work negatively on the handling.
- Costs **..** Diaphragm pumps are easy to rent in most of the countries. However, if the 100mm diaphragm pump is desired to use, it must be bought while these are not in the renting fleet.

Conclusion of the diaphragm pump: For the pilot project it is positive that the experiment of pumping fish eggs was a success in the paper of Ellen M. George (George et al., 2017). Furthermore, a self priming pump will cause less difficulties on board of the vessel. However, the fluid is pulsing through the system and will encounter accelerations and turbulence.

Centrifugal in progress

Centrifugal pumps are dynamic pumps which move fluids through a system using one or more impellers. They are the most common type of pump because of the simplicity and effectiveness of their design and operation. Because they are the most familiar, they also tend to cost less than other types of pumps. Compared to positive displacement pumps, they provide higher flow rates and lower pressures.(Engineering360,)

- Low shear forces **1**
  The centrifugal pump transports the fluid by accelerating it through the pump house by spinning it.
- Turbulence **1**
  Due to the high velocities in the pump housing, the probability on turbulence is high.
- Pressure differences **1**

- Self priming **1**
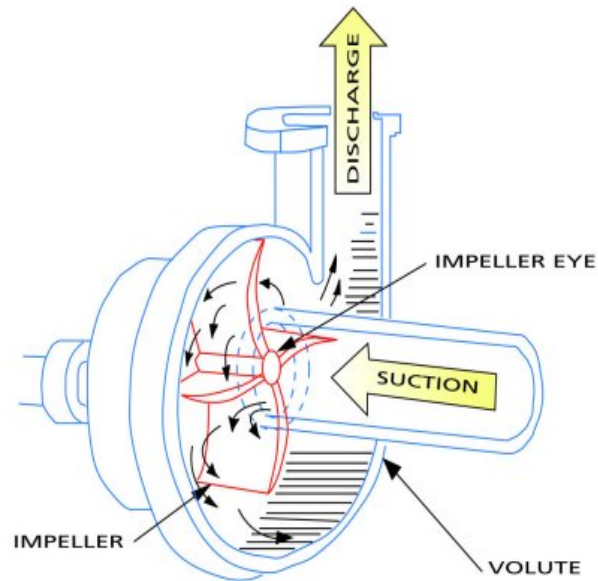
Figure B.15: Centrifugal pump principle (Engineering360,)

- Low local flow accelerations **1**

- Hydraulic head capacity **4**

- Scalability **4**

- Availability **3**
  All over the world, centrifugal pumps are good accessible.
- Handling **4**
  The system works with constant flow and easy to handle.
- Costs **..** Centrifugal pumps are easy to rent in most of the countries and relatively cheap.

Conclusion of the centrifugal pump: not a good pump for pumping coral embryo's but because it is very common and interesting to see what such a pump will do to fragile particles, it will be tested.

DESIGN FEATURES

Separate cable cap permits a new cable to be fitted without disturbing motor cover or bearing

High security cable entry assembly

Upper bearing temperature probe (optional)

High efficiency dry motor with class 'F' insulation with built in thermal sensors

Oil jacket with forced circulation for efficient cooling of immersible motor

Regreasing of bearings (certain models only)

Heavy duty shaft and bearings

Extensive monitoring

Oil circulation impeller locked onto shaft

Tandem mechanical seals

Finned back cover acts as heat exchanger

Heavy-duty hydraulic end incorporating the Hidrostal screw centrifugal impeller.

Figure B.16: Design features of a hidrostal pump (Hidrostal, 2018)

Appendix - Validation

C.1. Laboratory results

Figure C.1: Example of damage done to different proxies following pumping.

C.2. Example of a not optimal pumping system

To indicate pumping systems that are undesired for coral harvesting, this section presents a design that exceeds the thresholds. In Figure C.2 a representation of an undesired pumping system is presented for coral harvesting. The diameter is set on 50mm and the pump is positioned above the water surface. Large head differences are created by lifting the hoses to 4m in height. The length of the system is unnecessary long and the pump efficiency is very low.
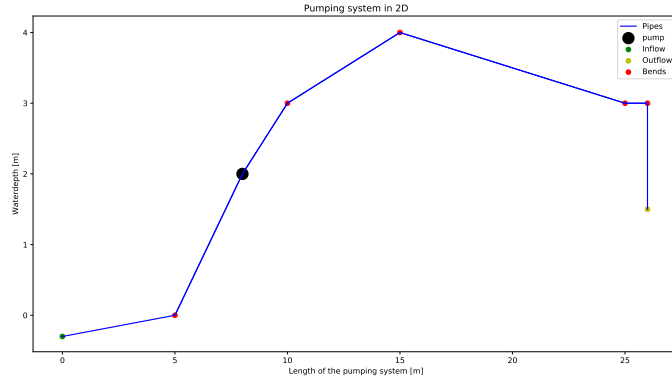
Figure C.2: Two dimensional presentation of an undesired pumping system

Very high head and energy losses are coupled to the system as presented in Figure C.3
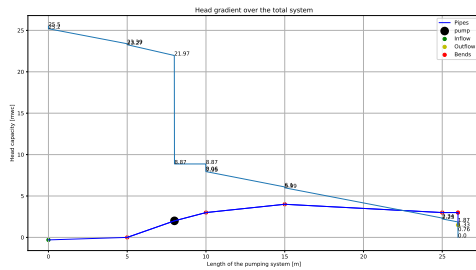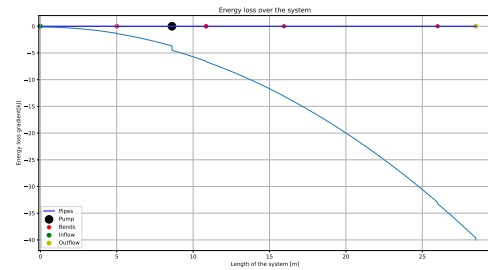
(a) Head losses over the pumping system   (b) High energy losses over the pumping system

Figure C.3

The local pressures become much lower than atmospheric pressure and even below the vapour pressure which indicates an high probability for cavitation occurrence as presented in Figure C.4.
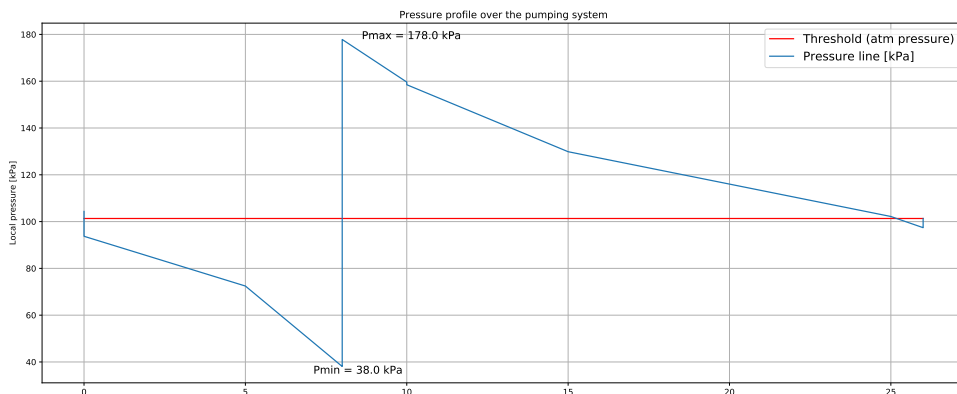
Figure C.4: Undesired local pressure variation over the pumping system

C.2.1. Harvesting coral colonies

Figure C.5: Harvesting coral colonies from the reef

C.2.2. Settled larvae on a tile

2.0 mm

Figure C.6: Settled larvae on a tile